MULTISCALE ANALYSIS OF NANOCOMPOSITE AND NANOFIBROUS STRUCTURES

A Dissertation

by

VINU UNNITHAN UNNIKRISHNAN

Submitted to the Office of Graduate Studies of
Texas A&M University
in partial fulfillment of the requirements for the degree of

DOCTOR OF PHILOSOPHY

August 2007

Major Subject: Civil Engineering

MULTISCALE ANALYSIS OF NANOCOMPOSITE AND NANOFIBROUS STRUCTURES

A Dissertation

by

VINU UNNITHAN UNNIKRISHNAN

Submitted to the Office of Graduate Studies of
Texas A&M University
in partial fulfillment of the requirements for the degree of

DOCTOR OF PHILOSOPHY

Approved by:

Chair of Committee,	J. N. Reddy
Committee Members,	Jose M. Roesset
	Luciana R. Barroso
	Xin-Lin Gao
Head of the Department,	David V. Rosowsky

August 2007

Major Subject: Civil Engineering

ABSTRACT

Multiscale Analysis of Nanocomposite

and Nanofibrous Structures. (August 2007)

Vinu Unnithan Unnikrishnan, B. Tech., University of Kerala;

M. S., Indian Institute of Technology, Madras

Chair of Advisory Committee: Dr. J. N. Reddy

The overall goal of the present research is to provide a computationally based methodology to realize the projected extraordinary properties of Carbon Nanotube (CNT)-reinforced composites and polymeric nanofibers for engineering applications. The discovery of carbon nanotubes (CNT) and its derivatives has led to considerable study both experimentally and computationally as carbon based materials are ideally suited for molecular level building blocks for nanoscale systems. Research in nanomechanics is currently focused on the utilization of CNTs as reinforcements in polymer matrices as CNTs have a very high modulus and are extremely light weight.

The nanometer dimension of a CNT and its interaction with a polymer chain requires a study involving the coupling of the length scales. This length scale coupling requires analysis in the molecular and higher order levels. The atomistic interactions of the nanotube are studied using molecular dynamic simulations. The elastic properties of neat nanotube as well as doped nanotube are estimated first. The stability of the nanotube under various conditions is also dealt with in this dissertation.

The changes in the elastic stiffness of a nanotube when it is embedded in a composite system are also considered. This type of a study is very unique as it gives information on the effect of surrounding materials on the core nanotube. Various configurations of nanotubes and nanocomposites are analyzed in this dissertation.

Polymeric nanofibers are an important component in tissue engineering; however, these nanofibers are found to have a complex internal structure. A computational strategy

is developed for the first time in this work, where a combined multiscale approach for the estimation of the elastic properties of nanofibers was carried out. This was achieved by using information from the molecular simulations, micromechanical analysis, and subsequently the continuum chain model, which was developed for rope systems. The continuum chain model is modified using properties of the constituent materials in the mesoscale. The results are found to show excellent correlation with experimental measurements.

Finally, the entire atomistic to mesoscale analysis was coupled into the macroscale by mathematical homogenization techniques. Two-scale mathematical homogenization, called asymptotic expansion homogenization (AEH), was used for the estimation of the overall effective properties of the systems being analyzed. This work is unique for the formulation of spectral/*hp* based higher-order finite element methods with AEH. Various nanocomposite and nanofibrous structures are analyzed using this formulation.

In summary, in this dissertation the mechanical characteristics of nanotube based composite systems and polymeric nanofibrous systems are analyzed by a seamless integration of processes at different scales.

To my parents

ACKNOWLEDGEMENTS

I would like to express my deepest gratitude to Professor J. N. Reddy, my dissertation advisor, for his guidance, support and his confidence in me during the course of my study at Texas A&M University. I am also deeply indebted to him for giving me the opportunity to pursue any research topic of my interest.

I am also grateful to Prof. Jose M. Roesset, Dr. Xin-Lin Gao and Dr. Luciana R. Barroso for serving on my doctoral committee and for their insightful knowledge and keenness in my research issues. I would like to specially acknowledge the help by Dr. Lisa M. Perez, of the Laboratory for Molecular Simulations, Department of Chemistry, Texas A&M University, for the computational and software support and the super computing facility at Texas A&M University. I am also thankful to Prof. Namas Chandra for his initial help on molecular dynamics.

My pursuit in academic studies would not have been possible without the support and help of many people, as goes the Sanskrit teaching "*Matha Pitha Guru Daivam*." I therefore am indebted greatly to my parents for all their support and wisdom.

My teachers have been a constant source of inspiration during my entire life. It would not have been possible but for all the encouragement by Prof. A. Meher Prasad and constant memories and inspiration of the late Prof. C. S. Krishnamoorthy.

I would also like to thank my friend Dr. Santhosh Sathyapal without whose help I would not have been able to embark on this journey. I am also thankful to my brother Mr. Ginu Unnithan who has been a wonderful friend and fellow researcher, and also to my younger brother Mr. Vipin Unnithan. Last but not the least, I would like to thank my wife Mrs. Deepa Mohan for her companionship, support and understanding that helped me immensely during the course of this study.

TABLE OF CONTENTS

CHAPTER Page

CHAPTER Page

LIST OF FIGURES

FIGURE Page

FIGURE Page

FIGURE Page

FIGURE Page

CHAPTER I

INTRODUCTION

A. BACKGROUND

Nanotechnology, the science and technology of precisely controlling the structure of matter at the molecular level, is widely viewed as the most significant technological frontier currently being explored. Nanoparticles, nanotubes, and nanocomposites exhibit extremely high mechanical strength, and they are of great interest to researchers. The perfect formation of the nano units and the ease by which the structural as well as functional units can be manipulated helps in finding exciting applications. For the manipulation of nanoscale systems, understanding of the mechanics involved is necessary. The mechanics in a molecular level are based on the assumption that the atomic interactions are described by means of classical mechanics models. These interactions have to be scaled up spatially as well as temporally for the realization of the cumulative effects. Analysis of various physical processes occurring at various higher scales of interest can be grouped as multiscale analysis. Nanomechanics involves coupling of the mechanics at various length and time scales for understanding the local interactions as well as phenomenological behavior occurring at larger scales.

Carbon based materials are ideally suited for molecular level building blocks for nanoscale systems design, fabrication and application because of its unique metallic, semi conducting and electromechanical properties and yet are extremely lightweight. From an engineering perspective, there has been a tremendous interest in studying CNTs as reinforcements in composites even as replacements to the high strength carbon fibers. With the high axial strength and low weight of the CNT, the resulting composite could be exceptionally light weight with enhanced strength. The computational analysis remains the main focus of this present research in nanocomposites.

This dissertation follows the style of ASME Journal of Biomechanical Engineering.

B. MOTIVATION

From a review of the literature it can be seen that there is a severe lack of comprehensive knowledge in estimating the mechanical properties of nanostructures in the atomistic level and how it affects the properties in the macroscale. Thus, there is need to combine methods from atomistic simulation to macroscale mechanical analysis by seamlessly integrating the transfer of information. This research is aimed at formulating a multiscale computational model that bridges different scales using the classical Molecular Dynamics (MD) model as the atomistic computation tool, the micromechanical methods in the micro scale, and ultimately applying homogenization techniques with higher order numerical methods in the macroscale. The proposed multiscale modeling strategy is developed to provide a better tool in understanding the characteristics that rule the transition from the atomistic scale to the macro scale. Having motivated the use of multiscale methods for the analysis of nanocomposites and polymeric nanofibrous systems, this dissertation undertakes the study of the effect of nanotube on the mechanical properties of a nanocomposite system and estimates the elastic properties of a complex polymeric nanofibrous structure. The properties estimated in the atomistic scale are scaled to the mesoscale and then to the macroscale by the use of a novel homogenization method with higher order finite element method.

The following results included in this dissertation are unique:

1. Estimation of elastic properties of silicon doped nanotubes and based nanocomposites.
2. Estimation of the effect of the surrounding structures on the core nanotube in a nanocomposite and multi-nanotube system.
3. Multiscale analysis and estimation of elastic properties of a polymeric nanofiber taking into consideration the properties in the atomistic scale up to the macroscale.
4. Formulation and use of higher order spectral/*hp* based finite element method for the homogenization of nanostructure by asymptotic finite element method.

C. SCOPE OF THE RESEARCH

Studies on nanostructures have been focused on the different scales of interest at the atomistic and the macroscopic levels. There is a need to develop theoretical formulations and associated computational procedures that take into account the physical processes that occur at different spatial and temporal scales and the coupling between these scales are obtained by sound physical reasoning and theoretical formulations.

The primary objectives of this study are divided into four main categories:

CARBON NANOTUBE BASED NANOSTRUCTURES

- Analysis of CNT structures like single and multiwalled carbon nanotubes, nanoropes, and the effect of spatial arrangement, chirality on the mechanical strength.
- Analysis of substitutional impurity on CNT structures, doping with silicon atoms.
- Analysis of multifunctional CNT structures by functionalization with chemical groups and study the effect on how functionalization modifies the fiber matrix interactions.

CARBON NANOTUBE BASED NANOCOMPOSITES

- Develop sound theoretical formulations for the study of CNT reinforced composites with special emphasis on the mechanical properties.
- Atomistic study using molecular dynamics to establish the properties of CNT-reinforced composites with multifunctional features.
- Analysis of interphase effect on the continuum properties of the composite.

ANALYSIS OF POLYMERIC NANOFIBERS

- Obtain elastic properties of polymeric materials by MD simulations.
- Homogenization of the Shish-Kebab models for multiscale modeling.
- Development of theoretical models to predict mechanical properties by using the proposed "modified Continuous Chain Model" (CCM).
- Study the effect of the size of fibrils and the effect on the tensile strength of the polymeric nanofiber.
- Be able to predict the elastic properties of the nanofiber and compare with experimental methods.

MULTISCALE ANALYSIS OF NANOSTRUCTURES BY HOMOGENIZATION TECHNIQUES

- Develop asymptotic expansion homogenization techniques for coupling mesoscale with the macroscale properties.
- Formulation and development of higher order finite element methods for the analysis of high gradient field problems.
- Application of the developed methods to the analysis of CNT based nanostructures and polymeric nanofibers.

In this dissertation work, novel multiscale modeling strategies are proposed for the analysis of carbon nanotube (CNT) fiber reinforced composite structures with CNTs of various morphologies (orientation, functionalization etc) and chiralities for application as multifunctional nanocomposites. This research provides a strong interlinking from the atomistic scale to the macroscale. With a full-scale mathematical basis, this methodology would be applied to the analysis of CNT reinforced nanocomposite structures and polymeric nanofibers. This research would provide a sound theoretical and computational tool for the analysis and design of an enhanced strength nanocomposite using CNTs and nanofibers.

The dissertation is organized as follows. In Chapter II, the theoretical analysis of CNT structures like single walled nanotube and double walled nanotubes are

presented. The atomistic simulation is carried by molecular dynamic simulation and a brief description is given in this chapter. The analysis of mechanical properties of CNT is also given in this chapter. This chapter also contains a discussion on the effect of doping of CNT structure and the estimation of the mechanical properties along with the discussion on the thermal stability.

Chapter III is concerned with the effect of matrix on the mechanical stiffness of CNTs. Apart from the effect of the surrounding matrix; this chapter also includes a discussion of the effect of functionalization of the nanotube and the effect when the functionalized CNT is embedded in a matrix or within nanoropes. The mechanical property estimation carried out in this chapter is for the core or central nanotube. The mesoscale coupling is also highlighted in this chapter with a micromechanical analysis of the nanocomposite system.

The analysis of polymeric nanofiber is carried out in Chapter IV, where the atomistic properties are estimated using molecular dynamic simulation and the mesoscale properties are estimated using micromechanical methods. The morphological characteristics are taken into consideration in the estimation of the overall elastic properties by considering the effect of the Shish-Kebab model and the use of a modified continuum chain model. This chapter also shows how the results compare with experimental studies in literature.

The mesoscale-macroscale coupling is achieved by using the Asymptotic Expansion Homogenization (AEH) techniques which is discussed in Chapter V. The homogenization of material properties is carried out by coupling with higher order spectral/*hp* finite element methods. This developed spectral based homogenization method is used in the estimation of the macroscale effective properties of nanocomposite systems as well as nanofibrous systems. Finally, in Chapter VI some concluding remarks are made with comments on ongoing and future research.

CHAPTER II

ANALYSIS OF UNDOPED AND DOPED CARBON NANOTUBES

In this chapter the general analysis of neat and doped carbon nanotubes using molecular dynamic simulations is presented. A discussion of different types of carbon nanotubes and the methods of analysis using atomistic simulation is presented. The chapter is organized as follows. In Sections A to C, carbon nanotubes and estimation of its mechanical properties are discussed. The concept of doping with silicon atoms on a CNT is also presented. Sections D and E contain numerical simulations of doped and undoped CNT using molecular dynamics. The chapter concludes with a summary in Section F.

A. INTRODUCTION

Carbon nanotubes are present mainly in three configurations: single-walled carbon nanotubes (SWNT), multiwalled carbon nanotubes (MWNT), and carbon nanotube bundles or ropes (see Figure 2.1). Carbon nanotubes (CNTs) are many orders of magnitude stronger, stiffer, conductive, and lighter than the best available carbon fibers [1-15]. The perfect formation of nano-units and the ease by which the structural as well as functional units can be manipulated helps in finding exciting applications. For the manipulation of nanoscale systems, molecular level study involving interactions in the atomic scale should be analyzed. The simulation of molecular systems is based on the assumption that the atomic interactions are described by means of classical mechanics models [2, 16-20].

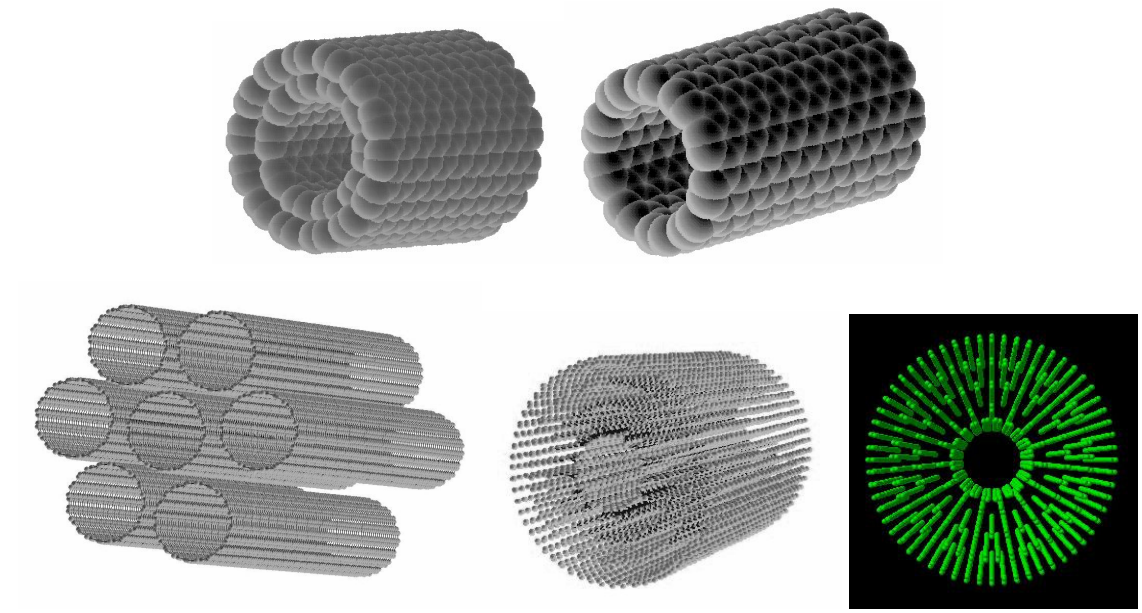

Figure 2.1 Zig-Zag double walled (DWNT) and single walled carbon nanotube (SWNT) nanoropes and nanocomposites

Analysis of CNT reinforced polymer composites (see Figure 2.2) [3, 11, 19] under the application of various forces is the computational problem that is primarily studied. The fiber phase materials, which are of a few orders of nanometers, interact with the surrounding polymer matrix. The primary requirement for the realization of the maximum effective property is that the reinforcements are required to be distributed homogeneously in the matrix and aligned in specific orientations to obtain the desired effective properties in a composite material system. Though the basic principles appear similar to conventional fiber reinforced composites [21], the scale of the conventional fibers (of the order of μm) is quite different from that of CNTs which are in the order of a few nano meters. This disparity in scales brings with it a new set of challenges. To achieve the promise of transferring the exceptional properties of the carbon nanotubes into practical devices, one need to understand how the processes that occur at the nanoscale affect those at macroscales (μm to mm to m). This can only be achieved through multi-scale modeling. This research is mainly focused on the analysis of CNT

and CNT-reinforced composite structures to obtain the macroscale properties by means of an efficient multiscale modeling method.

Silicon doped carbon nanotube (CNT) may find potential multifunctional applications where novel mechanical and electronic properties are desired. Ab-initio analysis of CNT doped with silicon has shown that the resulting structure is stable. However, simulation on the effect of silicon doping on the mechanical properties of the CNT structure, which has not been carried out to-date, is studied in this chapter. Analysis of silicon doped carbon nanotube for the estimation of elastic properties is also presented.

B. IDENTIFICATION AND PROBLEM DESCRIPTION

CNT reinforced polymer composites [3, 11, 19] under the application of various forces is the physical computational domain. To realize this, let us consider a plate structure acted upon by external forces and moments. This structure is reinforced with CNT fibers of finite length and of various chiralities, functionalization, spatial orientation with respect to the structural axis and other mechanical, chemical and thermal properties (see Figure 2.2). The fiber phase materials, which are of a few orders of nanometers, interact with the surrounding polymer matrix. The problem is very unique from a conventional fiber composite material in the sense that the fiber phase interacts with the matrix phase through molecular interactions. The material/mechanical properties of the participating phases in a conventional composite material analysis is widely studied and accepted. This is, however, not the case with the nanometric sized fibers, as the material properties are still being debated and even weak molecular interactions is found to alter the overall properties drastically [2, 13].

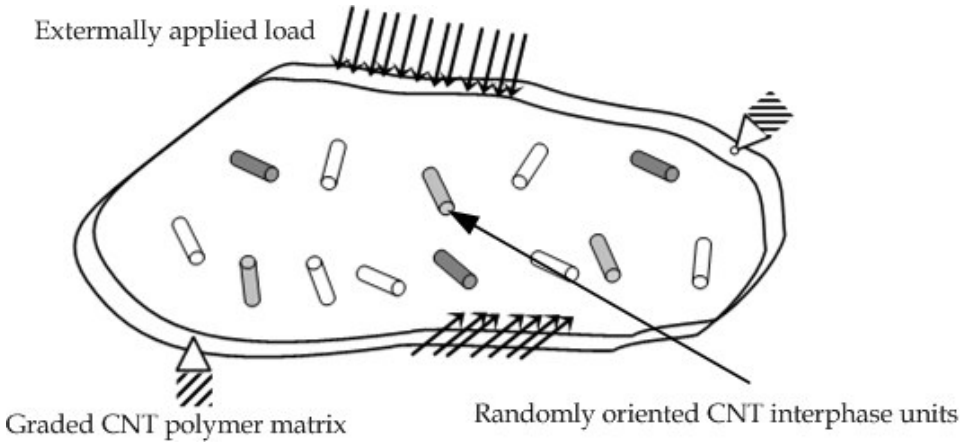

Figure 2.2 Nanotube reinforced polymer nanocomposite with graded dispersion of CNT

Research in the determination of overall properties of the composite was carried out earlier with a bottom to top approach. Of late, greater focus is on the accuracy in the prediction of lower order properties and hierarchical transfer of the material properties to the larger scale. In the previous works on multiscale modeling, the response in the atomistic level was transferred to the mesoscale or microscale by the explicit use of equivalence of the response variables [22]. This equivalency of the displacement or the stress field has a major drawback: the loss of essential information important in the atomistic scale is either not considered or averaged out in the higher scales [10]. Another multiscaling method involves the use of micromechanical schemes to model the mesolevel and subsequently use continuum formulation for scaling the domain of interest. The obvious drawback of such an approach is that the local variations in morphology and structure are not considered or do not translate to the macroscopic scale. Keeping these models in mind, a radical approach in the modeling and analysis of CNT filled polymer matrix composites is proposed. This model draws inspiration from various attempts in multiscale modeling thus far and improves upon them wherever necessary, such that a two-way coupling of information is achieved with a strong bottom to top coupling and a weak top to bottom coupling (see Figure 2.3).

The strong bottom-to-top approach analysis can be carried out by the use of explicit modeling of various atomistic configurations and simulating each of these configurations and subsequently relaying information to the higher scales. The various scales involved in a nanocomposite analysis are: atomistic level which spans a few orders of nanometers, mesoscale which spans a couple of μm to ~10^{-7} and finally the microlevel which spans a few μm to a few millimeters.

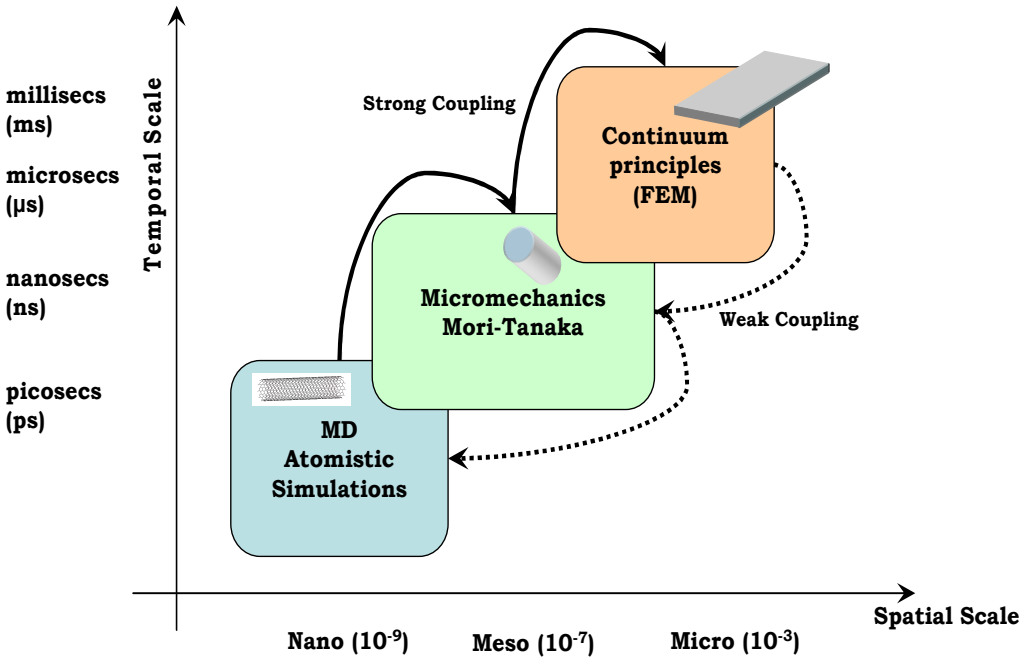

Figure 2.3 Scaling from atomistic to continuum by two-way coupling

In the atomistic level the interactions exists in the molecular level and are modeled using pair potentials to respond to externally applied disturbance. The response variables in the lower scales are passed on to the next higher scale, seeking change in the material properties. This method is justified, since the material response at an atomistic scale is highly nonlinear [18] and any change in the local environment has been found to vary the ensemble properties dramatically [2]. However, previous works in this area have not been able to capture the local variations in a global sense, which is achieved in this work. For example, changes in the chirality, orientations of the

fiber phase with the global orientation and chemical functionalization are found to change the atomistic ensemble properties. Thus these properties are captured and passed on to the higher scales which subsequently affect the macroscopic response.

Once the atomistic material properties have been determined for various morphologies of the fiber phase, the volume average over the ensemble would give the averaged material properties [22, 23]. The volume averaged properties are subsequently scaled to the mesolevel by applying the Eshelby's equivalent eigenstrain method and Mori-Tanaka formulation to obtain the effective material response in the mesolevel (see Figure 2.4). A weak coupling can be achieved by this method, but this is a definite improvement over conventional multiscale methods. The advantage of this coupling method is the ultimate realization of an analysis and design philosophy based on the macroscopic structural behavior, by predicting and enhancing the micro structural level.

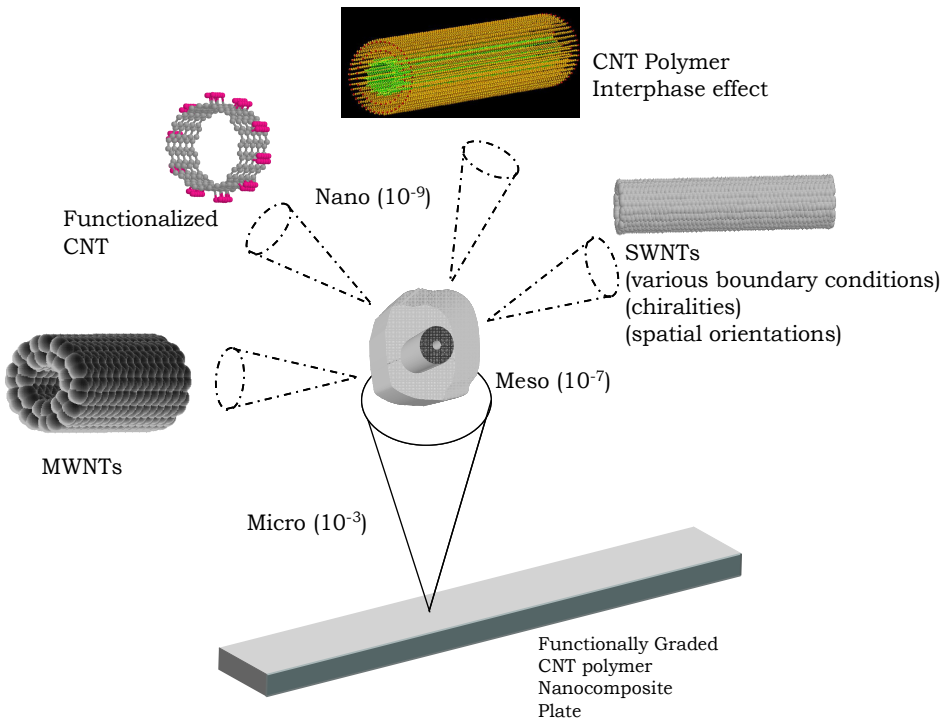

Figure 2.4 Top-down model of various spatial domains

C. CARBON NANOTUBES

Single-walled nanotubes are idealized as being formed by the folding of a graphene sheet into a hollow cylinder, which is composed of hexagonal carbon ring units referred to as graphene units [1, 18, 20, 24] (see Figure 2.5a). Each of the carbon atoms forming the tubules has three nearest neighboring bonds. In a fully relaxed structure, the angles between these bonds depend on the radius of the cylinder as well as on their orientation [1, 18]. All the three angles approach 120^o (perfect graphitic plane) with increasing cylindrical radius.

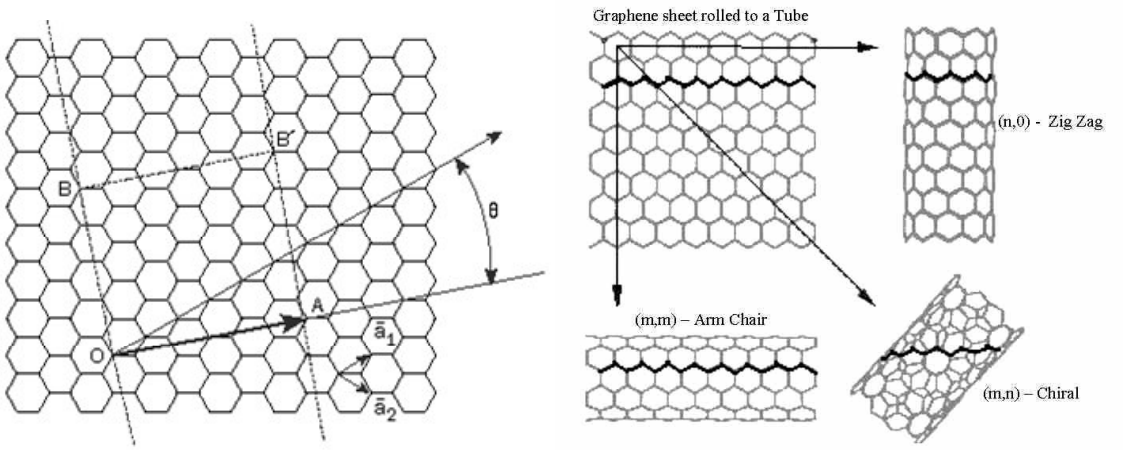

(a) (b)

Figure 2.5 (a) Graphene sheet representation (b) Type of CNT : Chiral, Zig-Zag and Armchair

The fundamental CNT structure can be classified into three categories: Armchair, Zig-Zag, and Chiral, in terms of their helicity. One of the advantages of atomistic simulation is the ease with which various configurations can be studied (see Figure 2.6a, b). The experimental investigation of CNT is extremely difficult as the capability is limited by the availability of high quality defect free CNTs of sufficient length and measurement of nanoscale structures [25]. Studies in the mechanical, electrical and thermal behavior of CNTs were focused primarily on the use of empirical potentials using Molecular Dynamics (MD) and continuum models using the elasticity theory [4, 6, 14, 15, 18, 19, 22, 26]. Despite the immense success of MD simulations in atomistic

scale, the computational adaptation to model macroscopic problems based on CNT's are not completely established. The application of continuum mechanics principles into nanomechanics demands the bridging of the two or more scales of interest. From a computational perspective, these techniques should be able to efficiently represent the processes in a fine scale and provide solutions to the analysis in the macroscale.

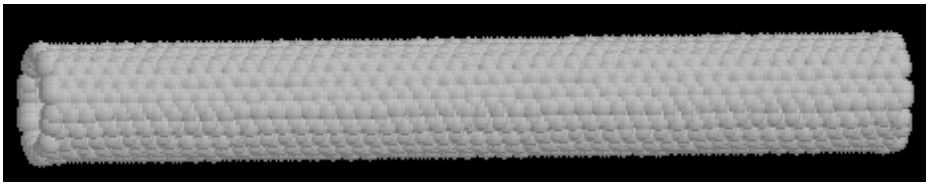

(a)

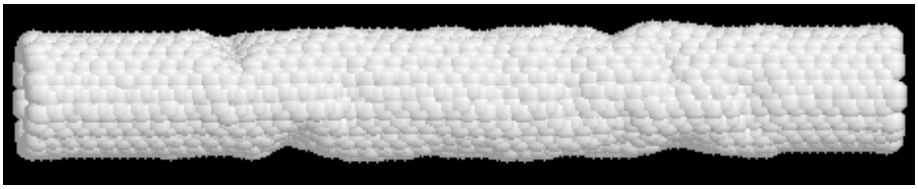

(b)

Figure 2.6 (a) CNT under elastic axial tension (b) CNT under elastic axial compression

D. MOLECULAR DYNAMIC SIMULATION

A completely quantum mechanical simulation is the ultimate analysis possible for an atomistic system. These are called the ab-initio methods and are either semi-empirical or fully quantum mechanical. The Density Functional Theory (DFT) and the Tight Binding methods are some of the ab-initio methods available in literature. These types of analysis are extremely time consuming and are only capable of simulating atomistic ensembles which consists of very few atoms. However, for a realistic estimation of the properties in the macroscale, simulation in the atomistic scale should consist of adequate number of atomistic entities for a longer period of simulation times.

There are numerous methods of analysis large atomistic systems and are based on empirical potentials to represent the interaction between atoms. Molecular Dynamics has been a very popular tool for the simulation of such atomistic structures for the determination of mechanical, thermal and other properties of interest [2, 8, 9, 20, 27]. Embedded atom method (EAM) which is also based on empirical potentials are found to be extremely useful for the investigation of structure, thermodynamic and atomic transport properties. The EAM is based on the concept of pseudopotential theory, where the atomic interactions are represented as a sum of each pairwise interaction and are dependant on the effective density around an atom [28].

The starting point of a molecular dynamics simulation is the non-relativistic quantum mechanical time dependant Schrödinger equation. The thermodynamic state characterized by the fixed number of atoms, volume and temperature called the Canonical Ensemble [27] forms the basis of the molecular dynamic simulation in this work. The simulated system and the heat bath couple to form a composite system. The conservation of the energy still holds in the composite system but the total energy of the simulated system fluctuates. The motion of the particles in the system is governed by the Hamiltonian which is a function of the position and momentum of the particles, and the Hamiltonian equations of motion. The Hamiltonian representing the total energy of an isolated system is given as the sum of the potential, kinetic energy terms and thermodynamic terms

$$\mathrm{H}(r, p, s, p_s) = \sum_{i=1}^{N} \frac{p_i^2}{2m_i s^2} + U(r) + \frac{1}{2Q} p_s^2 + N_d k_B T \ln s \qquad (2.1)$$

where $U(r)$ is the potential energy from intermolecular interactions as a function of the spatial ordinate r, $\sum_{i=1}^{N} \frac{p_i^2}{2m_i s^2}$ represents the kinetic energy which depends upon the momentum p of the particle i with mass m_i. s and p_s are the additional "thermostatting" variable and its momentum respectively and are introduced to control the "thermodynamic temperature" T, Q is the thermal inertia, N_d is the number of

degrees of freedom, k_B is the Boltzmann's constant. For an isolated Number-Volume-Energy (NVE) Ensemble, the Hamiltonian is given by

$$\mathrm{H}(r,p)=\frac{1}{2m}\sum_i p_i^2+U(r) \tag{2.2}$$

Using the time and spatial derivative of the Hamiltonian [29]

$$\frac{d\mathrm{H}}{dt}=\frac{1}{m}\sum_i p_i.\dot{p}_i+\sum_i\frac{\partial U}{\partial r_i}.\dot{r}_i\,;\ \frac{d\mathrm{H}}{dr_i}=\frac{\partial U}{\partial r_i} \tag{2.3}$$

the equations of motion ($F_i=m_i\ddot{r}_i$), of a particle i of an NVE system can be obtained.

$$\frac{d\mathrm{H}}{dr_i}=-\dot{p}_i=-m\ddot{r}_i\,;\ \frac{d\mathrm{H}}{dp_i}=\frac{p_i}{m}=\dot{r}_i \tag{2.4}$$

$$F_i=-\frac{\partial\mathrm{H}}{\partial r_i}=-\frac{\partial U}{\partial r_i} \tag{2.5}$$

Similarly, the equations of motion for the additional degrees of freedom in the NVT system can also be obtained (see Eqns 1-6 in Ref. [27]). The MD computational scheme in this chapter has been successfully used by various researchers to estimate the elastic properties of CNTs [2, 19, 30, 31]. After each straining process the ensemble is stabilized and the control temperature is maintained. The mechanical straining process imparts energy to the isolated system; the assumption is that the difference between the strained equilibrium energy and the unstrained equilibrium energy is the mechanical strain energy and this contributes to the mechanical stiffness of the CNT [10].

The reliability of a molecular dynamics simulation depends on the type of potential functions. In general, the total potential of the CNT structure is given by the sum of valence bond energies and nonbonding interactions

$$U^{tot}=\sum_j\sum_{j>i}\left[V_{ij}^{B}+V_{ij}^{NB}\right] \tag{2.6}$$

where V_{ij}^{B} is the potential energy due to bonding and V_{ij}^{NB} is the potential energy due to nonbonding interactions. Tersoff-Brenner empirical bond order potentials are found to

be excellent for the simulation of carbon based materials [2, 8, 10, 20, 27, 30, 32]. These potentials are capable of describing the changes in the bonding between atoms but lacks in describing the long range interactions [17]. The binding energy of an atomic many-body system can be computed in terms of pair-wise nearest-neighbor interactions modified by the local atomic environment. In this dissertation, the Tersoff-Brenner potential for the simulation of C–C interactions in nanotubes has been used, and the total potential energy of an atomic ensemble is given by

$$U = \sum_{j} \sum_{j>i} f_c \left[a_{ij} E_r(r_{ij}) - b_{ij} E_a(r_{ij}) \right] \tag{2.7}$$

where $r_{ij} = r_i - r_j$, $E_r(r_{ij}) = A_{ij} e^{-\lambda_{ij} r_{ij}}$ represents the repulsive pair-wise potential, such as the core- core interactions, of the potential function, and $E_a(r_{ij}) = B_{ij} e^{-\mu_{ij} r_{ij}}$ represents the attractive part of the potential function that represents the bonding due to the valence electrons. The parameters of the Tersoff-Brenner potential for carbon atoms have been taken from Brenner [32] which are widely used in the MD simulation of CNT based structures [2, 8, 10, 27, 31-33].

For a multicomponent system consisting of more than one species of atoms, the choice of potential functions becomes even more taxing. According to Tersoff [34], the potentials for a multicomponent system can be generalized by combining the parameters obtained for individual species of elements. In such a method, the parameters for the individual species are determined independently by curve fitting to the original elemental data and are generalized for multicomponent systems [34]. The parameters for Si atoms were taken from Tersoff (see Table 1 in Ref. [34]) and are combined with those of Carbon atoms as shown below.

$$\lambda_{ij} = (\lambda_i + \lambda_j)/2; \qquad \mu_{ij} = (\mu_i + \mu_j)/2 \tag{2.8}$$

$$A_{ij} = (A_i A_j)^{1/2}; \quad B_{ij} = (B_i B_j)^{1/2}; \quad R_{ij} = (R_i R_j)^{1/2}; \quad S_{ij} = (S_i S_j)^{1/2} \tag{2.9}$$

where, i and j represents the atoms in the system and X_{ij} represents the various parameters $\{\lambda, \mu, A, B, R, S\}$ that appear in the Tersoff equation for a bond ij. The accuracy of such a combination of potential parameters for multicomponent systems was guaranteed as was shown by Tersoff [34].

The force of attraction and repulsion (F_α) experienced by each atomic entity is obtained from the gradient of the potential field (α represents the direction vectors)

$$F_\alpha = -\frac{\partial U^{tot}}{\partial r_\alpha}. \tag{2.10}$$

The molecular dynamic time stepping is carried out by the standard veocity-verlet algorithm and the time step is normally in the range of a few femtoseconds [8, 12, 16, 31]. At the beginning of each simulation time step, updated velocities $v_i(t)$ are calculated for each particle using

$$v_i(t + \Delta t/2) = v_i(t - \Delta t/2) + \frac{f_i(t)}{m_i}\Delta t \tag{2.11}$$

where t is the time, Δt is the time step of the molecular dynamics simulation, $f_i(t)$ is the total force acting on the particle i given by

$$f_i(t + \Delta t) = \frac{\partial \Phi}{\partial r_i(t + \Delta t)} \tag{2.12}$$

and m_i is the mass of the particle. The coordinates of the particles $r_i(t)$ are updated from the velocities using

$$r_i(t + \Delta t) = r_i(t) + v_i(t + \Delta t/2)\Delta t \tag{2.13}$$

1. TERSOFF-BRENNER POTENTIAL

One of the best potentials which are capable of catering to a whole range of atomic entities is the Tersoff type of Tersoff-Brenner potentials [2, 7, 10, 27, 31-33]. In Tersoff type of potentials the binding energy of an atomic many-body system can be computed in terms of pair-wise nearest-neighbor interactions modified by the local atomic

environment. Tersoff employed this prescription to obtain the binding energy. The Tersoff-Brenner potentials are employed for the simulation of C-C interactions [12, 35]. The total potential energy for carbon-carbon interactions can be given as

$$E_{tot} = \sum_{i} \sum_{j(<i)} \left\{ V_R(r_{ij}) - B_{ij}^{*} V_A(r_{ij}) \right\} \tag{2.14}$$

where, E_{tot} is the total potential energy, $V_A(r_{ij})$ and $V_R(r_{ij})$ are the pair additive repulsive and attractive potential function terms which are dependant on the length of the bond (r_{ij}) between atoms i and j

$$V_A(r_{ij}) = f(r) \frac{D_e}{S-1} \exp\{-\beta\sqrt{2S}(r - R_e)\} \tag{2.15}$$

$$V_R(r_{ij}) = f(r) \frac{D_e S}{S-1} \exp\{-\beta\sqrt{2S}(r - R_e)\} \tag{2.16}$$

where, B_{ij}^{*} represents the many body coupling between the bond from atom i to atom j and the local environment of the atom i

$$B_{ij}^{*} = \frac{B_{ij} + B_{ji}}{2} \tag{2.17}$$

$$B_{ij} = \left[1 + \sum_{k(\neq i,j)} \{ G_c(\theta_{ijk}) f(r_{ik}) \} \right]^{-\delta}, \tag{2.18}$$

and $G_c(\theta_{ijk})$ is a function of the angle between bond $i-j$ and $i-k$, given by

$$G_c(\theta_{ijk}) = a_0 \left(1 + \frac{c_0^2}{d_0^2} - \frac{c_0^2}{d_0^2 + \left(1 + \cos\theta_{ijk}\right)^2} \right) \tag{2.19}$$

and

$$f(r) = \begin{cases} 1 & r < R_1 \\ \frac{1}{2} + \frac{1}{2}\cos\left\{ \frac{\pi(r - R_1)}{(R_2 - R_1)} \right\} & R_1 \le r \le R_2 \\ 0 & r < R_2 \end{cases}, \tag{2.20}$$

is the cut-off function. The cut-off function introduces a significant increase in the interatomic force near the bond breaking length [32, 36].

2. NUMERICAL SIMULATION PROCEDURE

The procedure employed for the estimation of the elastic modulus of doped, undoped nanotubes and for various nanotubes configurations (the same procedure is used for analysis in Chapter II) in this work is described below. The minimum energy configuration of the CNT is determined using the minimization of the total potential energy (PE) at 0 K using an NVE procedure. The CNT is minimized for each temperature increments (from 0 K) and the minimized energy at 3K is taken as the minimum PE of the CNT. Increment in displacement is applied to the relaxed structure and is allowed to equilibrate over a number of time steps. The straining process (see Figure 2.7) induces changes in the force experienced by each atom and determines the overall stiffness of the structure. This force is used in calculating the updated position of the atoms by the Velocity-Verlet time integration scheme [12]. Any change in the total potential energy is the strain energy induced by the applied stress or strain. The CNT is strained at a constant rate to calculate the strain energy of deformation by minimizing the total potential energy at each increment and the difference in the PE gives the strain energy due to deformation [2, 10, 12, 13, 24, 31, 37].

In a composite structure where the CNTs are dispersed in a polymer matrix, the orientations and morphological characteristics like diameter, length and chirality varies. These variations of the nanodimensional quantities results as variations in the macroscopic properties of the composite. The characteristics observed because of these morphological features of the CNT are different since the Tersoff-Brenner potential is anhormonic or non-isotropic in compression and tension [32]. Recent studies by Sears and Batra [10], also emphasises the nonsymmetry of the energy envelope in tension and compression [12, 13]: therefore, elastic tension and compression simulations of the CNT are carried out in this work (see Figures 2.8 A & B). The elastic property of the CNT obtained in our analysis matches closely with many of the theoretical [10, 27, 33] and experimental methods [14, 25, 38] and is shown in figure 2.9. Figure 2.6 shows the final configuration of a CNT subjected to tensile and compressive loading during the MD run.

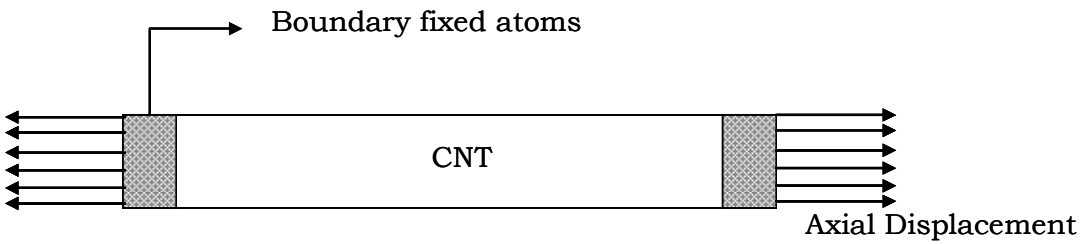

Figure 2.7 Applied boundary conditions on CNT fibers

For the analysis of silicon doped CNT, randomly selected carbon atoms of the equilibrated CNT are replaced by silicon atoms. The doped CNT structure is subsequently allowed to undergo energy minimization and is followed by mechanical straining by incremental displacement applied to the doped CNT as was carried out for the undoped CNT. On minimization of the doped CNT over a series of temperature increments, it is observed that the silicon atoms settle to a minimum position above the tubular structure, therefore having fewer interactions with the surrounding carbon atoms. This phenomenon was also observed by Baierle et al. [39] and is attributed to the weak bonding between the Carbon and Silicon atoms.

The application of any thermostat in an MD simulation should be carried out before the straining process and the elastic properties are extracted at the desired temperatures. In the "energy approach", the elastic constants is obtained directly from the second derivative of the potential energy [4, 10] with respect to the change in the spatial distance for doped and undoped [3, 12, 31] CNT. By this method, the use of an intermediate stress form or called the atomistic virial stress [2, 16], which contains the velocity term as used in some of the earlier works [2, 20, 31] can be avoided. The total potential energy due to the strain, the elastic strain energy can be expanded as a Taylor series for small displacements i.e. the initial position is represented by the equillibrium position. The components $C_{\alpha\beta\gamma\delta}$ of the elastic moduli tensor can be written as

$$C_{\alpha\beta\gamma\delta} = \frac{1}{2N\Omega_a}\sum_{j\neq i}\left[\frac{1}{r_{ij}^2}\left(\frac{d^2U}{dr_{ij}^2} - \frac{1}{r_{ij}}\frac{dU}{dr_{ij}}\right)a_{ij}^{\alpha}a_{ij}^{\beta}a_{ij}^{\gamma}a_{ij}^{\delta} + \delta_{\beta\delta}\underbrace{\frac{1}{r_{ij}}\frac{dU}{dr_{ij}}a_{ij}^{\alpha}a_{ij}^{\gamma}}_{A_{\alpha\gamma}=0}\right] \tag{2.21}$$

where $U = U(r_{ij})$ is the potential energy as a function of the interatomic distance r_{ij}; $A_{\alpha\gamma}$ is the internal stress tensor, and at equillibrium is equal to zero; Ω_a is the average volume of an atom and N is the number of atoms; $\delta_{\alpha\beta}$ is the Dirac-Delta function and $\alpha, \beta, \gamma, \delta$ are the spatial dimensions. a_{ij} is the undeformed value of r_{ij}, $u_{ij} = r_{ij} - a_{ij}$, and $u_{ij}^{\beta} = a_{ij}^{\alpha}\varepsilon_{\alpha\beta}$, $\varepsilon_{\alpha\beta}$ is the homogenous infintesimal strain tensor applied between atoms i and j. The force calculated during an MD dynamic time step is used in calculating the updated position of the atoms and is carried out by the Velocity-Verlet time integration scheme [12, 13].

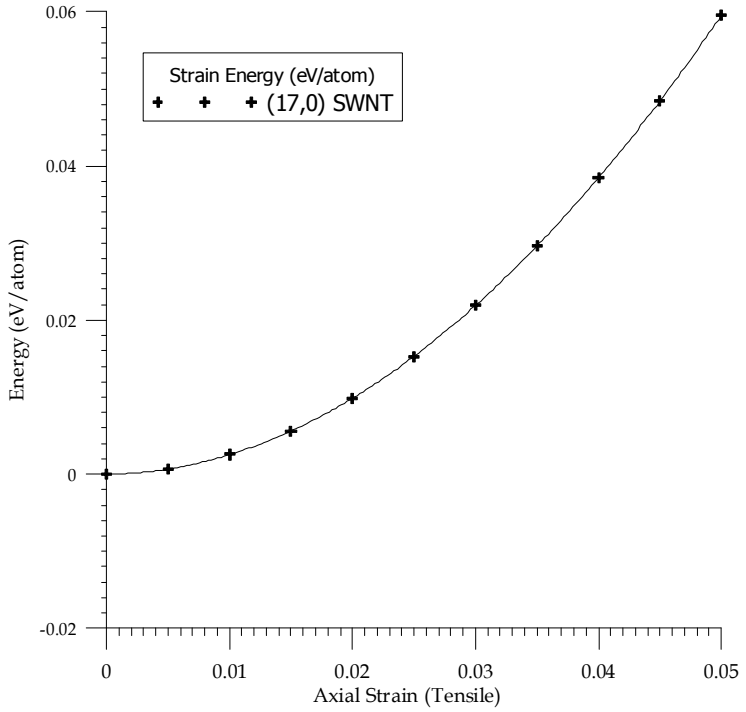

Figure 2.8 (A) Strain energy of (17,0) SWNT in axial tension

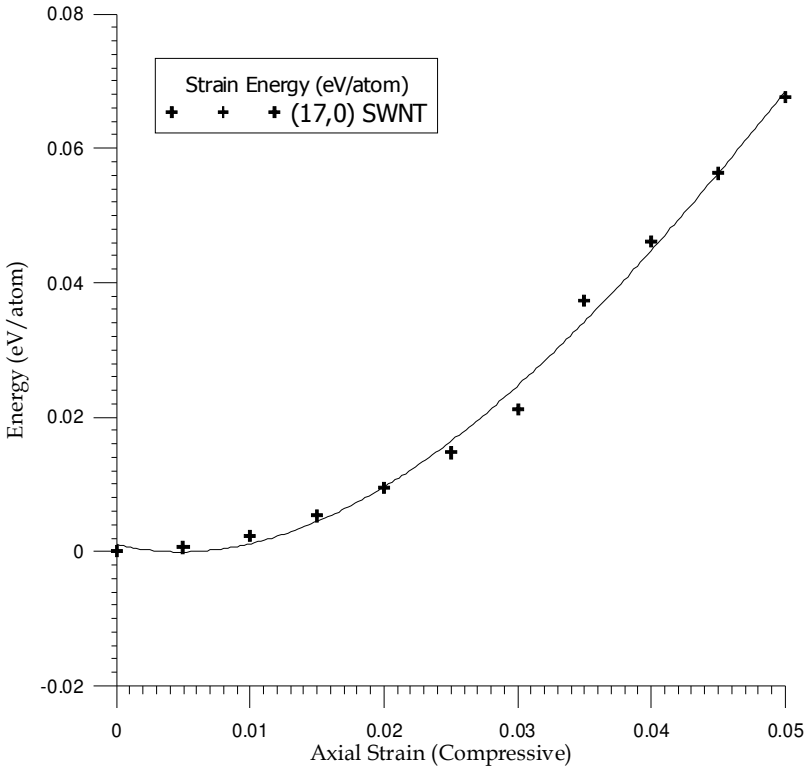

Figure 2.8 (B) Strain energy of (17,0) SWNT in axial compression

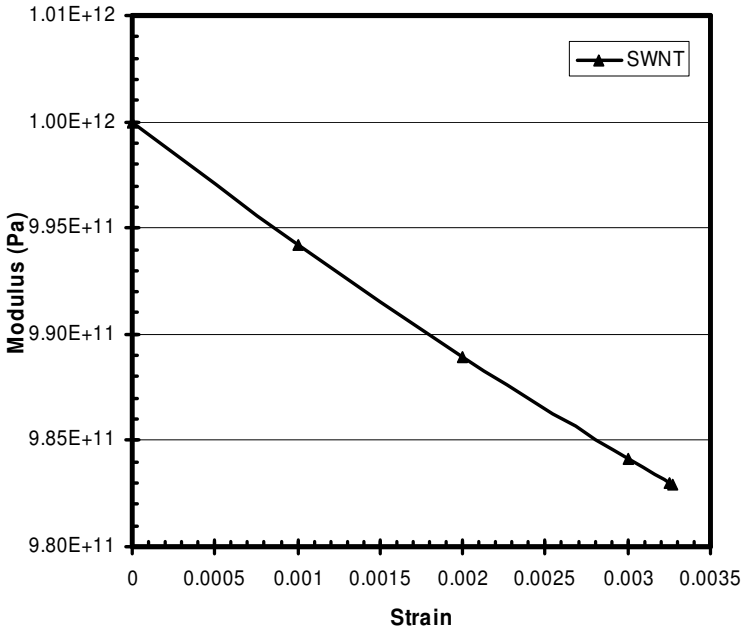

Figure 2.9 Variation of elastic modulus of CNT with strain applied

In this nanometer scale, material exists in atomic lattices and the elastic properties of this atomic system are obtained as an equivalent continuum (EC) method [22, 40]. One of the fundamental quantities that directly affect the elastic modulus is the physical dimension of the atomistic structure. Estimating the elastic property is a homogenization process, where the average potential energy is obtained from the total interacting atoms. The length, diameter and the thickness of the CNT are the fundamental quantities of interest here. It is assumed in earlier works in the mechanical simulation of elastic properties of nanotubes, that the tube thickness is equal to the interplanar spacing of graphite[4, 20]. However, recent research by Vodenitcharova and Zhang [41], and indirectly by Sears and Batra [10] has shown that the estimated thickness of the CNT (0.617 Å) is smaller than the interplanar spacing of graphite. This is one of the main reasons for the disparity in the range of the elastic properties estimated by various researchers. Continuum mechanics principles used for the estimation of the effective thickness cannot be strictly applied to atomistic systems. It should be obtained from chemical analysis or ab-initio studies. The thickness of the CNT is still an unsettled question and, therefore, the currently accepted/widely used thickness of the CNT (3.4Å) is used. It should also be emphasized that this constant, scales the estimated elastic modulus linearly. If a properly accepted thickness different from the currently used value is determined, the new modulus of the CNT can also be scaled accordingly. Also, note that the emphasis is on highlighting the characteristics of doping of a CNT by Silicon atoms and its effect on the elastic modulus.

E. SILICON-DOPED CNT DISCUSSION AND NUMERICAL ANALYSIS

Poor solubility and tendency to aggregate as bundles is one the main hindrance to the application of CNT in composites. In a CNT reinforced nanocomposite the load transferring properties can be increased by chemical functionalization [7, 8, 31]. The same effect can also be observed by doping or adding substitutional impurity: i.e. replacing the atom in a CNT chain by another atom. However, care has to be taken so as

not to disturb the tubular structure of the CNT necessitating very low orders of doping. With a low percentage of doping in a finite length CNT, the overall structural characteristics are found to change [39, 42-46]. CNT having some of the Carbon atoms replaced by Silicon atoms is a new and exciting area in nanotechnology. This doping of CNT, which broadly comes under functionalization of CNT holds the key for future applications of CNT. Most of the earlier studies have been concentrated on the electronic, mechanical and thermal stability and estimation of formation energy rather than on the structural properties of the CNT. The effect of CNT and the mechanical behavior due to the low order Silicon doping of the CNT is studied in this chapter.

The study of silicon substitutional impurities in SWNTs was first carried out by Baierle et al. The research carried out by this group is by far the best available literature in this area [39, 42-45]. The use of silicon as an impurity was chosen based on the fact that due to the different sizes of the Silicon and the Carbon atoms and the difference in the hybridization, an electronic hole would be formed at the doping location which leads to changes in the semiconductor properties of the nanotube. According to Baierle et al. [39] the electron density around the Silicon impurity changes thereby altering the chemical properties. This has motivated the present study on estimating the mechanical properties of Silicon doped CNT. Current research in nanotechnology is aimed at finding multifunctional applications of carbon nanotube based structures. Apart from the desired electrical/electronic properties the silicon doped CNT would also have to act conjunctionally as a mechanical structure. Since the doping with an isovalent impurity in CNT is relatively new [39, 42-44], this work is novel for the study of the mechanical properties of Si-doped Single walled CNT (see Figure 2.10). The variation of the stiffness of the doped CNT is studied for various low fractions of Silicon doping at a temperature of 3K. The stability of the doped CNT is an extremely important factor for potential application in real life situation and the effect of temperature on the stability is also discussed in this chapter.

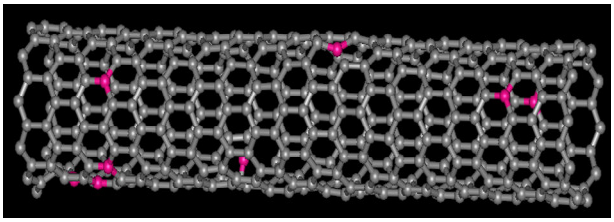

Figure 2.10 Silicon doped SWNT

Molecular Dynamic simulations of CNT of finite length using Tersoff-Brenner potential were carried out for a Zig-Zag (17,0) CNT (408 C atoms) at 3K with periodic boundary conditions. To exclude the boundary effect the atoms of the CNT for about one diameter length from the edge are restrained (see Figure 2.7) [2, 10, 31]. The second derivative of the strain energy profile obtained from the simulation gives the elastic modulus. From 0 K the temperature of the equilibrated CNT is slowly raised to 3 K over a sequence of temperature increments. The equilibrium position at 3 K is taken as the ground potential energy state. Atoms of the CNT are replaced randomly with Silicon atoms and are further allowed to equilibrate and the temperature is slowly raised to 3K. The Silicon atom in the relaxed configuration undergoes radially outward local distortion as reported by Baierle et al. [39]. The Silicon atoms in the CNT settle to a stable position above the CNT tubular structure. This is due to the weak bonding between the Carbon and Silicon atoms. The doped Si atoms have very low interactions with the surrounding carbon atoms as seen in Figure 2.11 [39].

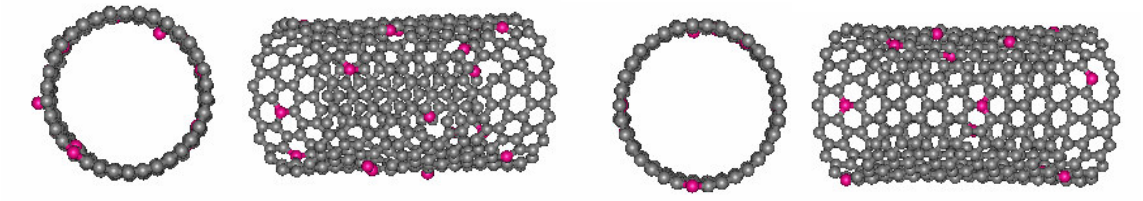

(a) (b)

Figure 2.11 Equilibrium configuration of (a) 4% and (b) 3% silicon doped CNT

The CNT units are strained at a constant rate to a maximum of 3% strain. The potential energy is determined at the end of each increment as shown in Figure 2.12a

for tension and Figure 2.12b for compression. The compressive strain applied is considerably less to cause buckling in the CNT. The elastic modulus for the tensile as well as compressive deformation is obtained from the variation of the potential energy with respect to the applied strain. It is observed that the strength of the silicon doped CNT changes with variation in the numbers of silicon doping (see Figure 2.13a, b) and the structure becomes unstable at larger doping percentages and temperatures. Even at low doping levels the CNT structure starts to become unstable at large strains and therefore the allowable strain is limited, to obtain a suitable estimate of the elastic properties. This is also due to the difference in bonding between the Si-C atoms in the CNT which is different from the strong C-C bonding. Also, the silicon atom which is smaller compared to the carbon atoms, settles to the surface of the CNT under equilibrium conditions. The silicon atom experiences weak interaction forces and are forced out of the tubular frame as the simulation proceeds. The elastic modulus of the Zig-Zag CNT falls within a range of 0.90-0.95 TPa for tensile and compressive modulus for Zig-Zag CNT which is in good agreement with published results [4, 9, 10, 24, 47] and the modulus of the doped CNT varies within a larger range of 0.15 – 0.16 TPa with change in the number of doping atoms (see Figure 13a, b) in tension and within 0.15 – 0.19 TPa for compressive modulus for 2 and 3 doped Si atoms in the CNT structure. The elastic modulus for a larger doping of 4 and 5 atoms further increases marginally for tension strain (0.32-0.5 TPa) while it increases considerably (1.16-1.05 TPa) for compressive strain. This variation in the modulus can be attributed to the low interaction of the C-Si bond strength which becomes pronounced during tensile loading and the repulsive effect between these atoms increases the modulus in compression. Another factor that is important is the random nature of the doping location.

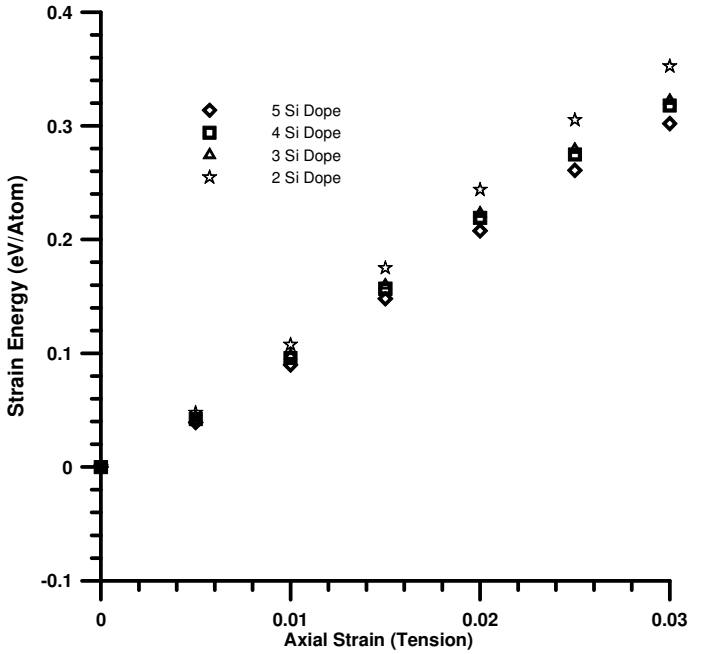

(a)

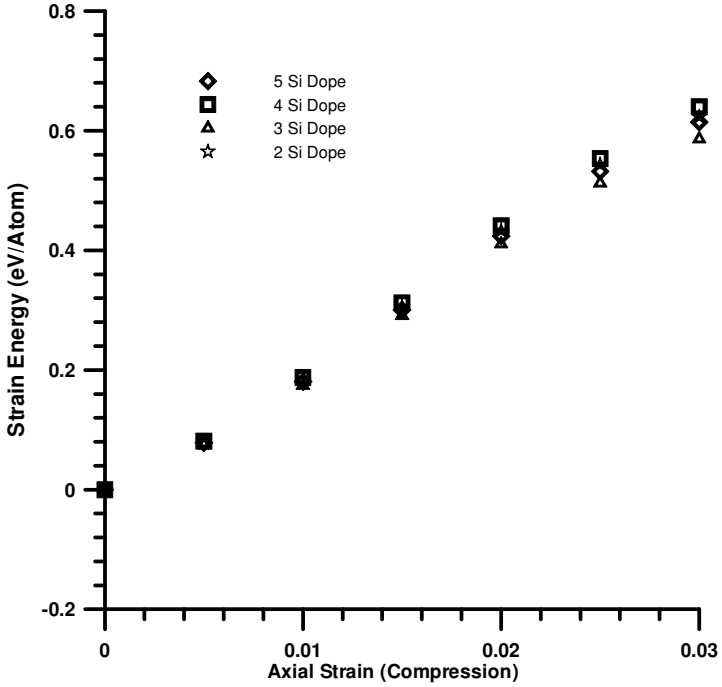

(b)

Figure 2.12 Strain energy of doped and undoped (17,0) SWNT in axial (a) tension and (b) compression (modified from [12])

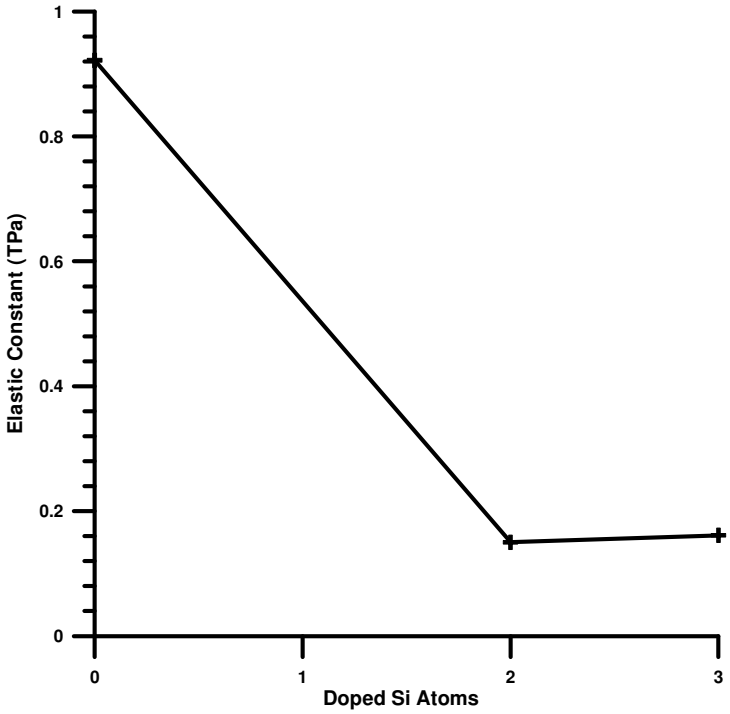

(a)

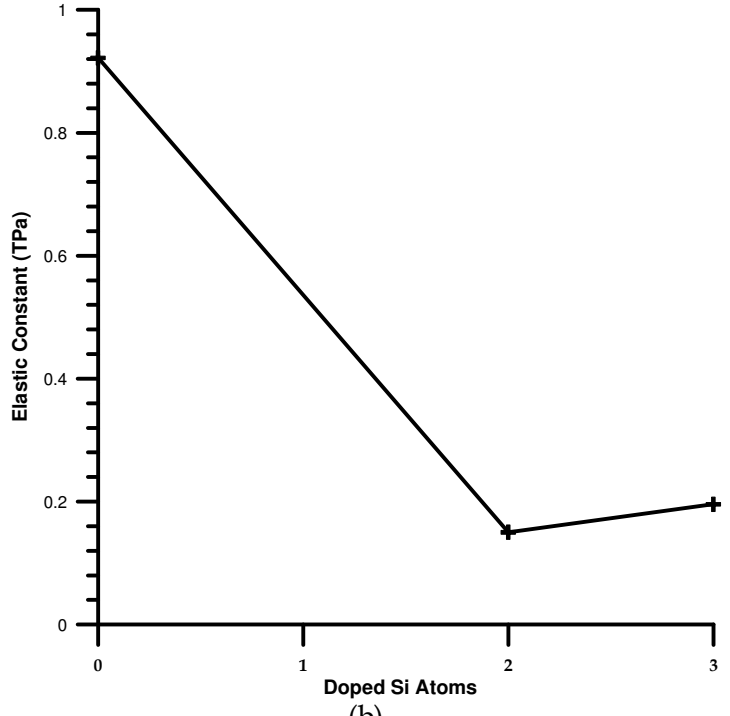

(b)

Figure 2.13 Modulus of doped and undoped (17,0) Zig-Zag SWNT (a) in tension (b) in compression (modified from [12])

F. CONCLUSIONS

In this chapter, the mechanical analyses by MD simulations were carried out with the estimation of the elastic properties of single walled nanotubes. These simulations were carried out using Tersoff-Brenner potential for isothermal strain conditions and the elastic modulus was obtained by the energy method. The estimated values were found to conform to the various published works in literature. Specialized CNTs can find significant multifunctional applications where novel mechanical and electronic properties are desired. Silicon as an impurity in CNT is found to form electronic holes leading to semiconductor properties in the resulting CNT. In the second part of this chapter, the analysis of Silicon doped CNT to estimate the elastic properties have been presented and some of the significant conclusions of this were enumerated. The doped CNT was found to be unstable at higher doping percentages and test temperature. Silicon atoms were found to attain an equilibrium position above the tubular structure of the CNT which had also been verified by earlier ab-initio studies. This instability was attributed to the low interaction with the surrounding Carbon atoms.

CHAPTER III

MECHANICS OF THE CORE NANOTUBE IN NANOCOMPOSITES, NANOROPES AND FUNCTIONALIZED NANOTUBE SYSTEMS

In this chapter, the properties of the central CNT when a functionalized CNT or other CNT structures are embedded in a matrix are studied. Functionalized involves the attachment of chains of foreign species on the nanotube surface to enhance the desired properties [25, 48]. This chapter also presents the effect of chemical functionalization on the stiffness of CNTs on the tubule axis along with matrix embedding. The nanometer dimension of a CNT and its interaction with a polymer chain requires a study involving the coupling of various length scales. There have been many attempts in predicting the overall bulk properties of such nanocomposites. These studies were based upon idealizations applicable only in a continuum framework. The investigation of mechanical behavior of nanostructure materials is carried out using Molecular Dynamics (MD) simulations and this interaction is subsequently idealized into an Equivalent-Continuum (EC) model. The interaction of the molecules of the CNT with the matrix creates an interphase with a reduced mobility. This chapter also discusses the variation of effective properties of the interphase region in a functionalized and neat CNT reinforced Poly-Ethylene (PE) nanocomposite systems.

This chapter is organized as follows. Section B gives a brief description of carbon nanotubes reinforced polymer composites. Section C through Section D discusses the simulation of nanocomposites, functionalized nanotubes, and nanoropes based on single-walled CNT and its behavior when embedded in a composite system.

Section E describes the interphase effect on a CNT reinforced nanocomposites, functionalized nanotubes, and nanoropes. Section G describes the estimation of effective properties using micromechanical methods and the effect of fiber orientation. Summary and conclusions are presented in Section H.

A. INTRODUCTION

Due to the atomically smooth nonreactive surface of nanotubes built of rolled graphene sheets, weak interfacial bonding inhibits load transfer from the matrix to nanotubes across the nanotube/polymer interface [49, 50]. The limited role of CNT as reinforcements in a composite, due to these weak bonding with the matrix, can be overcome by functionalization of the nanotubes, which provides multiple bonding sites to the organic/inorganic polymer matrix and thus inhibiting separation between the surfaces of polymer and nanotubes [25, 48]. Various researchers have studied the effect of different functional groups attached onto the nanotubes [2]. Some of the examples are fluorination of CNTs using alcohol solvents, functionalization by attaching hydrogen atoms through chemical and electric discharge processes, attachment of alkyl chains and carboxylic acids etc. Wei [51] studied the chemical bonding between the polymer and CNT using the Tersoff–Brenner potential. They found that multiple-site chemical bonding was energetically favorable, i.e., it enhanced the mechanical load transfer from the polymer chain to the CNT [49]. Liao and Li [6] observed that for a single-wall CNT composite system, the interfacial adhesion forces arises from the electrostatic and van der Waal interactions, the radial deformation induced by these forces, and the mismatch in the coefficients of thermal expansion for the polymer and the SWCNT. It was also reported that the interfacial shear stress of the CNT-polymer system due to CNT pullout is significantly higher than most carbon fiber reinforced composite systems.

CNT form agglomerates during its synthesis due to the strong surface area attractions between the carbon atoms and majority of the purification effort is spent on

the separation of the CNT units into individual units [38]. The molecular interactions and load transfer therefore would not only depend on the physical interactions between the nanotubes and polymer systems but also on the internal interactions within the nanotube rope systems. Therefore, the natural state for the production of the CNT based composite system would be a CNT rope – polymer composite system. However, from a computational perspective, the incorporation of CNT rope into a composite system would substantially increase the simulation time due to the large number of atoms involved in the model. Therefore, the search is on for a methodology that involves representation of the processes in the atomistic scale and translates the information efficiently into the next scale of interest using well established continuum theories [52].

There have been numerous experimental works that bring out the high strength aspects of CNT reinforced composite structures [11, 53]. However, a theoretical analysis is necessary for the accurate estimation of various interactions, especially in a multiscale framework. The objective of this chapter is to study the mechanics of the central CNT in a neat, functionalized and nanorope based CNT-nanocomposite system. Most of the earlier works in this area consider the effect of CNT-composite RVE in estimating the effective properties. However, in this chapter, focus is placed on the core or central CNT, and study how the mechanical properties are affected by the surrounding polymer, nanotubes, functionalizations, etc. This chapter also discusses the effect of the overall effective property of the interphase effect in a CNT reinforced polymer nanocomposite system.

B. CNT REINFORCED POLYMER COMPOSITE

Polymer based composites reinforced with carbon fibers have been widely used in advanced structures. Use of CNT as a potential composite reinforcement has many advantages over conventional fibers, enhanced mechanical strength of CNT being one of them. Few theoretical works have been undertaken to ascertain the effective

properties of CNT based polymers and experimental studies have found a 25% to 40% increase in strength [23]. CNT based composites are analyzed by considering the CNT as dispersed in a matrix and the interactions of the atoms of the CNT with the atoms of the matrix molecules is being studied by MD simulations [19, 20, 27, 30, 33, 49, 51]. The problem is different from a conventional fiber composite material in the sense that the fiber phase interacts with the matrix phase through molecular interactions. In a conventional composite material analysis, the material/mechanical properties of the participating phases are widely studied and accepted. This is however not the case with the nanometric sized fibers, as the material properties are still being debated and even weak molecular interactions is found to alter the overall properties drastically [2, 13]. Research in the determination of overall properties of the composite was carried out earlier with a bottom to top approach [2, 13, 22, 54]. Of late, focus is on the accuracy in predicting the lower order properties and hierarchical transfer of the material properties to the larger scale. In the previous works on multiscale modeling, the response in the atomistic level was transferred to the mesoscale or microscale by the explicit use of equivalence of the response variables [22]. This equivalency of the displacement or the stress field has a major drawback, where there is a loss of essential information that is important in the atomistic scale, which is either not considered or averaged out in the higher scales [10]. Another multiscale method involves the use of micromechanical schemes to model the mesolevel and subsequently use of continuum formulation for scaling the domain of interest [52]. The obvious drawback of such an approach is that the local variations in morphology and structure are not considered or do not translate to the macroscopic scale. Keeping these models in mind, a novel approach is used in the modeling and analysis of CNT filled polymer matrix composites. This model draws inspiration from various attempts in multiscale modeling. The interactions in the molecular level are modeled using pair potentials to respond to externally applied disturbance. The response variables in the lower scales are passed on to the next higher scale, seeking a change in the material properties**.** This method is justified, since the material response at an atomistic scale is highly nonlinear [18] and any change in the local environment has been found to vary the ensemble

properties dramatically [2]. However, previous works in this area have not been able to capture the local variations in a global sense, which is intended to be achieved in this chapter. For example, changes in the chirality, orientations of the fiber phase with the global orientation and chemical functionalization are found to change the atomistic ensemble properties. Thus, they are captured and can be passed on to the higher scales subsequently affecting the macroscopic response.

1. APPLICATIONS

The most exciting use of CNT is as reinforcements in polymeric nanocomposites. Polymer based composites reinforced with carbon fibers have been widely used in advanced structures. Use of CNT as potential composite reinforcements has many advantages over conventional fibers. The enhanced mechanical strength of CNT is one of the primary reasons. Apart from this enhanced strength, various multifunctional features can also be obtained by the use of CNT fibers. One of the most popular methods of analysis of the discrete atomistic system and scaling up to the continuous macroscale domain is through homogenization methods [13, 23, 55], similar to the analysis of heterogeneous composite structures.

2. MODELING OF CNT-POLYMER MATRIX RVE

Polyethylene is one of the simplest polymers studied due to a simple molecular structure. Majority of the works carried out so far has predicted an increase in the stiffness of the resulting PE composite RVE (Representative Volume Element or called Periodic Unit Cell) reinforced with CNT (see Figure 3.1) [1, 11, 23, 27, 30, 56]. This prediction of an increase in the effective modulus of the composite RVE is expected as the stiffness of a CNT is many orders higher than that of the surrounding polymer. However, what has to be estimated in this nano-molecular level is how the interactions of the surrounding molecules affect the properties of CNT. The properties estimated from the atomistic simulations, especially in crystalline materials, are always found to

be higher than the bulk properties of the same material. This was attributed to the microscale imperfections in the bulk material that degrades the higher scale properties. In estimating the properties due to the molecular interactions it is not always straightforward as predicting the material properties based on the principles of continuum mechanics.

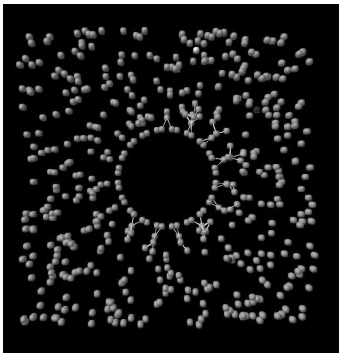

Figure 3.1 Modeling carbon nanotube-polymer nanocomposites

The large surface area and the nanometer dimensions of the CNT increase the quantum of molecular interactions between the molecules of the surrounding polymer and the atoms of the CNT. This has been experimentally observed especially in the works of Ding et al., [57]. These experiments categorically prove that the interfacial strength of CNT-Polymer interface are strong enough for an effective load transfer and hence mathematical simulations with perfect load transfer conditions are acceptable. Another important factor that affects the interfacial strength of the CNTs is that the nanotubes form agglomerates when free. This is due to the strong surface attractions between the neighboring nanotubes [50]. The emphasis of this study is on the characterization of the layer of polymer immediately surrounding the CNT, called the *interphase*, which is found to change the elastic modulus not related to the bulk of the material. Ding et al. [57] has observed that the total effective diameter of the MWNT embedded in a polycarbonate polymer is larger and this indicates that there exists stronger interaction between the polymer molecules immediately surrounding the CNT.

The minimum energy configuration of the CNT is minimizing at 0 K using an NVE procedure. The CNT is minimized for each temperature increments from 0 K up to 300K and is taken as the minimum potential energy of the CNT system. Increment in displacement is applied to the relaxed structure and is allowed to equilibrate over a number of time steps. The CNT system is strained at a constant rate to calculate the strain energy of deformation by minimizing the total potential energy at each increment and the difference in the potential energy gives the strain energy due to deformation [2, 10, 12, 13, 24, 31, 37].

a. ANALYSIS OF SINGLE AND DOUBLE WALLED CNT –POLYMER RVE

In this study, the Zig-Zag (17,0) CNT and compatible Zig-Zag multiwalled nanotubes are used to estimate the effective property of a CNT-reinforced polymer nanocomposite. These nanocomposites are ultimately used as coatings or as load bearing structures. The fundamental requirement of these materials is the enhanced mechanical strength and durability. As the first step in analyzing the material property of the macrostructure, the atomistic interactions need to be analyzed. The CNT which forms the reinforcements in a polymeric matrix material was analyzed using molecular dynamics. The second step involves the analysis of the mesoscale regime and subsequently the higher scales of interest.

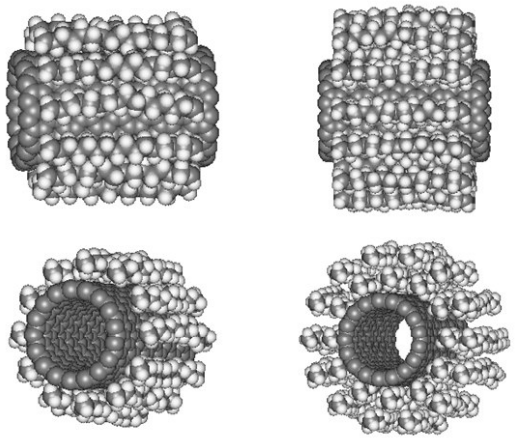

Figure 3.2 Study on the effect of polymer matrix on the property of carbon nanotube

For a complete understanding of the molecular effects and how these percolate into the upper scales, one has to study the effect of one medium over the other. In this case, it should be understood as to how the property of the CNT affects the polymer matrix and vice-versa (see Figures 3.2 and 3.3). It has been experimentally proven that the interface between the CNT and the polymer has an altered property compared to the polymer itself. This is due to the atomistic interactions of the polymer and nanotube. This also sheds light on the fact that the atomistic interactions not normally considered could affect the macroscopic material property considerably and therefore needs to be estimated for each case. In this study, estimating the effect of the polymer on the CNT is of primary interest. The analytical domain consists of an RVE (or Periodic Unit cell) of a CNT (Zig-Zag in this case) surrounded by layers of Poly-Ethylene (PE) molecules. The polyethylene molecules studied in this work are crystalline.

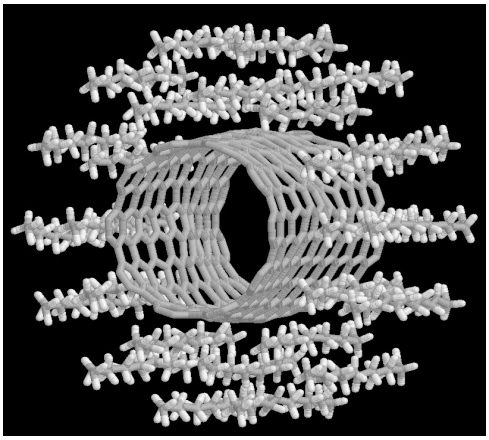

Figure 3.3 Deformation characteristic of SWNT under the influence of polymer

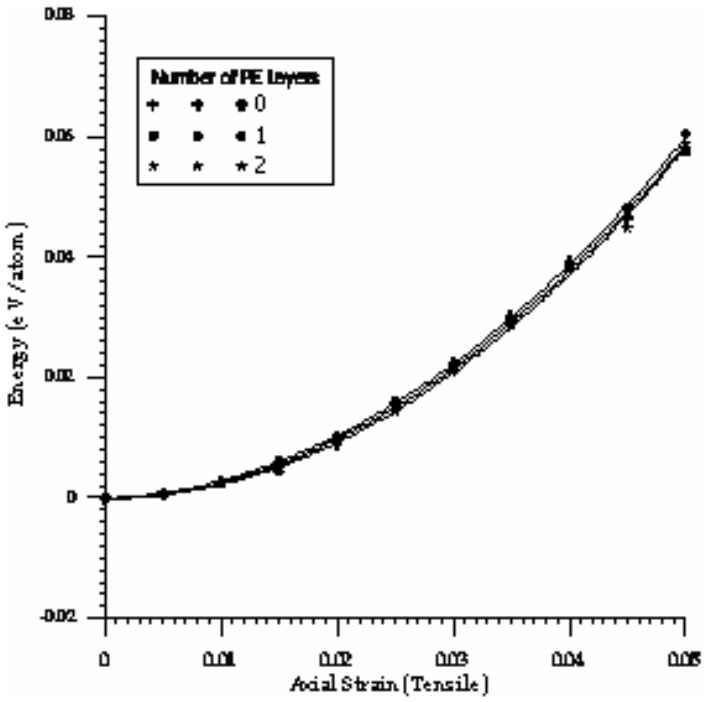

(a)

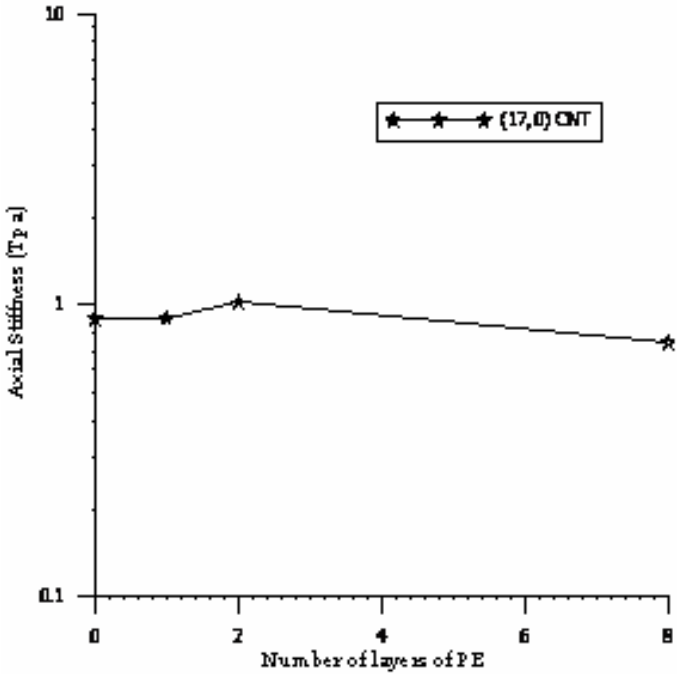

(b)

Figure 3.4 (a) Strain energy variation, and (b) axial stiffness with axial strain for SWNT-PE composite

It is found that the effective property of the CNT reduces during the tension and compressive loading stages. The analysis was also carried out for various numbers of surrounding polyethylene molecules for a detailed estimate. As the numbers of polyethylene molecules are increased the effective property reduces and reaches an asymptotic value when the number of polyethylene (PE) layers equals 8 (see Figure 3.4). This possibly suggests the effect of infinite polymer medium, normally encountered in nanocomposite specimens, on the CNT. This reduced effective property of the CNT will be used in the estimation of the higher scale properties by homogenization methods. No relevant works were found to compare this reduction in the property of the CNT under the influence of the surrounding polymer; however, it is very clear that the property has to change compared to a freely existing atomistic entity. Most of the works that estimate the effective property of the CNT-Polymer RVE calculate the effect of the total RVE as such or take into consideration the effect of the individual independent components. Analysis was also carried out for DWNT with surrounding polymer materials, and the effective property of the core DWNT was also found to be less than would be estimated for a neat DWNT (see Figure 3.5 and 3.6a&b).

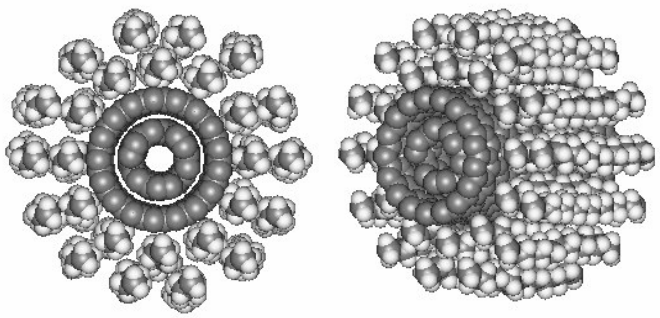

Figure 3.5 Modeling double walled CNT PE nanocomposites

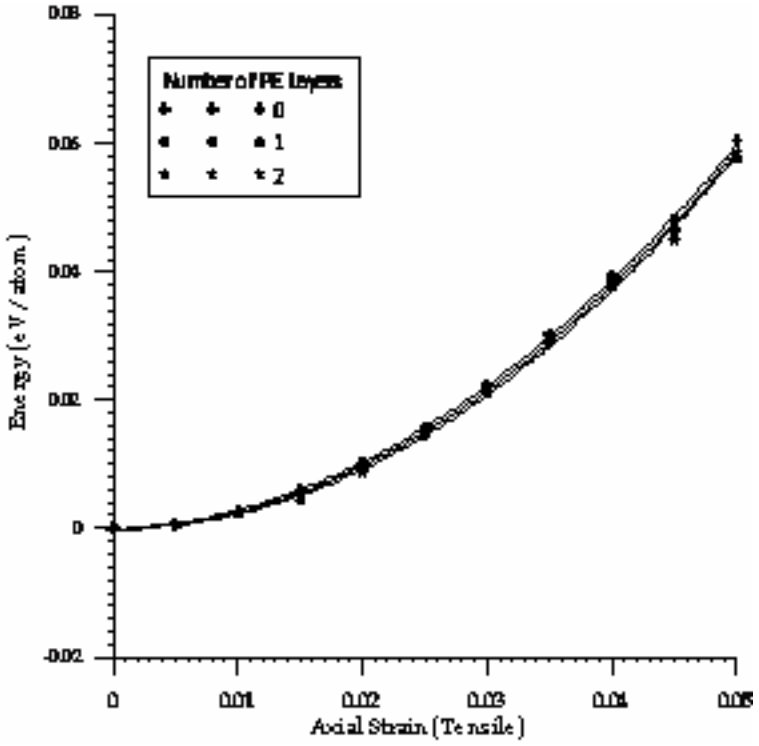

(a)

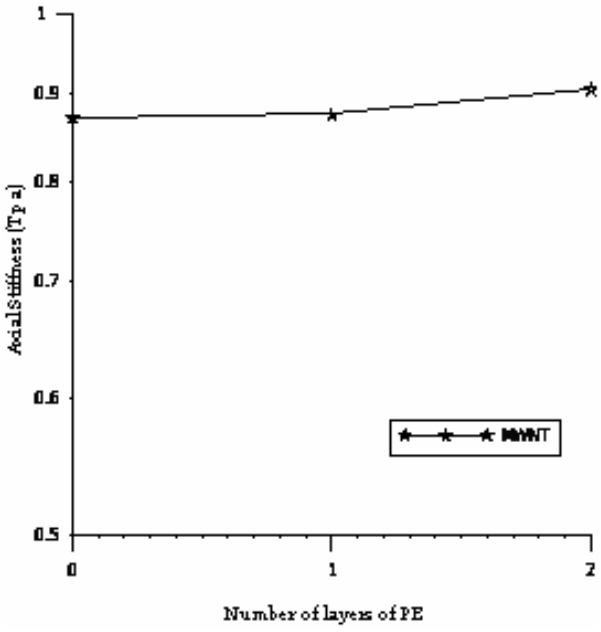

(b)

Figure 3.6 Strain energy variation with axial strain and axial stiffness for double walled CNT -PE composite

b. ANALYSIS OF SWNT NANOROPE –POLYMER RVE

Analysis was also carried out on the combined effect of surrounding polymer matrix and CNTs on the core CNT. This simulates the effect of the CNT nanorope embedded in a polymer matrix. The computational time required for the analysis increases prohibitively high for a large polymeric system RVE (see Figure 3.7) with nanoropes. The strain energy variation with the applied tensile and compressive deformation is given in Figure 3.8.

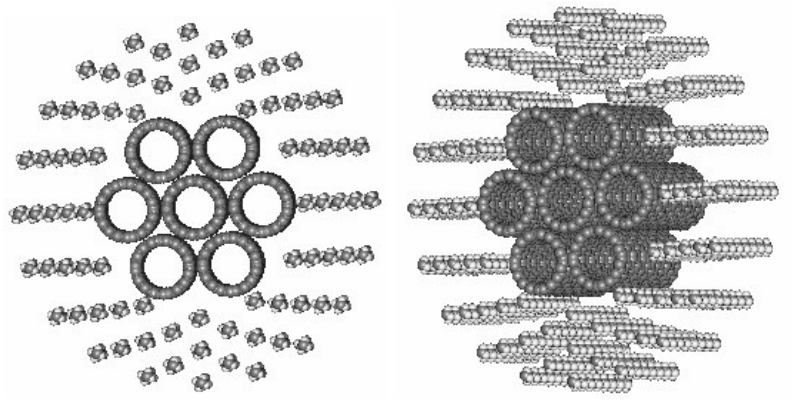

Figure 3.7 SWNT nanorope –polymer RVE – computational unit

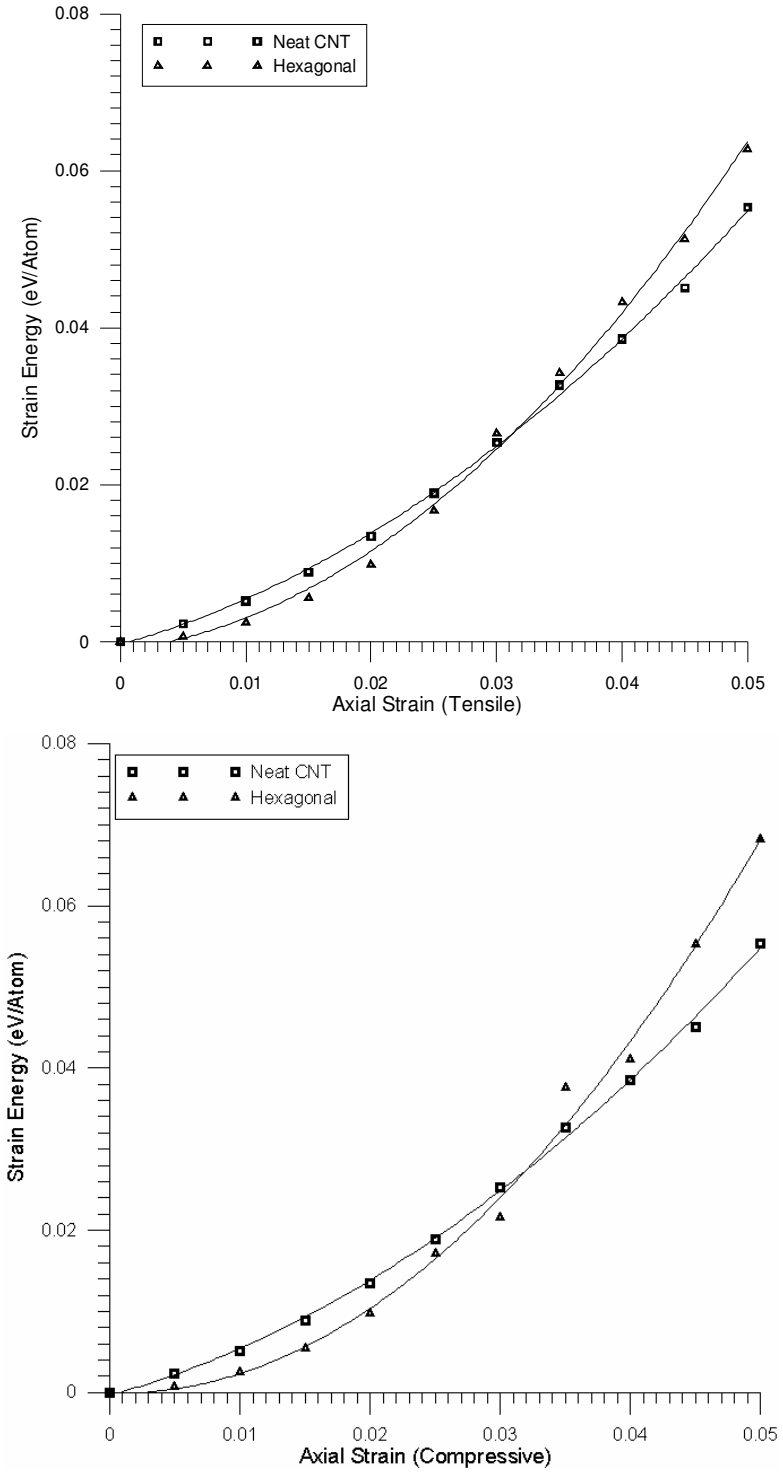

Figure 3.8 Strain energy variations with axial tensile and compressive strain for a SWNT-nanorope-polymer RVE

Perfect load transfer is assumed in many of the works in CNT-composite models. In some works where this perfect condition is not achieved, the effective load transfer is enhanced using functionalization of the CNTs. For the realization of the multifunctional property in the CNT, substitution impurity or doping the CNT is another promising area. This section is focused on the effect of the surrounding polymer on the stiffness of the neat (pure or non-functionalized) and functionalized CNT. In majority of the works carried in CNT composite structures, it is inaccurately assumed that the CNT does not undergo any change in its properties. In this work, however, the effect of the polymer on the degradation or enhancement of the CNT properties is investigated. By this approach, it is possible to take into consideration two factors that affect the stiffness of the composite. First, by considering the change in the property of the CNT under the influence of the surrounding polymer and incidentally, the effect of imperfect load transfer is indirectly taken into consideration. The argument for such a treatment is that if there is an imperfect load transfer then one can naturally surmise that the property of the CNT does not change under the influence of the matrix and on the other hand if it changes, then conclude that the polymer affects the property of the CNT. Second, by considering the property of the surrounding interphase layer greater accuracy is achieved in predicting the effective property of the composite structure. It should be emphasized that the simulations carried out in this work do not take into consideration the change in the effective property of the surrounding matrix.

C. ANALYSIS OF FUNCTIONALIZED CNT

A functionalized CNT with ethylene chains as the functional group is shown in figure 3.9. The sites of substitution is chosen randomly along the lengh of the CNT and therefore no specific order is used in the creation of the functionalized CNT. The ethylene group is of sufficient length so that it can also be attached to the surrouding polymer as in the case of an embedded CNT-matrix structure. After minimization of the functionalized CNT ensemble, tensile and compressive strains are applied incrementally. The change in the elastic modulus (in TPa) of the functionalized CNT is compared with a neat (meaning CNT with no functionalization) CNT as shown in figures 3.10 a & b. The properties thus obtained, can be used in the higher scale analysis for various CNT structures and morphologies for a multiscale analysis. When strain is applied to a composite material quickly, the chemical attachment generally breaks at the fiber wall. However, when the composite is deformed slowly the bonded chain gets sufficient time to get disentangled from the surrounding matrix. In either case, the movement of the attached polymer dissipates energy during deformation thus increasing the overall resistance of the material to failure [58]. This phenomenon of slow matrix re-entanglement is enhanced when the CNT is functionalized [2]. However, the rate of application of strain has to be controlled.

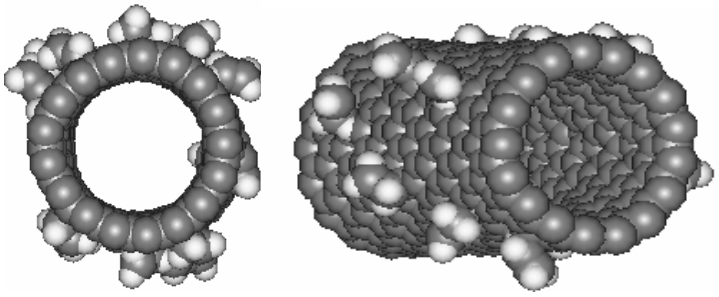

Figure 3.9 Functionalized singlewalled CNT

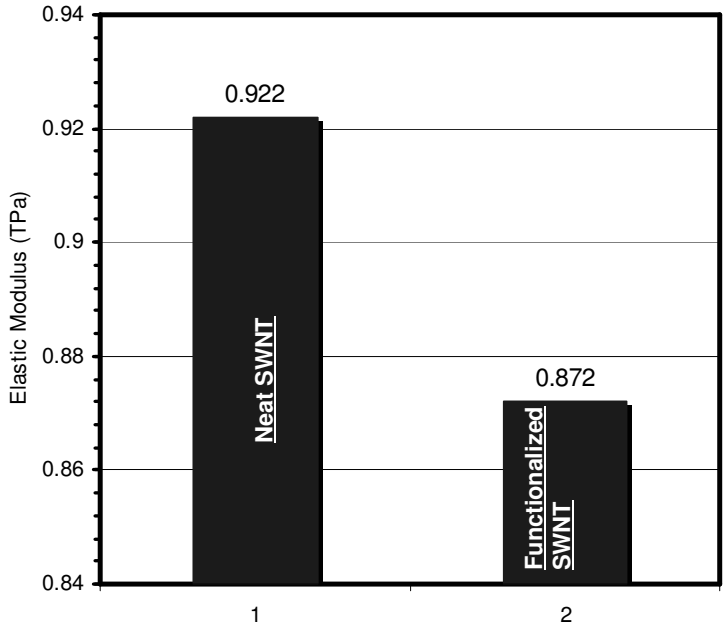

(a)

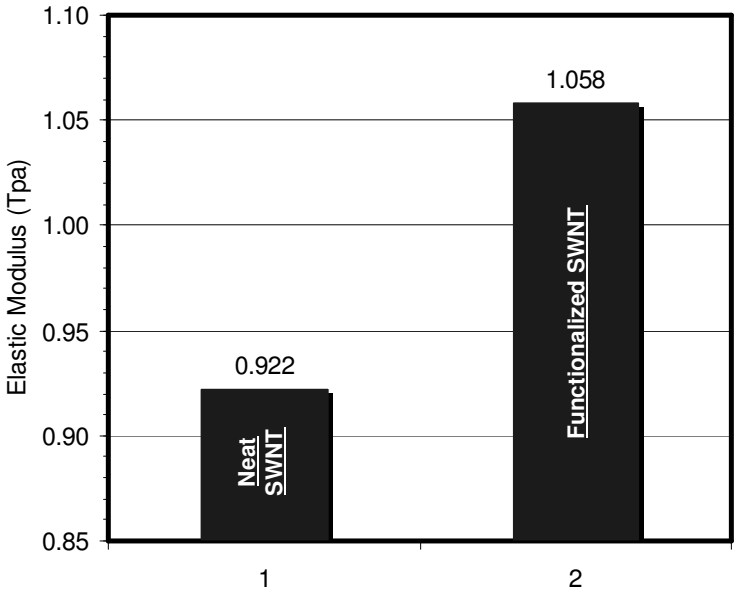

(b)

Figure 3.10 Elastic properties of functionalized SWNT in (a) tension and (b) compression (1. neat SWNT, 2. functionalized SWNT)

1. ANALYSIS OF FUNCTIONALIZED CNT REINFORCED POLYMER COMPOSITE

A functionalized CNT embedded in a matrix enclosure is shown in figure 3.11. The sites of substitution in this case is also chosen randomly along the CNT. The ethylene group is of sufficient length so that it can be attached to the surrouding polymer in this case. After minimization of the functionalized CNT ensemble, tensile strains are applied incrementally. The change in the elastic modulus (in TPa) with a neat and functionalized CNT is shown in figure 3.12. The properties calculated in this study is for the central CNT and not for the whole ensemble as it is very important to estimate the effect in-situ. In most of our simulations, it has been found that no direct correlation can be made on the effect of various features on the properties of CNT and therefore analysis needs to be carried out for each scenario.

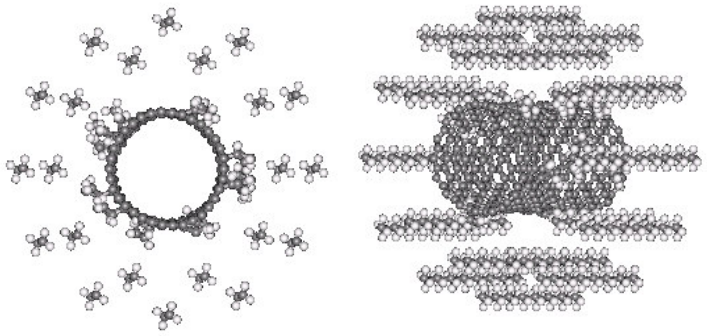

Figure 3.11 Functionalized SWNT embedded in a polythelene matrix

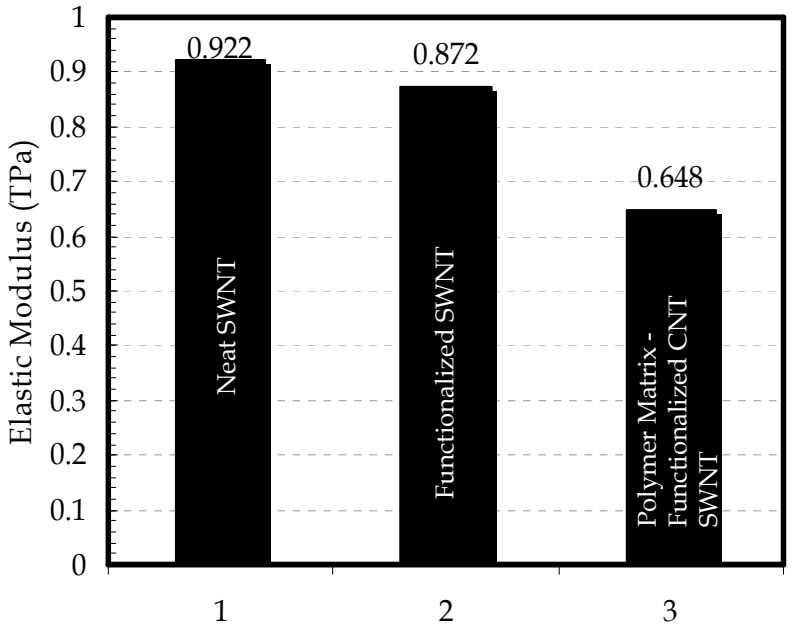

Figure 3.12 Elastic properties of various SWNT ensembles

Tensile tests carried out on the CNT-matrix RVE, interestingly shows that functionalized chains form attachments with the surrounding matrix. This series of bonding and rebonding has also been observed in pullout tests conducted on functionalized CNT-matrix interactions [31]. However, the important point in this simulation is the fact that even during energy minimization processes, the functionalized chains of the CNT establishes bonding with the matrix chains. This feature is important in the load transfer from the matrix to the CNT and vice-versa as can be seen in Figure 3.13. One of the most important characteristics of such a phenomenon is the effect of such an interaction on the macroscopic material property, where the interactions in the nanoscale affect the properties in the macroscale leading to a coupled multiscale model.

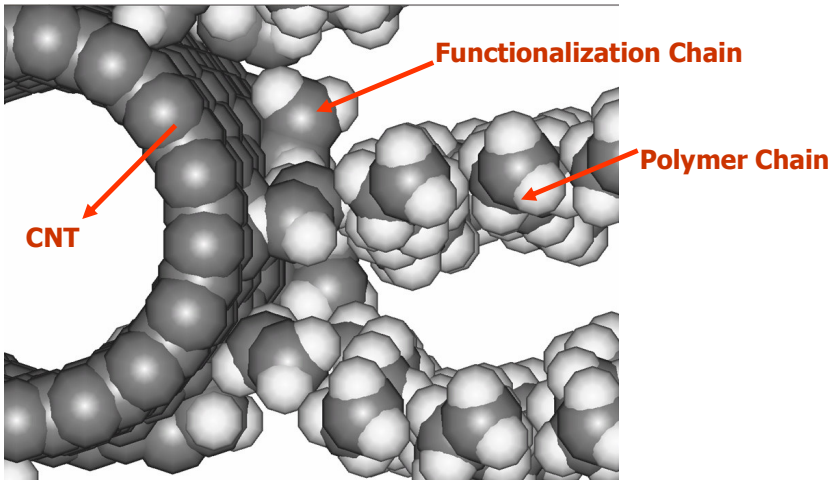

Figure 3.13 Re-attachment of ethylene chains in the CNT to the ethylene chains in the matrix after stabilization

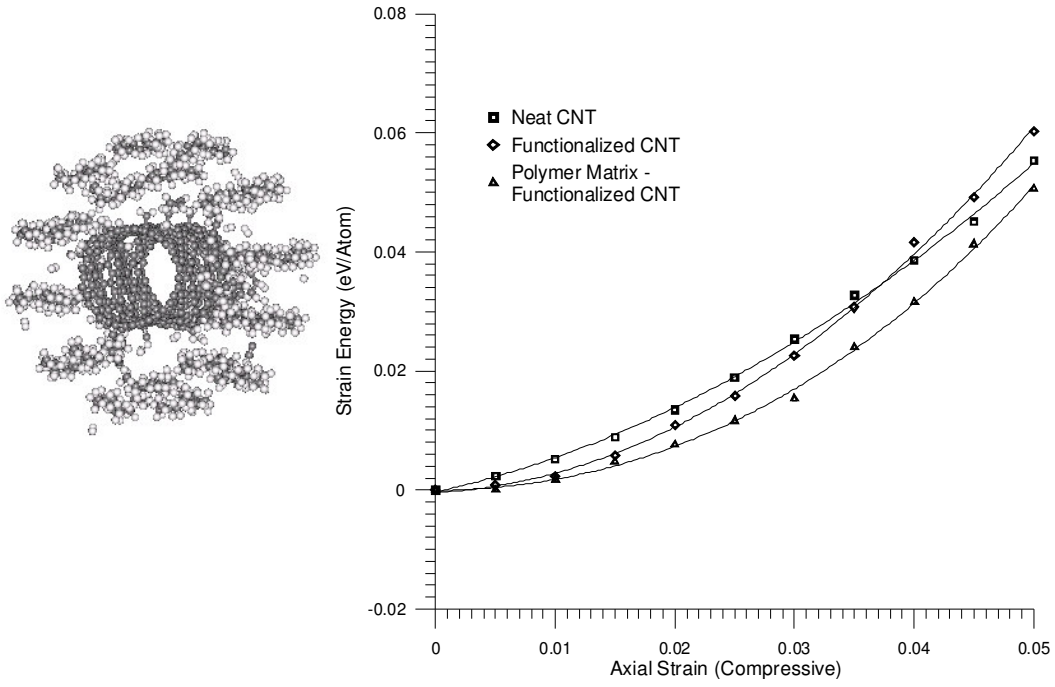

(a) (b)

Figure 3.14 (a) Functionalized SWNT surrounded by 2 polymer layers (b) strain energy variation with respect to the applied strain

The variation of the strain energy with respect to the applied strains in comparison with neat CNT, functionalized CNTs and matrix-embedded functionalized CNT is show in figures 3.14b. Figures 3.15a show a CNT matrix embedded in 4 layers of polymer matrix and Figure 3.15b show the corresponding strain energy variation. The difference in the strain energy between figures 3.14b and 3.15b is due to the effect of the number of polymer layers on the central or the core CNT.

When strain is applied to a composite material quickly, the chemical attachment generally breaks at the fiber wall. However, when the composite is deformed slowly the bonded chain gets sufficient time to get disentangled from the surrounding matrix. In either case, the movement of the attached polymer dissipates energy during deformation thus increasing the overall resistance of the material to failure [58]. This phenomenon of slow matrix re-entanglement is enhanced when the CNT is functionalized [2]. However, the rate of application of strain has to be controlled.

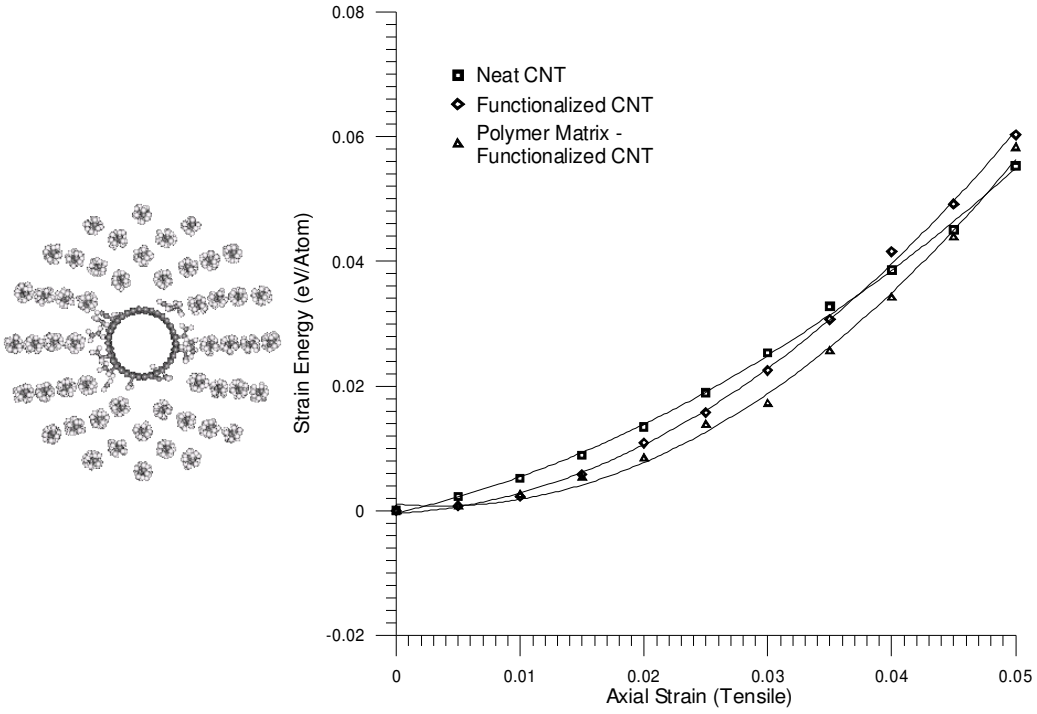

(a) (b)

Figure 3.15 (a) Functionalized SWNT surrounded by 4 polymer layers (b) strain energy variation with respect to the applied strain

The properties of the functional CNT and its behavior when embedded in a matrix structure and also the effect of chemical functionalization on the stiffness of CNTs along the tubule axis can also be established. For the macroscopic functionalized nanocomposite structure to be stable, the functionalized CNT atomistic unit has to be structurally stable under various thermal conditions. The stability of the CNT affected by the substitutional changes has to be studied by monitoring the structural change in the CNT profile under various loading and temperature conditions. These properties help in establishing the use of functionalized CNT in composite structures. It is found that the CNT functionalized with chemically active functional chains are stable to a sufficient strain level and there is no adverse effect on the tubular structural integrity of the CNT. Also, the functionalized CNT embedded in the matrix is found to be stable; however the material stiffness shows variation with the change in the number of layers of matrix molecules it is embedded in. Figure 3.16 shows the variation of the elastic stiffness of the CNT for various states of the neat and functionalized CNT in compression and is within the range of 0.5 -5.5 TPa as in the literature [23, 31]. It can be seen that with the increase in the number of polymer layers, the effective elastic modulus of the CNT is found to decrease as the number of farfield molecular interactions increases.

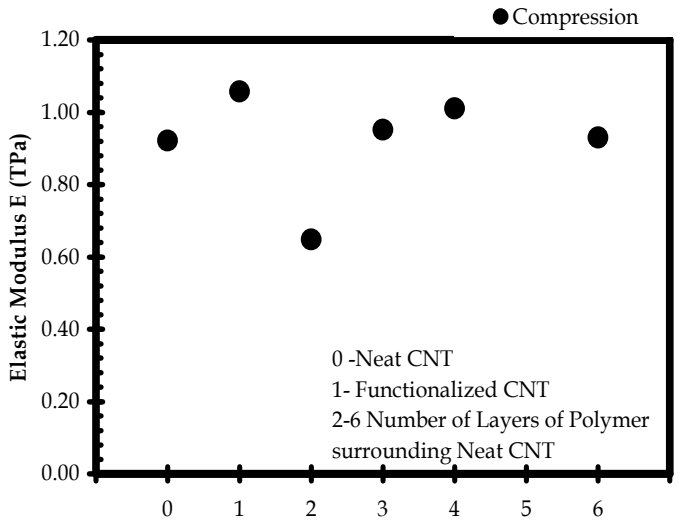

Figure 3.16. Elastic properties of various types of SWNT ensembles in compression

D. ANALYSIS OF CNT NANOROPES AND FUNCTIONALIZED CNT NANOROPES

1. CNT NANOROPES

Carbon nanotubes are normally found to exist in an aggregated state. It is infact a known property of carbon based nanotubes to form agglomerates during its synthesis and majority of the purification effort is spent on the separation of the CNT units into individual units. The tiny structure of single-walled carbon nanotubes has very high curvature, which results in a high surface energy [50]. Therefore, the individual nanotubes tend to self-organize into crystalline bundles or into a set few hundred aligned nanotubes arranged in a two-dimensional lattice in the plane perpendicular to the common axes. These highly uniform tubes which have a greater tendency to form aligned bundles have led Smalley to christen the bundles nanotube "ropes". Initial experiments indicated that the rope samples contained a very high proportion of nanotubes with a specific Armchair structure. Subsequent work has suggested that the rope samples may be less homogeneous than originally thought. Nevertheless, the synthesis of nanotube ropes (see Figure 3.17) gave an important boost to nanotube research. The incorporation of CNT rope into a composite system would substantially increase the simulation time due to the large number of atoms involved in the model. The molecular interaction and load transfer in such a system would not only depend on the physical interactions between the nanotubes and polymer but also on the internal interactions within the nanotube rope system. Hence it is required that the nanotube rope system should also be analyzed independently. The type of nanoropes used in the current analysis is shown in Figure 3.17, and it consists of a triadic arrangement of CNT.

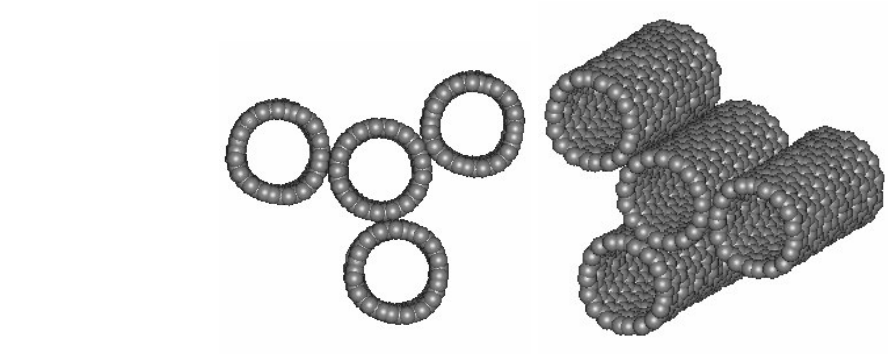

(a)

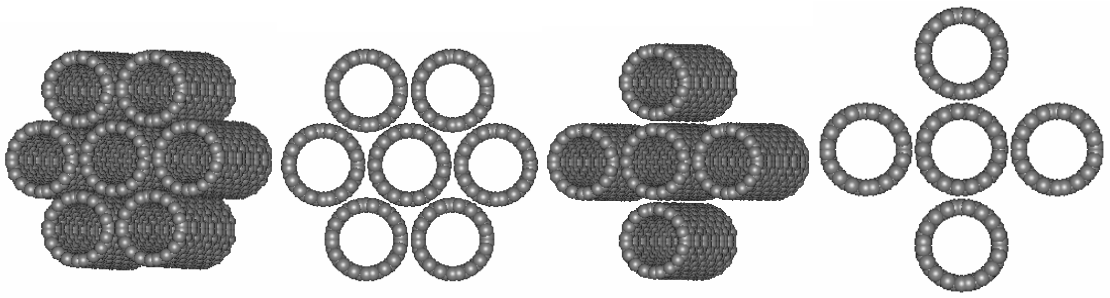

(b) (c)

Figure 3.17 (a) Triangular arrangement of SWNT – nanoropes (b) hexagonal and (c) pentagonal arrangement of CNT based nanoropes

Various configurations of nanoropes also under study are shown in Figure 3.17b&c however the results presented in this chapter pertains only to the triadic system. Experimental analysis by Atomic Force Microscopy (AFM) of nanoropes to estimate the elastic properties of CNT based ropes by Salvetat [38] is one of the few experimental works available, a couple of theoretical works exists in` the analysis of CNT based ropes [50, 59]. The experimental analysis by Salvetat has shown that the overall properties of the nanorope are less than the effective property of a single nanotube. This degradation in the property of the CNT is also reflected in this analysis (see figure 3.18). The property of the nanotubes is estimated indirectly in this analysis by considering the effect of the surrounding CNT on the core CNT. There is no direct study to compare this degradation of the property of the core CNT, due to the nature of the atomistic interactions at the nanoscale, the tensile and compressive (attractive and repulsive forces) forces on individual CNT atoms affect the strain energy thereby

affecting the elastic modulus. Any change in the property of this core CNT would be due to the effect of the surrounding CNT. This method of analysis is also aimed at studying the effect of a surrounding polymer or functionalization on a CNT. It has been stated that the interactions between the different non bonded CNTs is by van der Waals forces and this contributed to the radial deformability of individual nanotubes and also leads to changes in the inter-tube contact within a rope [50].

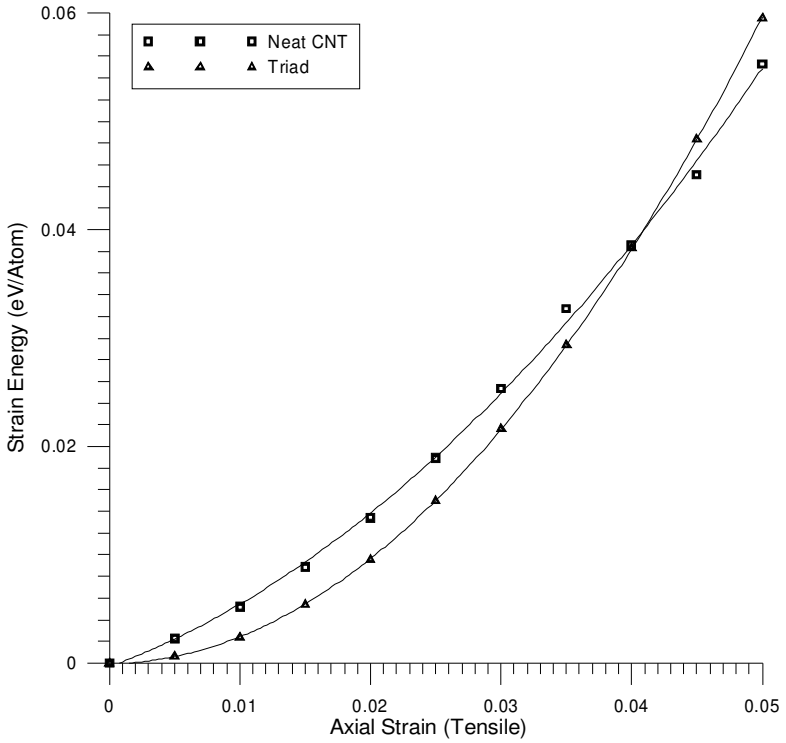

Figure 3.18a Elastic strain energy under tensile strains for CNT based nanoropes

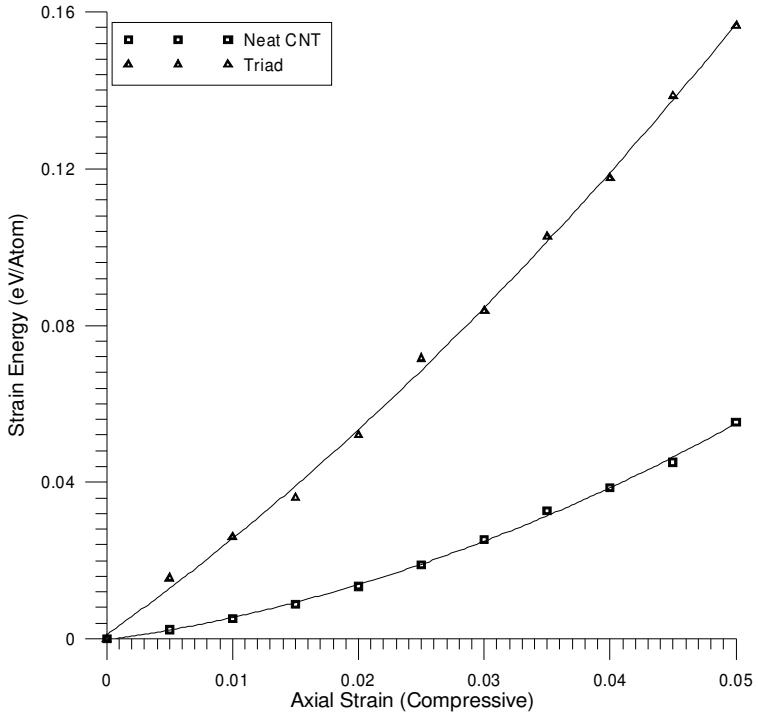

Figure 3.18b Elastic strain energy under compressive strains for CNT based nanoropes

The variation of the elastic strain energy for the core CNT in a Triad-Nanorope reveals the effect on the core CNT under tensile loading and is found to be marginal; however the compressive loading has a profound effect. This is because in compression the surrounding CNTs interacts more (repulsive effect) with the core CNT rather than in tension. The elastic modulus of the core CNT obtained by the above method (see Figure 3.19) closely matches with the experimental analysis of Salvetat [38] for the type of CNTs used in this analysis. Salvetat has observed ranges from 1.3TPa to 67GPa for various rope diameter and lengths. The elastic modulus was found to decrease as the physical dimension of the evaluated specimen increases.

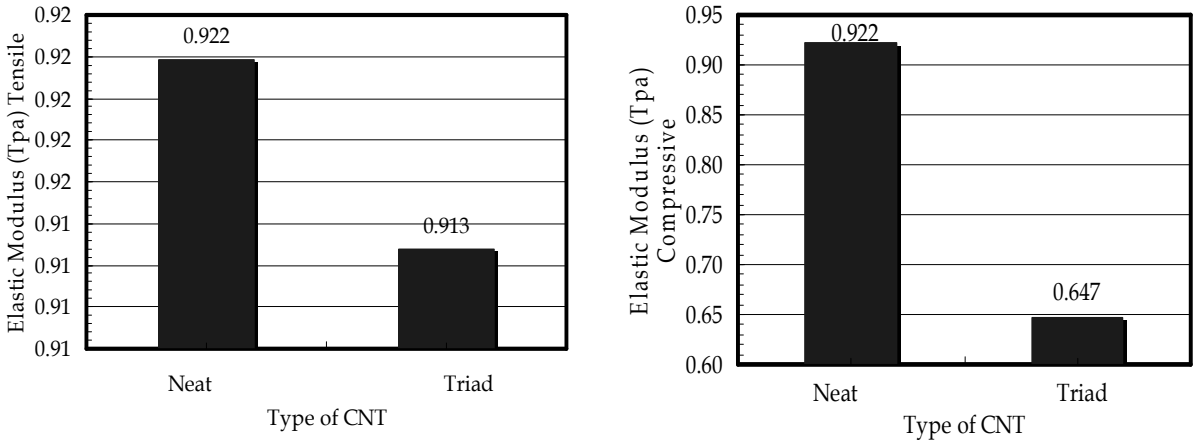

(a) (b)

Figure 3.19 Elastic properties of CNT based nanoropes in (a) tension and (b) compression

a. ARMCHAIR (10,10) CNT NANOROPE

To have a better estimate of the elastic properties of individual configurations that should be transferred to the higher scale, one need to do individual MD analysis on each of these CNT configurations. Therefore, MD analysis was carried out on an Armchair (10,10) CNT (see Figure 3.20) and the effect the core or central CNT would experience when it is surrounded by a layer of CNTs has been estimated.

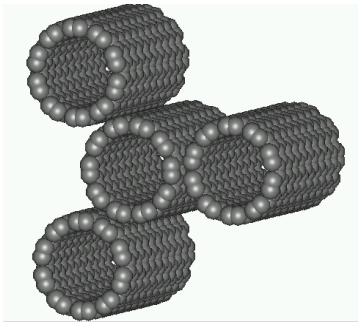

Figure 3.20 Undeformed and deformed configuration of Armchair (10,10) SWNT nanoropes

It should be noted that for the strains applied, there is no structural instability observed on the core or surrounding CNTs. The strain energy variation during the tensile deformation process is plotted in Figure 3.21(a). The variation of the strain energy has been found to be similar to what has been observed for the Zig-Zag CNT based nanorope and the elastic modulus obtained is shown in Figure 3.21(b).

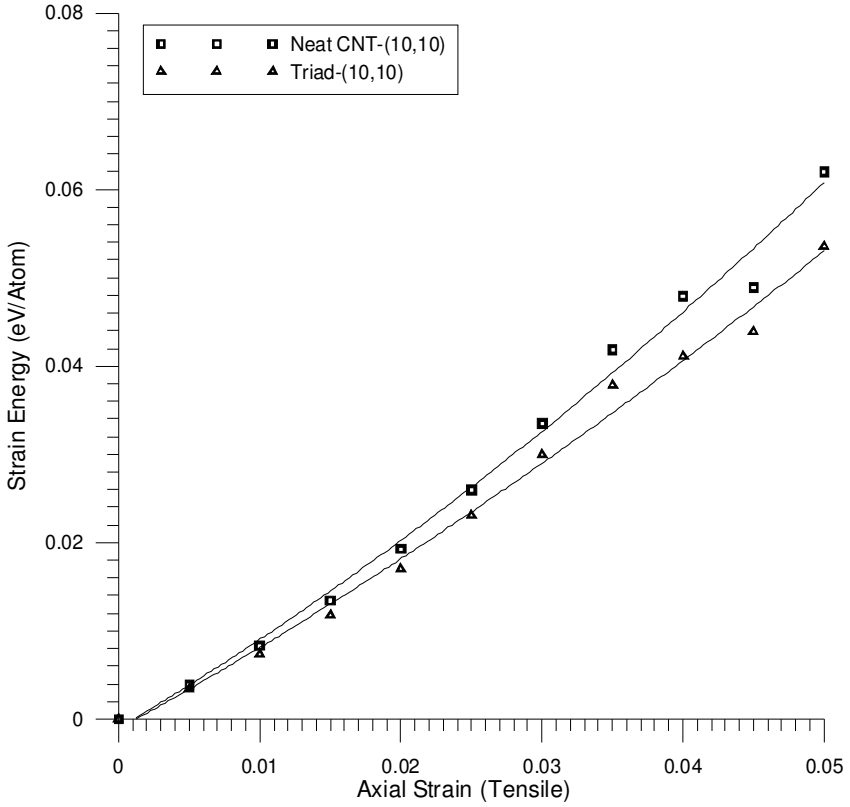

Figure 3.21. (a) Strain energy variation during the deformation process

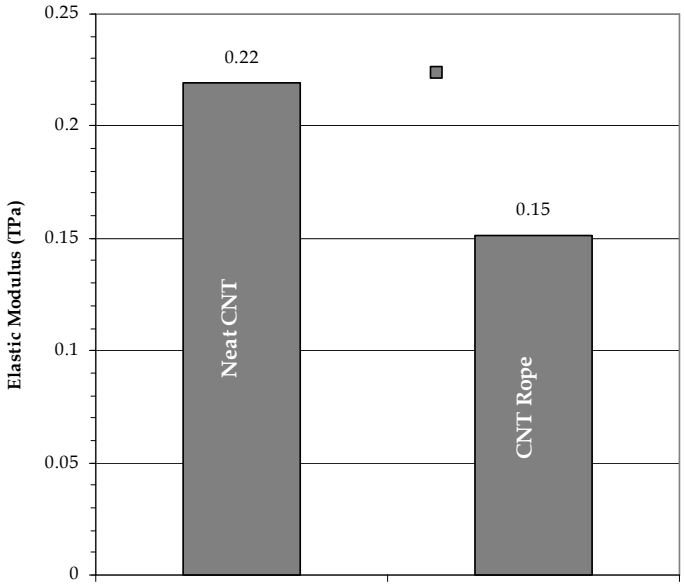

Figure 3.21 (b) Elastic modulus for a neat (10,10) CNT and core CNT of a nanorope

2. FUNCTIONALIZED CNT NANOROPES

As a continuation of the previous sections on the analysis of CNT nanorope, the effect of functionalization of CNT ropes and its interaction with the central neat CNTs are studied. The main interest is in the behavior of central CNT in the presence of the functionalization and peripheral nanotubes. Though various configurations of nanoropes are possible, this chapter mainly concentrates on the quad and hexagonal arrangements**.** The incorporation of CNT rope into a composite system would substantially increase the simulation time due to the large number of atoms involved in the model. The molecular interaction and load transfer in such a system would not only depend on the physical interactions between the nanotubes and polymer but also on the internal interactions within the nanotube rope system [50]. The type of nanorope used in the current analysis is shown in Figure 3.22a, which consists of a diamond arrangement of CNT. The variation of the elastic strain energy for the core CNT in a quad-nanorope in tension is shown in Figure 3.22b.

Functionalization studies on a hexagonal arrangement (see Figure 3.23a) of the CNT ropes are also being carried out. The strain energy variation with the applied strain for this configuration is shown in Figure 3.23b. The strain energy profile changes with the number of surrounding CNT's and due to the presence of the functional groups on the surface of the CNT. It can be seen that the strain energy profile is drawn to a point below the zero energy state in the case of the hexagonal nanorope. This is because due to the large number of atoms in the ensemble drastically increases the computational time required for total minimization. The minimization procedure is terminated before a true minimization may be achieved. The corresponding strain energy profile originating from this ensemble therefore shows a non-zero energy state and this residual strain energy is indicated (see Figure 3.23b).

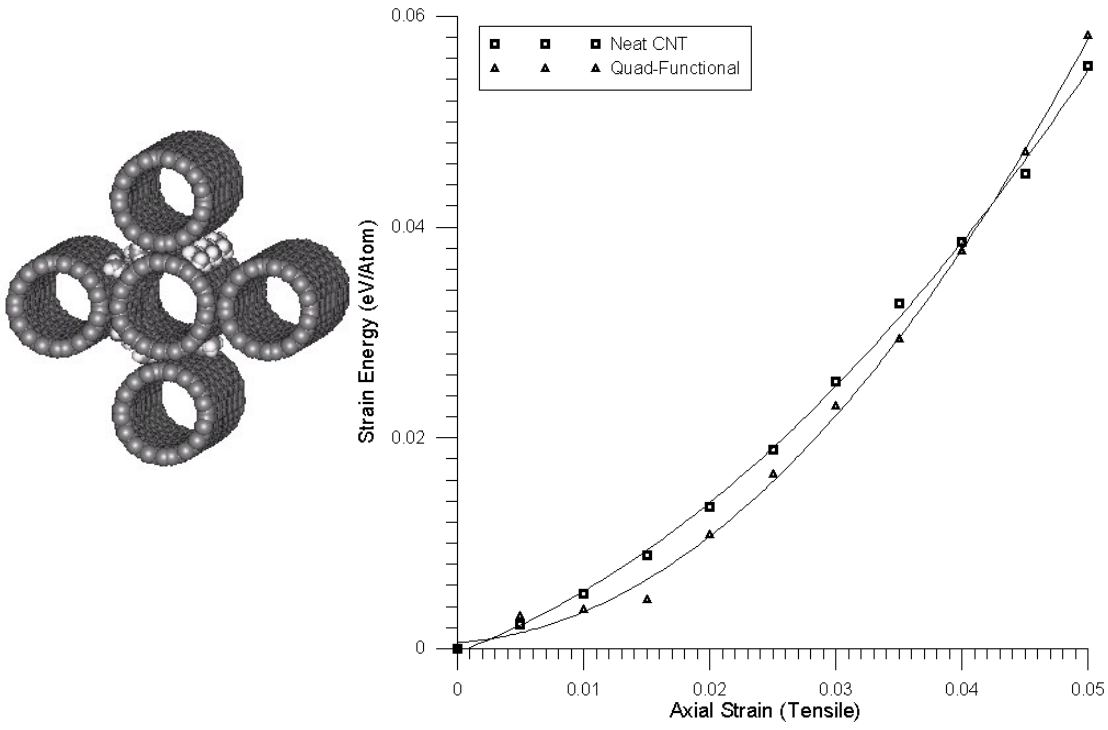

(a) (b)

Figure 3.22 (a) Functionalized SWNT quad-nanorope (b) Strain energy variation with respect to the applied strain

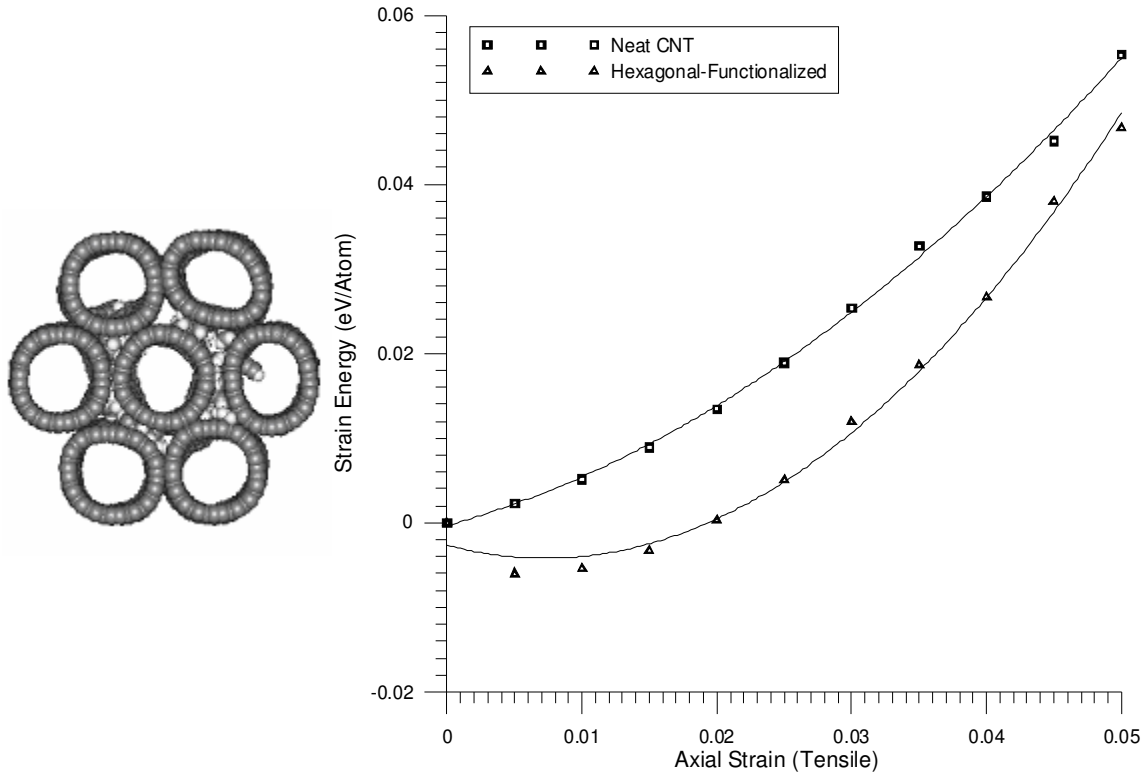

Figure 3.23 (a) Functionalized SWNT hexagonal-nanorope (b) variation of strain energy with respect to applied strains

E. INTERPHASES IN NANOCOMPOSITE

One of the most popular methods of analysis of a nanocomposite is the homogenization methods similar to the analysis of heterogeneous composite structures. Polyethylene is one of the simplest among the various polymers studied and the advantage lies in the fact that it has a simple molecular structure. Majority of the works carried out so far has predicted an increase in the stiffness of the resulting PE composite reinforced with CNT [1, 11, 27, 30, 56, 60]. The large surface area and the nanometer dimensions of the CNT increase the quantum of molecular interactions between the molecules of the surrounding polymer and the atoms of the CNT. This has been experimentally observed especially in the works of Ding [57] and Sandler [61] and Barber [62]. These

experiments categorically prove that the interfacial strength of CNT-Polymer interface is strong for an effective load transfer and hence mathematical simulations with perfect load transfer conditions are acceptable. The emphasis of this study is on the characterization of the layer of polymer immediately surrounding the CNT called the interphase, which is found to have an altered effective property not related to the bulk of the material. Ding has observed that the total effective diameter of the MWNT embedded in a polycarbonate polymer is larger and this indicates that there exists stronger interaction between the polymer molecules immediately surrounding the CNT.

According to Fisher and Brinson [60] the interphase thickness is of the order of the diameter of the CNT. Therefore the effect of the interphase cannot be completely eliminated in the analysis of the effective properties of the composite. Interphase analysis of fiber matrix composites due to various effects considers the variation of the interphase property based on Wacker's mathematical model [63] given by

$$E_i = \left(\alpha E_f - E_m\right)\left(\frac{r_i - r}{r_i - r_f}\right)^n + E_m \tag{3.1}$$

where $E_{i,f,m}$ is the modulus of the interphase, fiber and matrix phases respectively and $0 \le \alpha \le 1$, and $n = 2, 3, \ldots$. The effective average transverse modulus of the interphase is given by

$$E_i(r) = \frac{r_i - r_f}{\int_{r_f}^{r_i} \frac{1}{E_i(r)} dr} \tag{3.2}$$

It is also reported that for purely polyethylene based composites the value of α is around 0.21 with the value of n fixed and taken as 2 [63]. The stiffness of the matrix is taken as 610 MPa [27]. Since this model takes into consideration the polymer based composite systems, the direct application of the load transfer mechanism into the molecular regime can be implicitly assumed. Thus, one can model the effective properties of the interphase based on the properties of the surrounding matrix in the

outer layer and also the effective property of the CNT, which forms the inner core. The properties of the interphase vary within this layer according to this model. The effective property of the interphase is calculated from Wacker's model in the longitudinal direction to the fiber phase for CNT systems having neat and functionalized CNTs. It is not clearly established that the size of the interface layer is limited to only the diameter of the fiber phase. Figure 3.24 shows the variation of the axial stiffness of the interphase region along the radius. The stiffness of the CNT used is the modified stiffness of the CNT, due to the effect of the surrounding polymer or functionalization and this is one of the uniqueness of the current work.

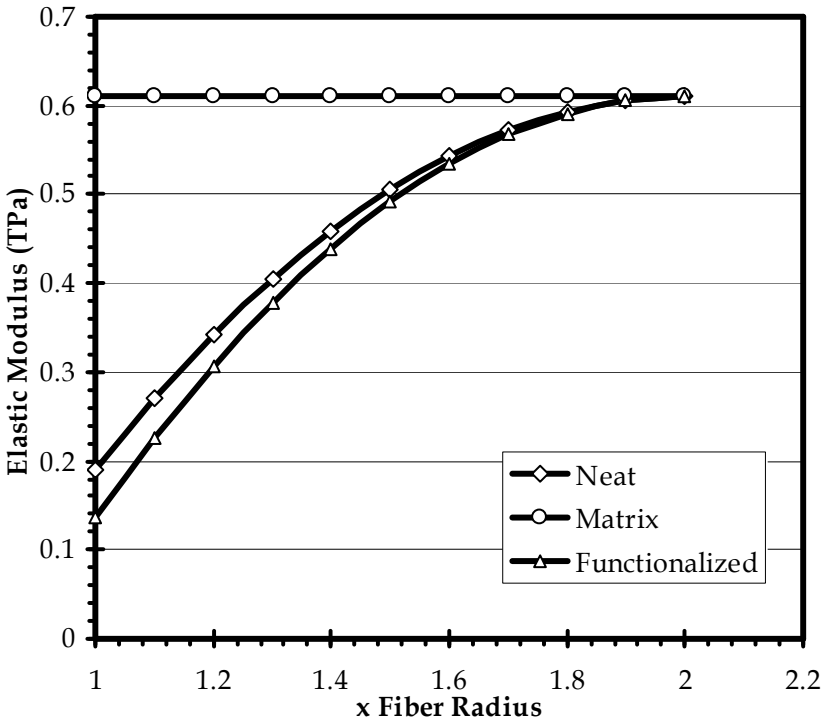

Figure 3.24 Variation of axial stiffness along the radius of the composite in the interphase region for neat and functionalized CNT systems

F. ADHESION ENERGY OF CNT COMPOSITE SYSTEMS

Most of the works in molecular simulation of the mechanical properties of CNT and CNT-reinforced composites has either been concentrated on the effect of the chirality of the CNT or the volume fraction of the CNT in composites. There have been very few reported studies [64-68] on the effect of strain on the adhesion energy of the CNT-based composite systems. The CNT-PE RVE has been analyzed using molecular dynamics with variation in the nanotube volume fractions. However, in an actual composite structure the matrix and fiber (CNT) phase undergoes strain variations. Since the effective property of the RVE is dependent on the current state of the system, a look at the adhesion energy is also important to get a reliable estimate of the bonding between the matrix and the fiber-phase. In the literature, the adhesion energy is calculated from the difference between the energy of the composite from the sum of the energy of the CNT and the polyethylene molecules [66-68]. However, in this study, a novel method of estimating the adhesion state of the CNT with the surrounding matrix is presented. The difference of the total strain energy of the deforming CNT and the CNT under the influence of the polyethylene matrix would give an estimate of the total amount of energy interaction that is occurring between the CNT and the matrix. This method can be applied to single-walled nanotubes (SWNTs) as well as doubled walled nanotubes (DWNT's).

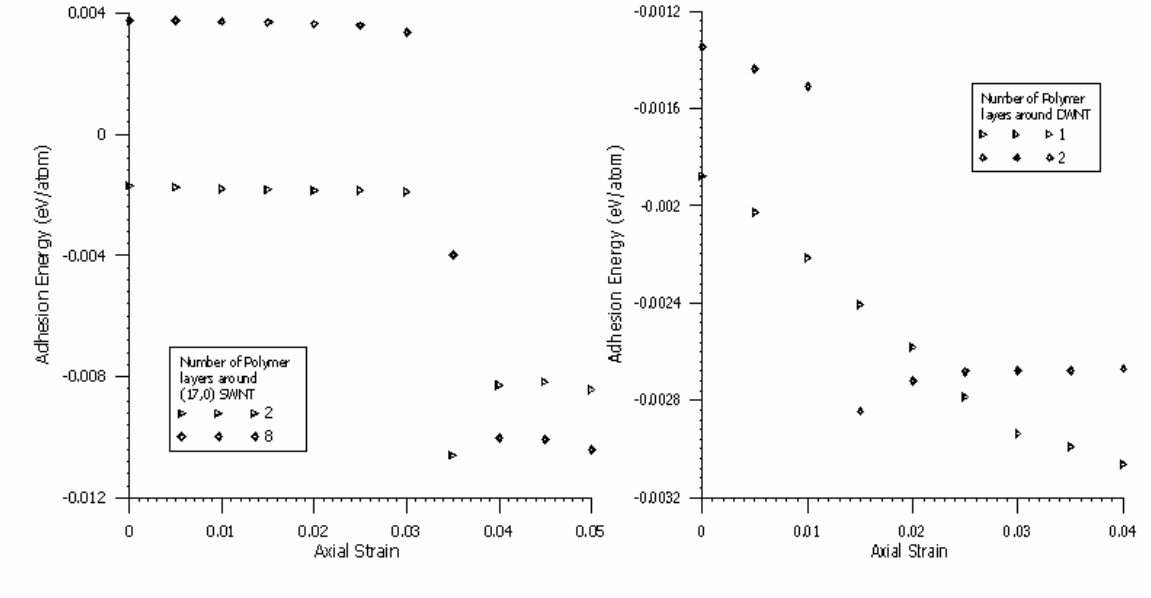

(a) (b)

Figure 3.25 Variation of adhesion energy for (a) SWNT and (b) DWNT CNT composite systems

The adhesion energy of the CNT obtained for the composite shows that there exists a zone of snap-through of the chemical bonds (see Figure 3.25a), leading to an enhancement in the interaction between the matrix and the CNT phases as been reported by Zhao et al. [67] and Heterl et al. [68]. The snap-through in the bonding is found to occur at a strain of 0.03 for SWNT, and for MWNT there does not seem to be a clear demarcation in the two zones. The zones are also found to depend on the number of polymer layers surrounding the CNT. For a large number of matrixes in the DWNT, a clear demarcation has not been observed but this does exist in a low percentage of matrix polyethylene (see Figure 3.25b). The matrix molecules in the low-volume-fraction CNT-Composite RVE have been arrested from deforming beyond a region of influence. By arresting these far away molecules, one can reduce the computational time taken for analysis. This method is justifiable because the actual effect of the surrounding molecules on the CNT is restricted to the immediate layers around the CNT and the farther the layers are, the lesser is the influence. That is to say, no direct

influence exists between a far away atom and near atom separated beyond the radius of influence of the carbon atoms in the CNT.

G. CONTINUUM VOLUME AVERAGING: MICROMECHANICAL METHOD

The outstanding scientific problem such as turbulence and nonlinear material behavior exemplifies multi-scale problems in time, length and/or energy scales. While in each of these multi-scale problems, processes occur simultaneously at various scales which affects parameters at other scales, what distinguishes one problem from the other is the degree to which each of those scales are coupled. Both experimental and computational strategies should recognize the strength of those couplings before devising methods to analyze them. In cases where the coupling is weak, each of those scales can be solved independently with a few selected parameters passing up and down the scales (e.g., elasticity, metal thermal conductivity, and so on). The main objective therefore is modeling the mechanical behavior of the heterogeneous macrostructure, made of nanocomposite materials, through numerical homogenization. The information of interest (e.g., mechanical, thermal properties, etc.,) in the atomistic level is usually "lumped" into very few macroscopic parameters like the elastic modulus, thermal conductivity etc. These properties depend on the symmetry properties of the macroscopic material [69]. These homogenization methods provide ways to predict the mechanical response of heterogeneous specimens by replacing the specimen with a homogeneous equivalent continuum through suitable averaged quantities [70]. For example the atomistic information of the mechanical properties of the individual atoms in the CNT is averaged for a CNT and this average is taken as the continuum equivalent of the elastic stiffness. The multiscale formulation, which combines the essential ideas of variational multiscale methods and Eshelby's equivalent eigenstrain principle [12, 13, 54, 55, 71], have being applied for homogenizing the displacement fields. Apart from the mechanical properties, this formulation can also deal with thermal properties in which only a few works have been reported. The method being proposed is generalized

in the sense that the cause of eigenstrain can either be due to material inhomogeneity or due to thermally or electrically induced strains.

Direct application of the micromechanical methods into the nanometer level raises several questions. A volume averaging of the constituent properties is one of the accepted methods for bridging the scales [11, 12, 19, 55, 72] and this forms the preliminary basis of a multiscale analysis. Let us consider a carbon nanotube, considered as a fiber, embedded in a matrix layer and subjected to far-field applied strain. In the eigenstrain formulation, the fiber is approximated as a distinct cylindrical inclusion in the matrix phase. Applying Eshelby's eigenstrain due to the inclusion [12, 13, 22, 73] on the matrix, the self-consistent model can be obtained (see Figure 3.26).

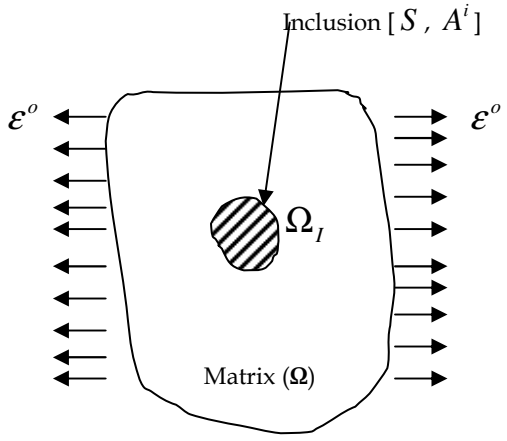

Figure 3.26 Matrix composite with an inclusion under far field - strain

The elastostatic equilibrium of a homogeneous matrix without an inclusion can be represented by the boundary value problem

$$\begin{aligned} \sigma_{ji,j} + b_i = 0 \quad & \forall x \in \Omega \in \Re^d \\ u_i = u_i^0 \ \ & \forall x \in \Gamma_u \\ \sigma_{ij} n_j = t_i^0 \quad & \forall x \in \Gamma_t \end{aligned} \tag{3.3}$$

In which σ_{ij} are the Cauchy stress components that are linked to the infinitesimal strain components by the generalized Hooke's law and the Lagrange strain defined by the gradient of the displacement field

$$\sigma_{ji} = C_{ijkl}\varepsilon_{kl} \tag{3.4}$$

$$\varepsilon_{ij} = u_{(i,j)} = \frac{1}{2}\left(u_{i,j} + u_{j,i}\right). \tag{3.5}$$

The solution of the boundary value problem with an inclusion (see Figure 3.26) can be expressed as the sum of the homogenous displacement field $\bar{u}$ and the deviation field u' caused due to the presence of an inhomogeneity given as

$$u = \bar{u} + u'. \tag{3.6}$$

By use of the far field strain conditions on a composite RVE, the deviation field can be modeled in terms of the equivalent eigenstrain. The proposed formulation involves the use of the corresponding eigenstrain in terms of the deviation field for modeling the effective modulus of the nanocomposite RVE. From the analysis carried out so far, one can estimate the stiffness variations of the functionalized CNTs as a structural unit and as embedded in the matrix. The elastic property calculated from these simulations helps in the multiscale formulations to estimate the macroscale properties of the CNT and CNT-reinforced composite structures. Estimation of the mechanical properties can be carried out by considering the volume averaging of the various measures in a mechanical straining process. For an elastic composite material, the effective constitutive relations are given by the volume average of the stress and strain [22]. Similarly, for each phase k on the micro/nano scale the constitutive relation can be given as

$$\left\langle \sigma \right\rangle_{tot}^{k} = C^{k} \left\langle \varepsilon \right\rangle_{tot}^{k} \tag{3.7}$$

In which $\langle . \rangle_{tot}^{k}$ is the volume averaged state of phase k, including the matrix, fiber and any interphase layers [13, 72], C is the elastic moduli and α, β are the Cartesian co-ordinates. The volume averaging of the state variables are given by:

$$\left\langle \bar{\sigma}_{\alpha\beta} \right\rangle_{EC} = \frac{1}{V}\int_{\Omega} \sigma_{\alpha\beta} dv\,; \qquad \left\langle \bar{\varepsilon}_{\alpha\beta} \right\rangle_{EC} = \frac{1}{V}\int_{\Omega} \varepsilon_{\alpha\beta} dv\,; \qquad \left\langle \bar{\sigma}_{\alpha\beta} \right\rangle_{EC} = C\left\langle \bar{\varepsilon}_{\alpha\beta} \right\rangle_{EC} \quad (3.8)$$

Whereas for an N particles atomic ensemble the state variables are:

$$\left\langle \bar{\sigma}_{\alpha\beta} \right\rangle = \frac{1}{N}\sum_{i=1}^{N} \sigma_{\alpha\beta}\,; \qquad \left\langle \bar{\varepsilon}_{\alpha\beta} \right\rangle = \frac{1}{N}\sum_{i=1}^{N} \varepsilon_{\alpha\beta}\,; \qquad \left\langle \bar{\sigma}_{\alpha\beta} \right\rangle = C\left\langle \bar{\varepsilon}_{\alpha\beta} \right\rangle \quad (3.9)$$

For a simple EC (see Figure 3.27) the average stresses due to the atomic ensemble is equal to the average stress due to volume averaging, establishing the relationship between the material constants derived from the MD simulation and volume averaging for use in the micromechanical techniques [22]. Applying the Eshelby eigenstrain formulation, the effect of the fiber phase on the matrix stress is captured by means of an averaged strain concentration tensor [23]. For the analysis of multiphase materials, the Mori-Tanaka (MT) method has been used to model the effective behavior of composites [19, 23, 55, 56].

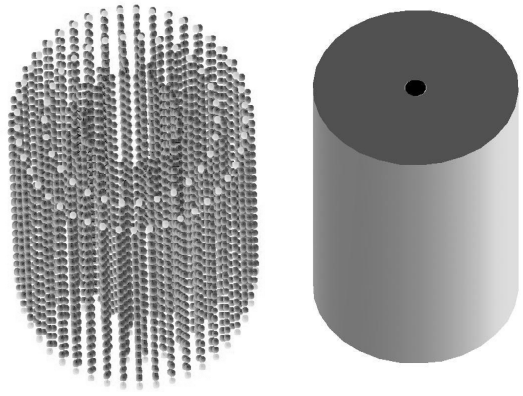

Figure 3.27 MD computational unit cell of CNT-matrix and equivalent continuum model

Consider an RVE in a CNT reinforced composite (see Figure 3.28) subjected to a homogenous displacement boundary condition which produces a uniform strain ε_{ij}^{o} in an infinite homogenous material containing an embedded inclusion shown in figure 3.26. Eshelby has shown that under the above conditions, the ellipsoidal inclusion experiences a uniform eigenstrain ε_{ij}^{*}. By applying the eigenstrain method the effective modulus of the composite RVE can be calculated (see Figure 3.19). One of the well known methods of approximation is Mori-Tanaka Method (MT). MT theory was originally concerned with the calculation of internal stress in a matrix containing inclusions with eigenstrains. The concentration matrices are determined for each phase having different properties. However, this theory is valid only for cases where the concentration of the inclusion phase is small.

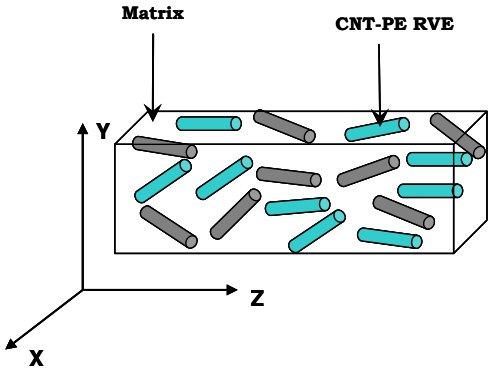

Figure 3.28 Representation of CNT reinforced composite

The MT method treats the different phases as distinct regions and does not take into consideration the geometry [23, 73]. The MT formulation followed in this work follows closely with the works of Fisher et al. [23, 60]. In a multiphase model as in the case of a fiber-interphase-matrix RVE the different regions are represented as distinct cylindrical phases equivalently dispersed in the matrix. This model is further used in the study of fiber orientations. To elucidate the expressions for MT method, assume the composite is composed of *K* phases. The stiffness of the matrix is given by C_m and the volume fraction of the matrix given by v_m. The k^{th} phase has a stiffness of C_k and

volume fraction of v_k. The dilute strain concentration factor for the k^{th} phase, A_k^{dil} relates the volume averaged strain in the k^{th} inclusion to that of the matrix [23, 73] and is obtained from

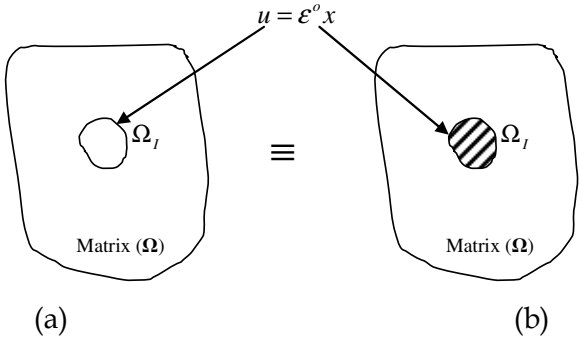

Figure 3.29 Equivalent eigenstrain inclusion for far field strains

To elucidate the expressions for MT method, assuming the composite is composed of k phases. The stiffness of the matrix is given by C_0 and the volume fraction of the matrix by v_0. The k^{th} phase has a stiffness of C_k and volume fraction of v_k. The dilute strain concentration factor for the k^{th} phase, A_k^{dil} relates the volume averaged strain in the k^{th} inclusion to that of the matrix is given by

$$A_k^{dil} = \left[I + S_k C_0^{-1} \left(C_k - C_0 \right) \right]^{-1} \tag{3.10}$$

I is the Identity tensor, S_k is the Eshelby Tensor for the k^{th} phase dispersed inclusion. The values of the Eshelby tensor for various fiber phase geometries can be obtained from literature [23, 73]. The effective modulus of the composite C is found from

$$C = \frac{\sum_{k=0}^{K-1} v_k \left\{ C_k A_k^{dil} \right\}}{\sum_{k=0}^{K-1} v_k \left\{ A_k^{dil} \right\}} \tag{3.11}$$

Thus effective material relation for the homogenized composite structure is given by

$$\left\langle \sigma \right\rangle_{tot} = C \ \left\langle \varepsilon \right\rangle_{tot} \tag{3.12}$$

The effective modulus of polyethylene matrix polymer is taken as 610 GPa [27] with a Poisson's ratio of 0.3. Mori Tanaka method has been applied to estimate the effective property of undoped CNT reinforced composites [12, 55]. In this dissertation, the applicability of this micromechanical method is extended to doped-CNTs. The continuum form of the tensile and compressive modulus of the undoped CNT is obtained by the equivalence of the strain energy and according to equations (3.7) - (3.9). The effective modulus of the doped CNT based composite is obtained using Mori Tanaka method. The overall effective strength of the matrix composite increases with increasing fiber phase as expected (see Figure 3.30 for tension and Figure 3.31 for compression of Zig-Zag CNT). One of the limitations of this analysis is the assumption that perfect load transfer exists between the CNT and the polymer matrix. Even though not ideal, valuable information on the effective strength of the resulting composite can still be determined. The significant contributions of this work are in the study of stability and estimation of elastic properties of silicon doped CNT and the estimation of effective property of doped CNT based nanocomposites.

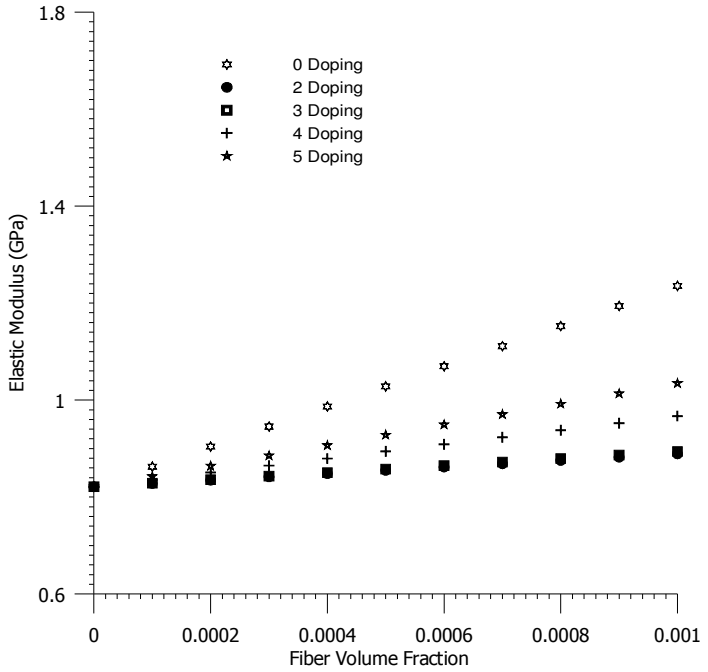

Figure 3.30 Effective tensile modulus of doped and undoped (17,0) Zig-Zag SWNT reinforced composite (modified from [12])

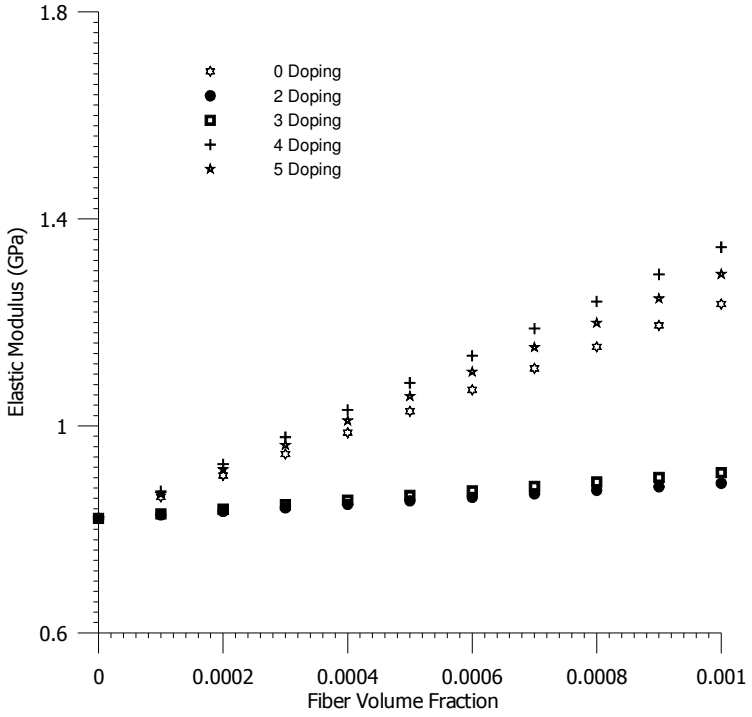

Figure 3.31 Effective compressive modulus of doped and undoped (17,0) Zig-Zag SWNT reinforced composite (modified from [12])

1. FIBER ORIENTATION MICROMECHANICAL ANALYSIS OF NANOCOMPOSITE

Micromechanical analysis of composite materials provides an estimate of their overall behavior from the known properties of the individual constituents and their detailed interaction. However, the behavior of short-fiber-reinforced composites is not only a function of the constituent properties, but also of the interfacial quality, which governs nearly all properties of a composite material. For any fibrous composite, the orientations of the fibers affect the overall properties. Apart from the molecular structure and the molecular interaction of the CNT with the matrix polymer, the large-scale morphology also affects the overall properties of the composite material. Attempts in studying the effect of CNT fiber orientation [19] were initiated by considering different orientation angles of the fiber [74-76]. In this work, the fiber orientation of the CNT-PE RVE has been studied by the Mori Tanaka method for two-phase composites

[12, 55]. Also, one can extend the model to include the CNT-Interphase RVE with the interphase and CNT RVE as equivalently distributed in the matrix (Figure 3.32).

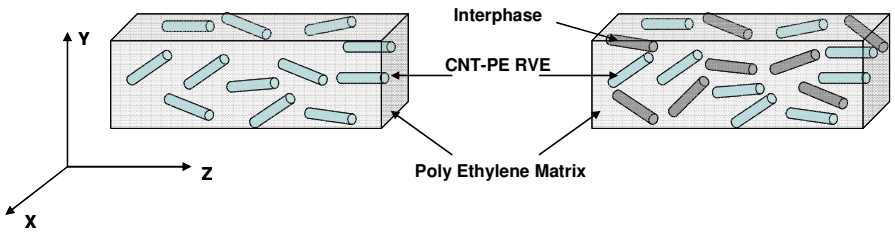

(a) without interphase (b) with interphase as a dispersed phase in the matrix

Figure 3.32 Micromechanical model of the CNT-fiber RVE orientations

The orientation of the CNT fibers affects the strain concentration tensor, and has to be modified accordingly. The strain concentration tensor is transformed from the fiber direction to the global direction by a simple transformation. The orientation average of this tensor is obtained by an averaging scheme [22, 74-76], which depends on an *orientation distribution function*. A random distribution of the fibers as well as an aligned fiber distribution is also considered in this work.

The dilute strain concentration factor for the kth phase, A_k^{dil} relates the volume-averaged strain in the kth inclusion (local direction) to that of the matrix and is obtained from

$$\left[S_k + C_m\left[C_k - C_m\right]^{-1}\right]A_r^{dil} - \sum_{n}^{K-1} v_n S_n A_n^{dil} = -\mathrm{I} \tag{3.13}$$

In which $(k,n) = \{f, g, ...K-1\}$ and S_k is the Eshelby tensor for the dispersed inclusions. The stiffness of the matrix is given by C_m; volume fraction of the matrix given by v_m. The kth phase has a stiffness of C_k and volume fraction of v_k is given as

$$\overline{A}_k^{dil} = T\, A_k^{dil} T^T \tag{3.14}$$

where T is the transformation tensor; $\overline{A}_k^{dil}$ is the transformed strain concentration tensor; and $\lambda(\phi,\gamma,\psi)$ is the orientation distribution function

$$\langle A_k \rangle = \frac{\int_{-\pi}^{\pi}\int_{0}^{\pi}\int_{0}^{\frac{\pi}{2}} A_k^{dil}(\phi,\gamma,\psi)\lambda(\phi,\gamma,\psi)\sin(\gamma)d\phi d\gamma d\psi}{\int_{-\pi}^{\pi}\int_{0}^{\pi}\int_{0}^{\frac{\pi}{2}} \lambda(\phi,\gamma,\psi)\sin(\gamma)d\phi d\gamma d\psi} \tag{3.15}$$

$\lambda(\phi,\gamma,\psi) = e^{-s_1\phi^2}e^{-s_2\phi^2}$, s_1, s_2 are factors that control the orientation [19], $s_1 = 0, s_2 = 0$ for the random distribution, and $s_1 = \infty, s_2 = \infty$ for the aligned distribution. The orientation analysis of the fiber distribution is carried out by the transformation of the fourth-order tensor followed by a spatial averaging over the RVE corresponding to the material point in the continuum, thus giving the overall averaged properties (see Figure 3.33). The fiber orientation in the RVE is subsequently defined by the orientation distribution function of the Euler angles.

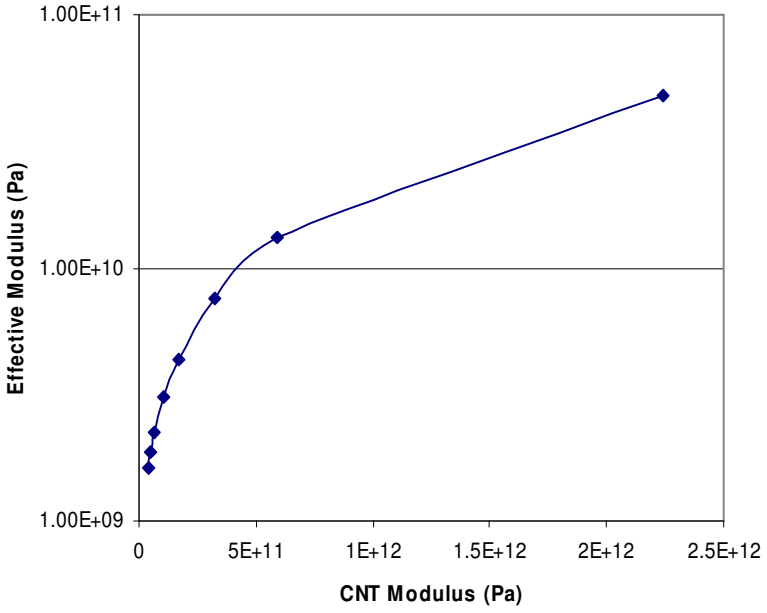

Figure 3.33 Two-phase variation of effective properties of the CNT-reinforced nanocomposite for aligned fiber

H. CONCLUSIONS

For the accurate and reliable estimation of the properties of nanocomposites an efficient multiscale modeling strategy is imperative. A multiscale computational framework would unify and improve the existing methods of analysis in the individual scales of interest and provide adequate mathematical stability and accuracy. In this chapter, the mechanical properties of the central CNT are determined when a functionalized CNT or other CNT structures are embedded in a matrix structure. In this study, the effect of chemical functionalization on the stiffness of CNTs along the tubule axis is also estimated. For the macroscopic functionalized nanocomposite structure to be stable, the functionalized CNT atomistic unit has to be stable under various conditions. The stability of the CNT affected by the substitutional changes is studied by monitoring the structural change in the CNT profile under various loading conditions. These properties help in establishing the use of functionalized CNTs in composite structures. Micromechanical techniques are used to obtain the effective properties in the homogenized mesoscale thereby bridging the different scales. This study also features a procedure for the estimation of the effective properties of the doped CNT based composite using Mori-Tanaka methods.

CHAPTER IV

ATOMISTIC-MESOSCALE COUPLED MECHANICAL ANALYSIS OF POLYMERIC NANOFIBERS*

In this chapter the theoretical analysis of Poly-(L)-Lactic Acid (PLLA) nanofibers is presented. This study aims to analyze the mechanical properties of PLLA nanofibers so that optimal scaffolds in tissue engineering applications can be developed. Analysis of PLLA nanofibers is carried out to estimate the mechanical properties from basic building blocks to the nanofibrous structures. A single PLLA nanofiber is made up of shish-kebab like fibrils intertwined together and can contain both amorphous and crystalline phases. The elastic modulus of the Lactic acid monomeric formation in the crystalline phase is derived using second-derivative of the strain energy using molecular dynamics simulation. The mechanical property of the Shish-Kebab fibril is derived by homogenization. The fiber modulus is then obtained using the Northolt and van der Hout's continuous chain theory. One of the significant contributions in this dissertation is the use of modified continuous chain theory, where a combined multiscale approach is used in the estimation of the mechanical properties of PLLA nanofibers. The theoretical results correlate well with reported experimental data.

This chapter is organized as follows. Section B describes the atomistic simulation of crystalline lactic acid using MD simulation for the estimation of the mechanical properties in the atomistic scale. Homogenization and description of the Shish-Kebab model is discussed in Section C.

---

*Part of the numerical results presented in this chapter appear in "Atomistic-Mesoscale Coupled Mechanical Analysis of Polymeric Nanofibers," by Unnikrishnan, V. U., Unnikrishnan, G. U., Reddy, J. N., and Lim, C. T., *Journal of Materials Science*, Accepted for publication. (DOI: 10.1007/s10853-007-1820-6). The original publication is available at http://www.springerlink.com.

The multiscale transfer of quantities of interest from the atomistic scale to the mesoscale by micromechanical methods is discussed in Sections D and E. In Section F, the formulation of the continuum chain model to scaleup the material properties is discussed. Section G combines the results from various methods and finally the chapter concludes with a summary in Section H.

A. INTRODUCTION

Polymeric nanofibers are attractive materials for a wide range of applications in the bio-medical, textile and other emerging technologies. This is primarily due to their large surface area to volume ratio and the unique features at the nanometer scale [77]. Structures of fibrous polymers are generally very flexible, and their conformation is easily deformed against mechanical extension or induced motion between its atoms. In any industrial application, the suitability of a material and/or structure relies significantly on their physical properties, especially their mechanical and electrical properties. Whilst the mechanical design ensures dimensional stability and structural integrity, the electrical design aims to fulfill the functionality of the products.

In recent years, polymeric nanofibers have been developed for a variety of applications such as tissue engineering, molecular filters, sensors and protective clothing [78-82]. For example, polymeric nanofibers can be used to form nanofibrous scaffolds for tissue engineering application [83]. These polymeric scaffolds allow cells to proliferate and grow into tissues with defined sizes and shapes for transplantation purposes [84, 85]. An understanding of the structure–property relationship is essential for the engineering applications of polymeric nanofibers since they are affected by the mechanical properties arise from the internal molecular structures. Tremendous savings in cost can be achieved if preliminary experimental designs can be evaluated theoretically to eliminate inferior designs and reduce the number of experiments. The proposed theoretical work in the analysis of nanofiber is primarily aimed at providing a computational framework for the estimation of the mechanical properties and to

provide a strong connection between experimental observations and theoretical analysis.

Fibers prepared from polymer solution or melt by conventional methods (melt, dry and wet spinning) have diameters in the range of 5–500 mm [86]. Recently, there has been increased interest in the fabrication of nanofibers (with diameters in the range from tens to hundreds of nanometers) using electrospinning [77, 86, 87] for mechanical characterization studies. Using molecular dynamics (MD) simulation, crystalline lactic acid monomer units are equilibrated and thermostatted to the experimental conditions by a series of NVE ensemble (Microcanonical ensemble) and NVT ensemble (Canonical ensemble) analysis and subjected to isothermal strain conditions to obtain the mechanical properties [12, 88]. To develop an optimal scaffold for tissue engineering application, it is required to manipulate the mechanical characteristics of the nanofibrous scaffolds. There has been numerous experimental studies on the design of optimal scaffolds [84]. However, very few theoretical studies exist in predicting the mechanical properties and behavior of nanofibers under external mechanical loads using multiscale simulation. This chapter aims to analyze the mechanical properties of PLLA nanofibers via an atomistic-mesoscale stimulation method.

Analysis of the orientation process during uniaxial drawing of a polymer has long been investigated in many theoretical and experimental studies [83, 89, 90]. Based on the deformation of cellulose fibers, analytical models were developed for rodlets connected by crosslinks. These models were modified with the various additions like cross-linking with forces applied to the ends of the chains as well as changes in material properties. This research leads to two different formulations for the analysis of polymeric chains: the rubber elasticity theory based on complex constitutive relations and the orientation based mechanism for the analysis of semi-crystalline polymers leading to the aggregate model [91]. The fibrils in a nanofibrous material are found to intertwine to form polymeric nanofibers. The fiber modulus is obtained using the Northolt and van der Hout's continuous chain theory [89, 92-94]. This is an enhancement over conventional homogenization techniques, because the effect of shear deformation of the fibrils is not taken into consideration. The continuum chain

formulation used in this chapter gives relationships between the macroscopic elastic constants and the orientation parameters based on the spatial distribution of the nanofibrils.

B. ATOMISTIC SIMULATION

The knowledge of structure and molecular motion in polymers is essential to understand the properties of practical interest. Theoretical simulation of the physical processes forms the first step in this work. The estimation of the mechanical properties of the PLLA fibers needs to be carried out. There are various methods of estimating the physical properties of atomistic structures, molecular dynamics (MD) simulation being one of them and is used here. Molecular dynamics has been a very popular tool for the determination of mechanical, thermal and other properties of interest in atomistic structures [2, 8, 9, 20, 27]. The starting point of a MD simulation is the non-relativistic quantum mechanical time dependent Schrödinger equation. The thermodynamic state characterized by the fixed number of atoms, volume and temperature called the canonical ensemble [27] forms the basis of the MD simulation.

The knowledge of structure and molecular motion in polymers is essential to the understanding of mechanical and thermal properties. The crystallization behaviour of PLLA shows that it is a semicrystalline polymer that crystallizes from melt and from solution to form fibres [95]. Studies on crystal structure of lactide copolymers by various studies have shown that the unit cell of PLLA is a pseudo-orthorhombic structure (a = 10.6 Å, b = 6.1 Å, and c = 28.8 Å), which is used here [96-99]. X-ray diffraction experiments and Nuclear Magnetic Resonance (NMR) analysis for the estimation of the fibrous and crystal structure of PLLA has shown that the crystalline structure of PLLA differs slightly [99] from that used by Hoogsteen et al. [96] and De Santis et al. However, these differences are not high enough to cause a change in the properties of the PLLA structure. MD analysis of crystalline PLLA is carried out with the crystal structure and the entire computational model is equilibrated to the experimental conditions (see Figure 4.1). The minimum energy condition is the starting

point for the thermostating analysis, where the crystal structure is analyzed under the influence of thermal energies. Isothermal strain conditions were applied to the thermally equilibrated unit cell and the elastic constants were obtained using second derivative elastic constant analysis [12, 31, 54].

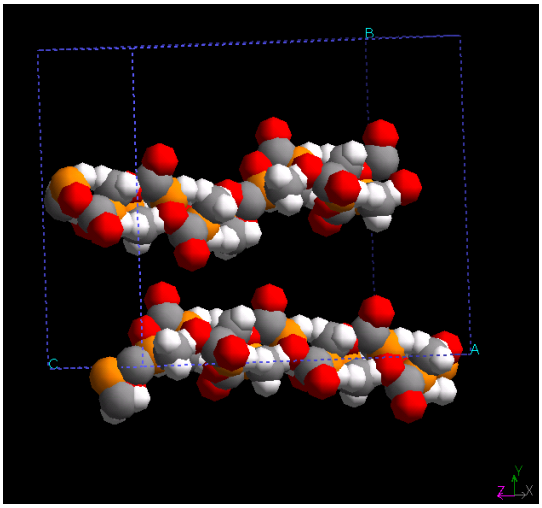

Figure 4.1 Computational domain of the cryastalline PLLA unit cell

C. SHISH-KEBAB MODEL- ELECTROSPUN NANOFIBERS

Orientation and extension of molecules in a polymer melt affects the crystallization kinetics, structure and morphology. In an entangled polymer, one of the most common crystallization formations is the Shish-Kebab structure [100-102]. The innermost portion of a Shish-Kebab structure is a long and macroscopically smooth extended chain which is crystalline in nature, called a shish. The kebabs are folded chain crystalline structures entangling the shish. The direction of growth of the kebab is normal to the shish [88]. There are various views on the formation of the Shish-Kebab structure in a crystallization process; however, in this study the interest is only in the experimentally observed shish structures in some of the very latest works on crystalline PLLA

nanofibers. Shish-Kebab structure can be found in many of the crystallization inducing processes like electro-spinning, melt spinning, etc. [87, 90, 103].

For the polymeric nanofiber, AFM imaging also reveals a ''Shish-Kebab'' structure [87, 102]. The elastic property obtained from MD analysis is used in the homogenization of the Shish-Kebab model. In this work, the homogenization of the Shish-Kebab model is proposed assuming that the homogenized axial modulus of shish is obtained from the crystalline modulus using MD simulations and the kebab modulus is obtained from the average of the modulus of the RVE in all the directions (see Figure 4.2). This assumption is valid since the Shish-Kebab model consists of only crystalline formations.

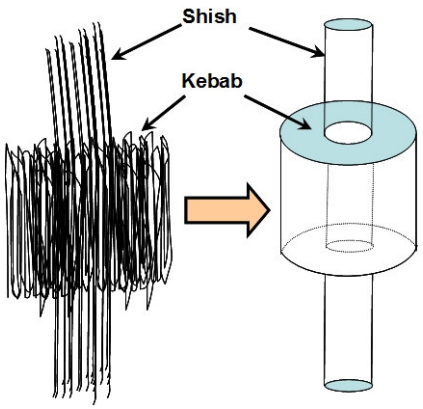

Figure 4.2 Shish-Kebab model and the homogenized equivalent continuum Shish-Kebab model

D. MICROMECHANICAL ANALYSIS

For a simple EC, the average stresses due to the atomic ensemble is equal to the average stress due to volume averaging, establishing the relationship between the material constants derived from the MD simulation and volume averaging of the state variables for use in the structural homogenization and micromechanical techniques. Structural models have been developed for foams and cellular materials based on a unit cell. Though these models are based on the information that the porosity of the material is above 70%, this method can be used in the present analysis, as there is a large expected

range of porosity of the polymeric fiber based on experimental studies [54]. The effective modulus by the structural model is given as [104]

$$\frac{E^*}{E} = 2.3\left(\frac{\sqrt{3}}{2}(1-\Phi)\right)^3 \tag{4.1}$$

Another structural-based homogenization procedure for porous material such as foam, called the 3D open cell material model, is from Gibson and Ashby [104]. The effective modulus of the porous material is related to the fiber modulus by [104]

$$\frac{E^*}{E} = (1-\Phi)^2. \tag{4.2}$$

According to Thelen et al. [104], the 3D open cell model is based on assumptions of high porosity; and it gives good predictions of modulus for materials with porosities in the range of 10 to 90%. The nanofibrous materials definitely fall in this range, and therefore, this model can be used in the conservative prediction of the elastic modulus [95, 105, 106]. However, the major drawback of the methods mentioned above is that the actual amount of voids present in the nanofibers is not known for comparing with experimental data. Hence the porosity based methods cannot be used for a reliable estimate of the stiffness of the nanofiber and, therefore, one need to look at theories that take into consideration both the porosity and orientation of the nanofiber constituents.

E. CONTINUUM VOLUME AVERAGING

Applying the Eshelby eigenstrain formulation, the effect of the fiber phase on the matrix stress is captured by means of an averaged strain concentration tensor [12]. The strain concentration tensors for various morphologies of the fiber phase are considered to cause corresponding eigenstrains on the matrix layer. This can be analyzed using the Mori-Tanaka (MT) method which has been discussed in Chapter II. The MT

formulation used in this work follows closely with that of Fisher et al. [23]. In a multiphase model (i.e. material with multiple inclusions), as in the case of a void-PLLA RVE, the different regions are represented as distinct cylindrical phases equivalently dispersed in the matrix (see Figure 4.3). This model is further used in the study of fiber orientations.

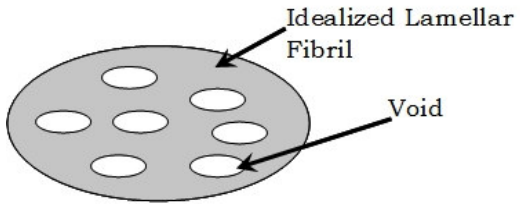

Figure 4.3 Idealized lamellar fibril homogenized model

F. CONTINUOUS CHAIN MODEL OF POLYMERIC FIBERS

Subsequent to the homogenization of the Shish-Kebab model, it is found that a fibril intertwines around other fibrils to form the nanofiber. Tan and Lim [87] have reported that a fibril might terminate by connecting another fibril or it may branch into two others. This type of complex intertwining cannot be modeled by simple homogenization techniques and therefore a detailed analytical procedures need to be considered. The deformation characteristics of an oriented crystalline polymeric fiber have to take into consideration, apart from the mechanical properties of the material, the molecular arrangement in the nanoscale, and at larger length scale [94, 107]. The model used in this chapter is based on the analysis of extension of oriented crystalline fibers called the continuum chain model. However, this theoretical formulation is extended by incorporating the effect of the smaller-scale material properties by adequate homogenization techniques. It has also been experimentally shown that a polymeric fiber experiences shear deformation when subjected to a tensile test [93]. The elastic deformation of a crystalline fibril is the result of the extension of the chain, which is the predominant effect, and the shear between adjacent chains is the secondary effect [89, 108].

The continuous chain model (series model) developed by Northolt and van der Hout [89, 94, 109] is used for the description of the tensile deformation of the fibers (see Figure 4.4). This model describes the deformation of a polymeric fiber as the sum of a linear extension and a rotation of the chains towards the fiber axis. The deformation of the fiber is taken as the average deformation of a polymer chain in the direction of the fiber axis as is shown in Figure 4.5. Detailed description of the continuous chain model can be found in Northolt [95], and Northolt and van der Hout [89]. The elastic and shear modulus (E_c, G_c) of the chain used is modified in this model by the homogenized elastic and shear modulus ($E_c(S, v_S, v_k)$, $G_c(S, v_s, v_k)$), which are functions of (1) the Eshelby tensor (S) for the circular inclusions, and (2) the volume fraction of the shish and kebab (v_S, v_k) or an equivalent homogenized structure. Thus, the effective fiber modulus is obtained by

$$\frac{1}{E_{fiber}} = \frac{1}{E_c(S, v_s, v_k)} + \frac{\left\langle \sin^2\theta \right\rangle_E}{2G_c(S, v_s, v_k)} \tag{4.3}$$

where E_{fiber} is the fiber modulus, $\left\langle \sin^2\theta \right\rangle_E$ is the strain orientation parameter and is given by the equations (4.4) and (4.5) [89, 93]:

$$\left\langle \sin^2\theta \right\rangle_E = \frac{\int_0^{\pi/2} \rho(\theta) \cos\theta \sin^3\theta \, d\theta}{\int_0^{\pi/2} \rho(\theta) \cos\theta \sin\theta \, d\theta} \tag{4.4}$$

The modified fibril strain can subsequently be written as the sum of the elastic strain and the strain due to elastic rotation or shear of the fibrils as given by

$$\varepsilon_f = \frac{\sigma}{E_f(S, v_s, v_k)} + \frac{\left\langle \sin^2\theta \right\rangle_E}{2} \left(1 - e^{-\frac{\sigma}{g(S, v_s, v_k)}} \right) \tag{4.5}$$

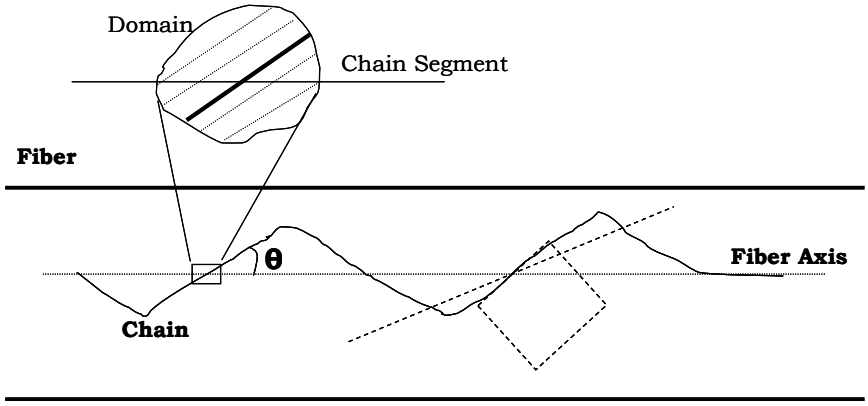

Figure 4.4 Schematics of a chain, a chain segment and the surrounding domain in the analysis using a continuous chain model

G. RESULTS AND DISCUSSION

There is a wide range in the reported values of the mechanical properties of PLLA fibers [89, 93, 94, 108, 109]. These are primarily affected by various factors like rate of drawing of the polymer, temperature and crystallinity of the polymer material [89, 93, 109]. Most of the studies carried out so far do not take into consideration the porosity of the nanofiber. There have been very few studies on the internal structure of an electrospun nanofibrous material and most of these studies have been aimed at providing the factors affecting the nanofiber dimensions [110, 111]. The mechanical stiffness of the nanofiber obtained by using Timoshenko beam theory and ordinary beam bending theory give conservative values. These results are not reliable since they do not capture the inherent orientation inhomogeneity of the nanofiber. The material modeling strategy used here is novel as it considers the inhomogeneity of the nanofiber and the orientation of the fibrils [83, 87, 90, 103]. This modeling procedure is carried out by using mathematically well established multiscale modeling simulation techniques coupling the atomistic scale to macroscopic scales. To the best knowledge of the authors, such a methodology of extracting the material properties from a completely computational point of view (independent of experimental data) for nanofibers has not

been attempted**.** As homogenization methods considering only the individual aspects of material modeling at different scales are available in literature, a multiscale computational framework is being proposed in this work. The material properties are extracted from the molecular to the macro level, and finally validated with independent experimental results. The uniqueness is in the multiscale approach proposed here.

High strength PLLA fibers of the order of 16 GPa with high crystallinity and porosity has been produced by dry spinning [106]. Leenslag and Pennings has reported a tensile modulus of 14 GPa for solution-spun PLA fibers [105]. Numerous studies by researchers have produced high modulus PLLA fibers for various uses, having elastic modulus ranging from 1 - 20 GPa. For example, Tan and Lim [103] reported elastic modulus values of 1 GPa to 10 GPa, Hoogsteen et al. [96] 16 GPa, Yuan et al. [112] 1 to ~5 GPa, Broz et al. [113] 3.0 GPa, and Cicero and Dorgan [114] reported 1.5 to 3.0 GPa for different draw ratios. Inai et al. [77] reported the elastic modulus in the range of 2.9 ± 0.4 GPa for semi-crystalline electrospun polymeric PLLA fibers. Most of the above reported values were attained by the estimation of elastic stiffness in tension. Flexural modulus in the range of 6-9 GPa was obtained by Lim et al. [115].

The Young's modulus obtained from MD analysis of crystalline lactic acid should conform to the experimental value of the modulus of crystalline PLLA [116]. The experimentally obtained elastic modulus for a ~90% crystalline PLLA made by a hot drawn (melt spinning) process is 9.2 GPa [116] and a Poisson's ratio of 0.44 has been reported by Balac et al. [117]. In this study, an elastic modulus of 9.44 GPa and a Poisson's ratio of 0.4 were obtained using MD simulations. As the elastic modulus obtained in this analysis conforms to the experimental values, it is used in the higher scale homogenization processes.

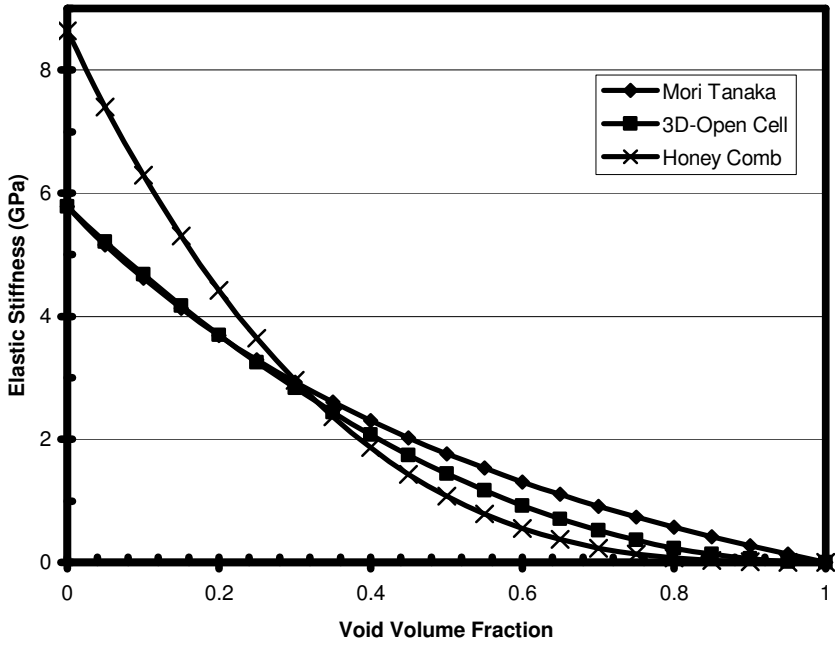

Figure 4.5 Variation of elastic modulus of nanofibers with void volume fractions

The elastic stiffness calculated using the Mori-Tanaka, 3-D open cell and honeycomb structure models is given in Figure 4.6. It can be seen that the predicted stiffness values has a maximum of 5.9 GPa and decreases with an increase in porosity. The amount of porosity is also indicative of the diameter of the fiber, as the diameter increases the porosity of the fiber also increases as seen from experimental observations [87]. It can be seen from Figure 4.5 that with an increase in diameter the elastic stiffness would decrease. This method, however, fails to provide an accurate estimation of the elastic modulus of nanofibrous materials, when compared to experiments (see, for example, Inai et al. [77]). The average elastic property obtained by homogenization of the Shish-Kebab model is used in the modified continuum chain model. In this continuum chain model, the homogenized elastic property is predicted by Equation 17 using the strain orientation parameter derived from the birefringence data (Equation 18). This analytically predicted elastic modulus of PLLA fibers (as shown in Figure 4.6) closely matches with the experimental values of Mezghani [118]. The stress-strain

curves, using the continuum chain model and the experimentally determined values for different draw velocities by Inai et al. [77] is compared in Figure 4.7. From the figure, it can be seen that the predicted stress-strain curve lies closer to the higher draw velocity curve. The modified continuum chain model predicts a stiffer fiber due to the inadequate information on the internal structure of the nanofiber. With a better understanding of the internal structure a more refined estimate of the stress-strain curve can be obtained.

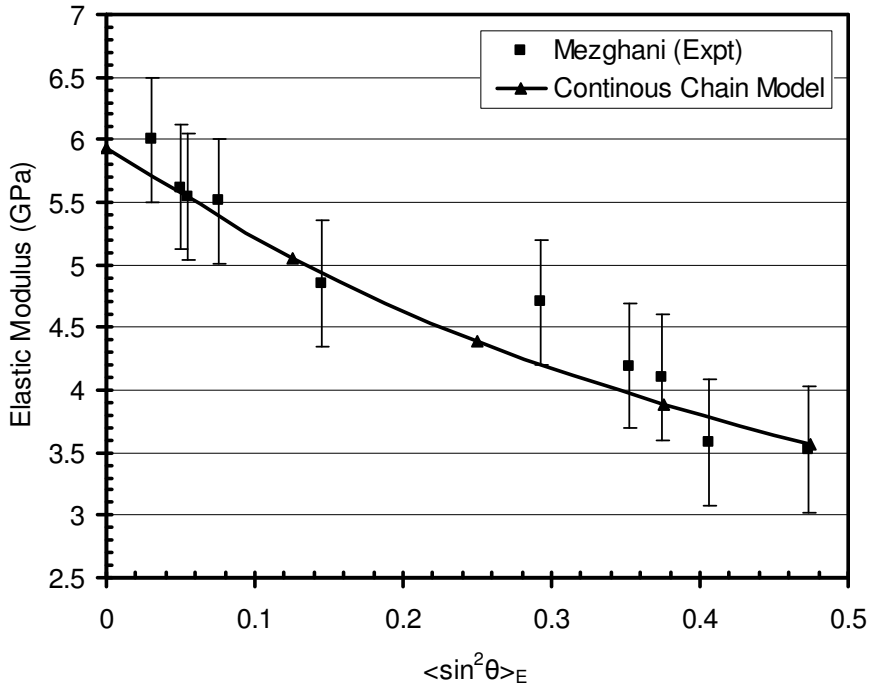

Figure 4.6 Variation of elastic modulus with the strain orientation parameter

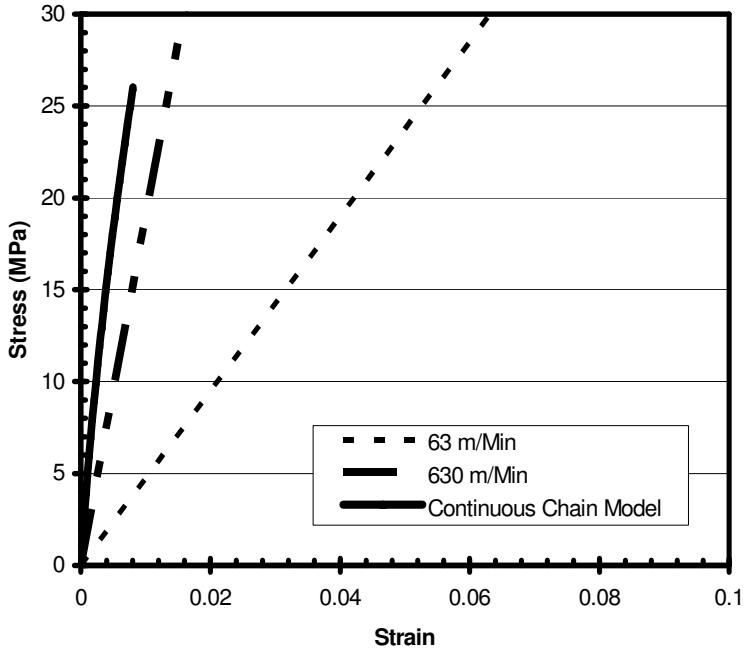

Figure 4.7 Comparison of stress- strain curves with that obtained from experiments

H. CONCLUSIONS

In this study, a multiscale modeling approach is used to obtain the effective elastic modulus of the PLLA nanofiber. The analysis is carried out from the atomistic level using MD simulation to obtain the crystalline elastic modulus. The next scale of modeling is the homogenization of the Shish-Kebab model using the Mori-Tanaka method. Based on this homogenization principle, the modified elastic constants are obtained and are subsequently used in the homogenized-continuum chain model to obtain the macroscale homogenized elastic modulus. The highlight here is the multiscale method of estimating the elastic properties of PLLA nanofibers, as compared to previous computational procedures that depend solely on either the conventional continuum chain model or atomistic simulations only. The simulation results obtained show excellent correlation with that of experiments, even without involving any experimental data in the analysis.

CHAPTER V

SPECTRAL/*hp* BASED ASYMPTOTIC EXPANSION HOMOGENIZATION OF HETEROGENEOUS MEDIA: ANALYSIS OF NANOSTRUCTURES

In this chapter a two scale asymptotic expansion homogenization of heterogeneous structures is carried out using spectral/*hp* finite element methods. For a realistic estimation of the properties of the processes that occur in the mesoscale and how they affect the macroscopic mechanical properties, multiscale computational homogenization models needs to be employed. The model should take into consideration the volume average of the properties in the atomistic scale and transfer of these properties to the next higher scales of interest. Two scale asymptotic expansion homogenization methods is a mathematical homogenization procedure where the material heterogeneities with a periodic microstructure are homogenized. For applications having high-field gradients the use of lower order finite element methods are unsuitable and requires higher order finite element methods. The developed computational procedure is applied to the multiscale homogenization of carbon nanotube based nanocomposites and self reinforced Poly-Lactic acid composites.

This chapter is organized as follows. The physical problem is described in Section B followed by the asymptotic expansion homogenization method. This section also deals with the spectral/*hp* finite element method along with the formulation of the combined spectral/*hp* with the AEH. Numerical examples with both verification and analysis of CNT-based nanocomposites and the analysis of polylactic acid nanofiber are given in Section C. The chapter concludes with a discussion of the results and a summary in Section D.

A. INTRODUCTION

In a multiscale model, the material and structural behavior is manifested as processes occurring in different time, length and energy scales. For each of these multi-scale problems, the processes occurring simultaneously at one scale affect the parameters at the other scales. However, what distinguishes one problem from the other is the degree to which each of these scales is coupled. For both experimental and computational strategies, one need to understand the strength of those couplings before devising methods to analyze them. The information of interest (e.g., mechanical, thermal properties, etc.,) at the atomistic level is usually "lumped" into very few macroscopic parameters like the elastic modulus, thermal conductivity etc. These lumped-up properties depends on the symmetry properties of the macroscopic material [119]. The homogenization methods provide ways to predict the mechanical response of heterogeneous specimens by replacing the specimen with an equivalent homogeneous continuum through suitable averaged quantities [70].

The mathematical homogenization methods are based on the assumption that there exist two or more scales of interest. These are the nanoscale, the microscale, mesoscale and the macroscale. In this homogenization principle two scales of interest are considered The microscale is being homogenized into the mesoscale where continuum principles are assumed to be valid. Homogenization reduces the computational size of the problem by decoupling the scales of interest into what can be considered as a macroscale problem and a microscale problem. Homogenization method based on a two-scale asymptotic expansion was developed for composites by Bensoussan et al [120, 121]. The common homogenization methods currently are based on three principles namely: conventional mechanics based modeling, homogenization theory, and finite element methods based homogenization techniques. This method is effective in evaluating both macroscopic constitutive equations and microscopic distributions of stress and strain in such composites. The advantage of asymptotic expansion based homogenization method is that the microscopic as well as the macroscopic stress and strain states in composites can be analyzed [122].

Asymptotic expansion homogenization (AEH) methods have been applied for the simulation of various applications in elasto-plastic and structural problems [120, 123-131]. The macroscale and the microscale problems essentially mean that the physics of the problems defined in these scales are different and therefore the bridging can be done by various methods. Most of the works in AEH uses the conventional finite element methods. However, the use of higher order finite element methods like spectral element methods is important for the analysis of problems involving complex geometries or high gradient fields. The *spectral element method* was first presented by Patera [132] for the solution of Navier-Stokes equations. A detailed history of the development of spectral element methods can be found in [133]. Based on the immense popularity of the spectral/*hp* finite element method in the solution of problems in solid and fluid mechanics [133-139], they are combined with the asymptotic expansion homogenization method for the multiscale simulation of Carbon Nanotube (CNT) based nanocomposites.

The nanometer dimension of a CNT and its interaction with a polymer chain requires a study involving the coupling of the different length scales [6, 14, 15, 18, 26, 140, 141] using multiscale modeling techniques. Modeling phenomenon in the continuum scale was mainly carried out by describing conservation laws and constitutive relations. These methodologies were successful and great strides were made in the understanding of solid and fluid mechanics problems [52, 136, 142]. One of the biggest drawbacks of the continuum theory of macromechanical processes is that as one goes down the scale, the theories defining the continuum formulations becomes questionable [143]. In this chapter, the mechanical properties of the CNT-based nanocomposite structures are analyzed using the developed multiscale modeling by spectral/*hp* asymptotic expansion homogenization method.

Polymer nanofibers are very attractive materials for wide range of applications in bio-medical industry, textile industry and other emerging technologies. This is because of their large surface area to volume ratio and the unique features in the nanometer dimensions [77]. Structures of fibrous polymers are generally flexible, and

their conformation is easily deformed against some mechanical extension or induced motion between the atoms.

An understanding of the structure–property relationship is essential for the engineering applications of polymeric nanofibers since they are affected by the mechanical properties arise from the internal molecular structures. Tremendous savings in cost can be achieved if preliminary experimental designs can be evaluated theoretically to eliminate inferior designs and reduce the number of experiments. To develop an optimal scaffold for tissue engineering application, it is required to manipulate the mechanical characteristics of the nanofibrous scaffolds. There has been numerous experimental studies on the design of optimal scaffolds [84]. However, very few theoretical studies exist in predicting the mechanical properties and behavior of nanofibers under external mechanical loads using multiscale simulation. The multiscale analysis of Poly-Lactic acid fibers has been carried in an earlier study by Unnikrishnan et al. [54] using Modified Continuum Chain Model [89, 94]. In this chapter, the mechanical properties of PLLA nanofibers are analyzed via the developed multiscale spectral/*hp* AEH finite element method.

B. THE DESCRIPTION OF THE PHYSICAL PROBLEM

The main feature of this multiscale method is to use the homogenized material properties derived from the atomistic or Y- scale (nanometer) and apply them in the micro level or X-scale (micrometer) as shown in Figure 5.1a. This process of homogenization uses the concept of volume averaging. The micro-level property can subsequently be translated to the structural level by considering the homogenized region as representing an inclusion surrounded by a homogenous matrix layer. Since the macroscopic continuum formulations are valid in this regime, computational techniques for the analysis of macroscopic bodies can be applied. The equivalent body which in the ε-space, is a realistic representation of the heterogeneous structure with proper boundary conditions and under the action of various external forces (see Figure 5.1a). The AEH therefore isolates the atomistic from the mesoscale by approximating

with a homogenized body in X and a scaled representative unit cell in Y. The solution in the smooth scale (here mesoscale) is affected by the ε–scale inhomogeneity and the solution gets modified appropriately (see Figure 5.1b).

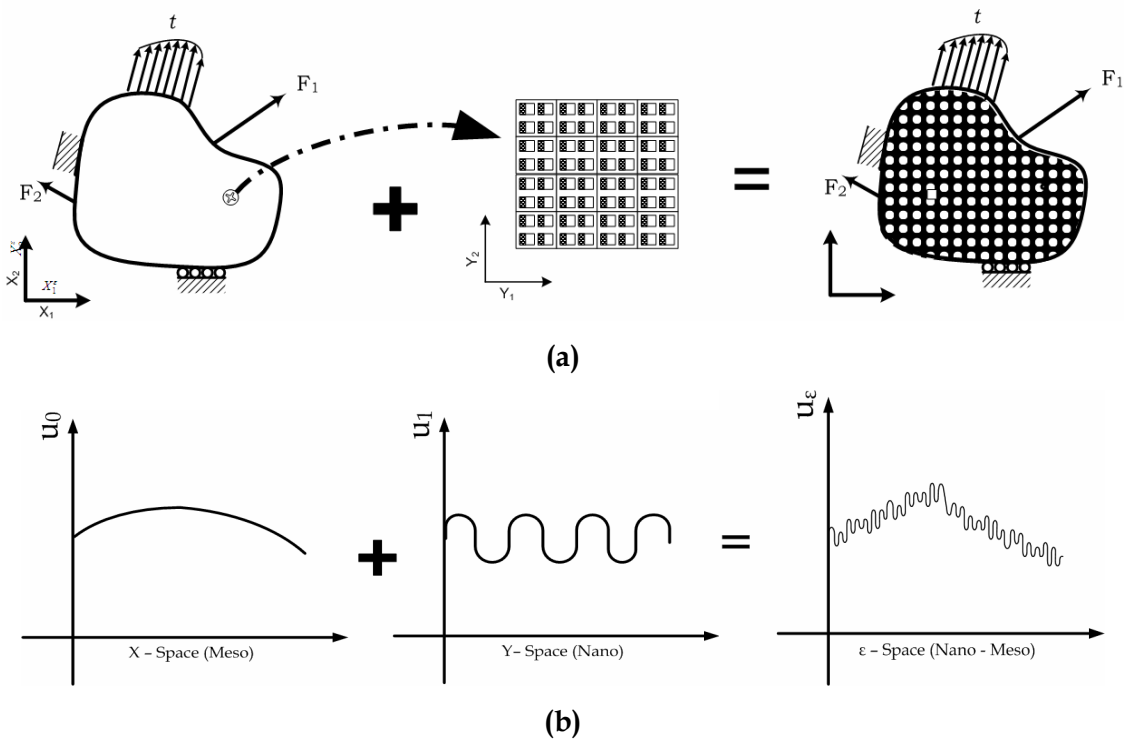

Figure 5.1 (a) Physical representation of a multiscale heterogeneous structure and (b) the mathematical solution of the problem

1. ASYMPTOTIC EXPANSION HOMOGENIZATION

Asymptotic expansions are applied in the analysis of mathematical functions to describe its behavior in a limiting situation. Such methods are called "perturbation methods". A perturbation method is a method of approximating the solution of problems involving a small parameter that can be obtained by expanding in an asymptotic series. When a function $y(x,\varepsilon)$ depends on a small parameter ε and the solution of the governing equation for this function is known when $\varepsilon = 0$, then a

perturbation method may prove useful in obtaining a solution for small values of ε. Such an approach is particularly attractive when the governing equation is nonlinear and no general techniques are available for exact solution. If ε appears as a multiplicative factor in a term in the governing equation, the standard approach is to try a power series solution as given in equation (5.1). This series function is now substituted in the governing equations and boundary conditions. The coefficients of the same powers of ε are grouped to yield an equivalent number of equations which are solved sequentially.

$$y(x,\varepsilon) = y_0(x) + \varepsilon y_1(x) + \varepsilon^2 y_2(x) + ... \tag{5.1}$$

Two-scale asymptotic expansion homogenization method is one such method of mathematical homogenization in which the material heterogeneities with a periodic microstructure are homogenized. The material can be considered to consist of two scales, (1) a micro Y scale described by atoms interacting through a potential and (2) a macro X scale described by continuum constitutive relations (see Figure 5.2). The periodic Y scale can have inhomogeneities like dislocations, impurity atoms etc. This type of multiscale homogenization substantially decreases the computational size of the problem by decoupling the scales into a micro scale and a macro scale.

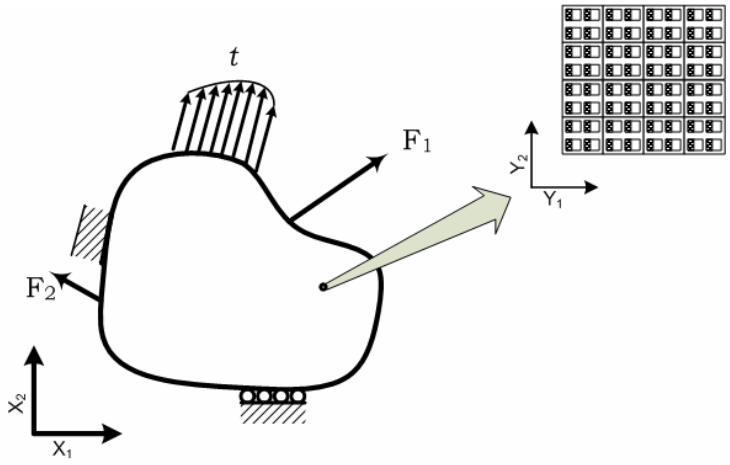

Figure 5.2 Two-scale system of composite structure for AEH

To begin with let us consider a simple case in which a body **Ω** with an internal periodic structure consisting of atleast two constituents is subjected to macroscopically uniform strain and stress. Consider a two-coordinate system, i.e., macroscale coordinate system $X(x_1, x_2)$ and a mesoscale coordinate system $Y(y_1, y_2)$, related by the scale ratio ε as:

$$\frac{Y(y_1, y_2)}{X(x_1, x_2)} = \varepsilon \tag{5.2}$$

where X can describe the global structure as well as the local region and Y describes the microstructure [125, 128, 138, 144, 145]. A homogenization framework thus facilitates this weak coupling between the lower scale and the higher scale. In order to decouple the length scales, one must appreciate the weak convergence properties by considering the limit of the time-independent asymptotic expansion parameter $\varepsilon \to 0$. When a load is applied to a composite structure, the periodicity of the local region is maintained and therefore the mesoscale is assumed to deform uniformly. This assumption forms the basic premise of the deformation characteristic of a two scale material structure. Let us consider a simply connected domain in $\Re^d$ $(d = 1, 2)$, with body force b under equilibrium. The solution is to find a set of admissible function u^ε. The field equations for overall material $\left(X^\varepsilon\right)$ can be given by:

$$\frac{\partial \sigma^\varepsilon}{\partial x^\varepsilon} + f = 0 \qquad \forall\, x \in \Omega \in \Re^d \tag{5.3}$$

with boundary conditions

$$\begin{aligned} u^\varepsilon &= u \qquad \forall\, x \in \Gamma_u \\ \sigma^\varepsilon n &= \bar{t} \qquad \forall\, x \in \Gamma_t \\ \sigma^\varepsilon &= C\ e^\varepsilon \\ e^\varepsilon &= \frac{\partial u^\varepsilon}{\partial x} \end{aligned} \tag{5.4}$$

σ_{ij} is the Cauchy stress component and is related to the Lagrange strain (ε_{ij}^{e}) component by the elasticity tensor (C_{ijkl}). Now, expanding the primary variables as an asymptotic series, one obtains

$$u^{\varepsilon} = u^{(0)}(x,y) + \varepsilon u^{(1)}(x,y) + \varepsilon^2 u^{(2)}(x,y) + .. \tag{5.5}$$

The functions $\mathrm{u}^{(\mathrm{i})}(\mathrm{x},\mathrm{y})$ are Y periodic in variable y and are independent of the scaling parameter ε. Strain can be expanded in an asymptotic expansion

$$e\left(u^{\varepsilon}\right) = \frac{1}{\varepsilon}\left(\frac{\partial u^{(0)}}{\partial y}\right) + \left(\frac{\partial u^{(0)}}{\partial x} + \frac{\partial u^{(1)}}{\partial y}\right) + \varepsilon\left(\frac{\partial u^{(1)}}{\partial x} + \frac{\partial u^{(2)}}{\partial y}\right) + \ldots \tag{5.6}$$

The constitutive equation is substituted in the equilibrium equation and the coefficients of the powers of ε are separated to get the three hierarchical equations as shown below.

$$\frac{\partial}{\partial y}\left(C\frac{\partial u^{(0)}}{\partial y}\right) = 0 \tag{5.7}$$

$$\frac{\partial}{\partial y}\left(C\left(\frac{\partial u^{(0)}}{\partial x} + \frac{\partial u^{(1)}}{\partial y}\right)\right) + \frac{\partial}{\partial x}\left(C\ \frac{\partial u^{(0)}}{\partial y}\right) = 0 \tag{5.8}$$

$$\frac{\partial}{\partial y}\left(C\left(\frac{\partial u^{(1)}}{\partial x} + \frac{\partial u^{(2)}}{\partial y}\right)\right) + \frac{\partial}{\partial x}\left(C\left(\frac{\partial u^{(0)}}{\partial x} + \frac{\partial u^{(1)}}{\partial y}\right)\right) + f\ = 0 \tag{5.9}$$

In the homogenization process, the terms with the same order of the perturbation parameter must be equal to zero so as to ensure the asymptotic series approximation to be valid as this parameter approaches zero. From equation (5.7), $u^{(0)}$ is independent of the local co-ordinate system y as shown in equation (5.10).

$$u^{(0)}(x,y) = u^{(0)}(x) \tag{5.10}$$

Now, using the transformation as shown in equation (5.11), where, χ_i^{kl} is called the elastic corrector or characteristic function and is clearly independent of $u^{(0)}$,

$$u^{(1)} = \chi \frac{\partial u^{(0)}}{\partial x} \tag{5.11}$$

the microscale equation in equation (5.8) becomes

$$\frac{\partial}{\partial y}\left(C \left(\delta.\delta + \frac{\partial \chi}{\partial y} \right) \right) \frac{\partial u^{(0)}}{\partial x} = 0, \tag{5.12}$$

which in variational form, is given as

$$\int_Y C \frac{\partial \chi}{\partial y} \frac{\partial v}{\partial y} dY = \int_Y v \ \frac{\partial C}{\partial y} dY . \tag{5.13}$$

The corrector term in macro scale is due to microscale perturbations. The Y scale here is composed of a finite element mesh depicting a composite RVE and the macroscopic behavior can be solved by the following equilibrium equation.

$$\frac{\partial}{\partial y}\left(C \left(\frac{\partial u^{(1)}}{\partial x} + \frac{\partial u^{(2)}}{\partial y} \right) \right) + \frac{\partial}{\partial x}\left(C \left(\frac{\partial u^{(0)}}{\partial x} + \frac{\partial u^{(1)}}{\partial y} \right) \right) + f \ = 0 \tag{5.14}$$

Upon application of the mean operator on this equation, by virtue of Y-periodicity of $\mathrm{u}^{(2)}$, the above equation reduces to

$$\frac{\partial}{\partial x}\left(C^H \left(\frac{\partial u^0}{\partial x} \right) \right) + f \ = 0 \tag{5.15}$$

where C^H is the homogenized elasticity matrix for the overall region given by

$$C^H = \frac{1}{|Y|}\int_Y \left(\delta.\delta + \frac{\partial \chi}{\partial y} \right) dy \,. \tag{5.16}$$

2. SPECTRAL/*hp* FINITE ELEMENT METHOD

The spectral element method was developed to combine the advantages of the spectral method with the ability of the finite element method to handle higher gradient fields and geometries [146]. Spectral element methods require fewer degrees of freedom to obtain the required accuracy than the normal finite element methods however requires more work per degree of freedom as the degree of the element is generally higher [147].

Let $\bar{\Omega}$ be the closure of an open bounded Lipshcitz domain $\Omega \subset \Re^2$ and let $\mathrm{x} = (x, y)$ be a point in $\bar{\Omega} = \Omega \cup \partial\Omega$ where $\partial\Omega = \Gamma$ is the boundary of Ω. The *hp*-version of the finite element method [148] is of interest here. In *h*-, *p*-, *hp*-FEM, the approximation spaces V are spaces of the piecewise polynomials. While the formulation of the finite element methods is independent of the actual choice of the polynomial basis, using the basis of the spatial approximation the analysis can be easily carried out in the framework of Legendre methods [134, 135].

Given that $V \subset H_0^1(\Omega)$ then the finite element method states: find $u \in V$ such that $H_0^1(\Omega) = \left\{ \psi \in H^1(\Omega) \middle| \psi(\Gamma) = 0 \right\}$; where, Γ denotes the boundary of Ω. Discretization of the governing differential equation is based on the spectral element method (SEM), which is a high-order weighted residual technique similar to the finite element method. The nodes of the Lagrange polynomials are taken to be the Gauss-Lobatto-Legendre (GLL) quadrature points [149, 150]. Within each element the basis functions are based on tensor-products of n^{th}-order Lagrange polynomials [132, 151-153]. For two-dimensional elements, one can construct two-dimensional basis functions as the tensor product of one-dimensional Legendre basis functions as given below:

$$\psi_i(\xi,\eta) = h_j(\xi) h_k(\eta) \text{ where } i = 1,.....P^2 \text{ and } j,k = 1,.....P \tag{5.17}$$

Here, P denotes the number of Gauss-Legendre-Lobatto (GLL) points in each direction (ξ,η) and $P = p+1$ where p denotes the polynomial order of the Legendre basis functions. The one dimensional Legendre basis function given by

$$h_i(\xi) = \frac{\left(1-\xi^2\right) L_p'(\xi)}{p(p+1) L_p(\xi_i)(\xi-\xi_i)} \tag{5.18}$$

in which L_p is the p[th] order Legendre polynomial and L_p' is the derivative. In order to keep the Legendre basis function general the following form of the shape functions is utilized.

$$h_i(\xi) = \prod_{\substack{j=1 \\ j\neq i}}^{P} \left(\frac{\left(\xi-\xi_j\right)}{\left(\xi_i-\xi_j\right)} \right) \tag{5.19}$$

$$\frac{\partial h_i}{\partial \xi}(\xi) = \sum_{\substack{k=1 \\ k\neq i}}^{P} \prod_{\substack{j=1 \\ j\neq i}}^{P} \left(\frac{1}{\xi_i-\xi_k} \right) \left(\frac{\xi-\xi_j}{\xi_i-\xi_j} \right) \tag{5.20}$$

where ξ_i, ξ_j and ξ_k are the permutations of the collocation points. In the spectral element method the control points or nodes of the finite element mesh are chosen to be the n+1 Gauss-Lobatto-Legendre (GLL) points which are roots of the relation given below:

$$\left(1-\xi^2\right) L_h'(\xi) = 0 \tag{5.21}$$

where $L_h'(\xi)$ denotes the derivative of the Legendre polynomial of degree p. It is due to the fact that the combination of the LaGrange interpolants with the GLL quadrature leads to an exact diagonal mass matrix. The nodes of the Lagrange polynomials are

taken to be the Gauss-Lobatto-Legendre (GLL) quadrature points as shown in Figure 5.3.

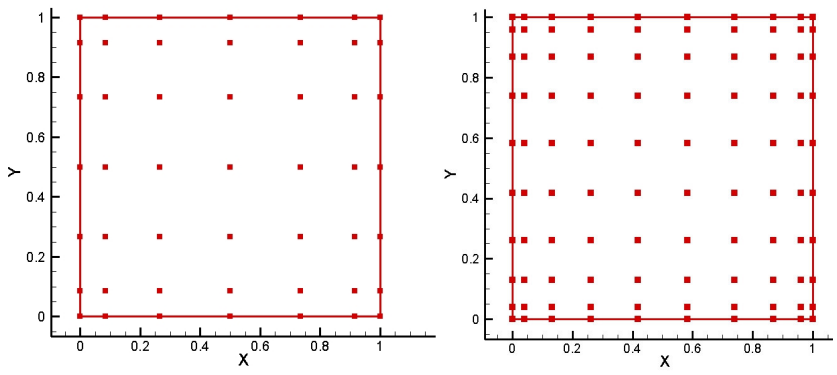

Figure 5.3 Computational domain of the Y-periodic unit cell

3. SPECTRAL/*hp* – AEH FORMULATION

In this chapter the AEH – homogenized constitutive equation in equation (5.16) is solved by the finite element method with appropriate boundary conditions (BC) to give the solution corrected for atomic scale effects. This method needs to be applied by considering the unit cell to be under periodic boundary conditions. In this simulation, the periodic boundary condition (PBC) is maintained by arresting the corresponding degrees of freedom at the edges of the unit cell. The variational form of the microscale equation in equation (5.22) can be discretized using Lagrange shape functions and suitable quadrature rules.

$$\int_Y C \frac{\partial \chi}{\partial y} \frac{\partial v}{\partial y} dY = \int_Y v \frac{\partial C}{\partial y} dY \tag{5.22}$$

This form of the variational statement can be considered by assuming the usual finite element strain matrix which is related to the displacement field by the element strain matrix given by

$$\{e\} = [B]\{u\} \tag{5.23}$$

in which

$$[B] = Dh = \begin{bmatrix} \frac{dh_1}{dx} & 0 & \frac{dh_2}{dx} & 0 & \dots & \frac{dh_n}{dx} & 0 \\ 0 & \frac{dh_1}{dy} & 0 & \frac{dh_2}{dy} & \dots & 0 & \frac{dh_n}{dy} \\ \frac{dh_1}{dy} & \frac{dh_1}{dx} & \frac{dh_2}{dy} & \frac{dh_2}{dx} & \dots & \frac{dh_n}{dy} & \frac{dh_n}{dx} \end{bmatrix}, \tag{5.24}$$

and the stress would be given by

$$\{\sigma\} = [C][B]\{u\} \tag{5.25}$$

Thus, the finite element analogue of the variational equivalent of the BVP in the y-periodic domain is given by [128]

$$\int_{Y^e} [B]^T [C][B] dy^e [\chi] = \int_{Y^e} [B]^T [C] dy^e \tag{5.26}$$

Subsequently, the solution of the homogenized material property would reduce to the following for each element in the FE Mesh as

$$\left[C^h\right] = \sum_{e=1}^{n_{elm}} \frac{V_e}{V_{tot}} [C]\left([I] - \left[B^e\right]\left[\chi^e\right]\right) \tag{5.27}$$

In which $\left[C^h\right]$ is the homogenized property matrix; n_{elm} is the number of elements in the unit cell; $[I]$ identity matrix; $\left[B^e\right]$ is the element strain matrix; $\left[\chi^e\right]$ is the matrix of nodal χ values.

C. NUMERICAL STUDIES

1. VERIFICATION OF THE FORMULATION

To illustrate the foregoing methods by a numerical example, let us consider a glass-epoxy composite material with varying volume fractions [125, 144, 154, 155]. The following material properties have been taken:

Epoxy: E = 3.5 GPa; v = 0.35
Glass: E = 70.0 GPa; v = 0.2.

The computational domain is shown in Figure 5.4a and the variation of corrector term in the unit cell is shown in Figure 5.4b. . In the computations, the periodic boundary conditions are enforced in the unit cell by arresting the degrees of freedom in all the external nodes. Spectral element analysis of the asymptotic expansion homogenization is carried out for various spectral degrees using Lagrange polynomials. The homogenized stiffness values obtained from AEH have been compared with the variationally consistent Hashin-Shtrikman upper and lower bounds as well as the Voigt and Reuss bounds. It was also observed by various researchers [125, 154-156] that the homogenized material properties actually lies close to the lower bounds as observed in Figure 5.5. The homogenized elastic constants is now given against the fiber phase volume fraction for various polynomial expansions using the developed spectral/*hp* finite element as is shown in Figure 5.6. It should be noted that there is a rapid convergence in the homogenized material constant, as the spectral degree was increased and therefore polynomial order above 4 are not required [157].

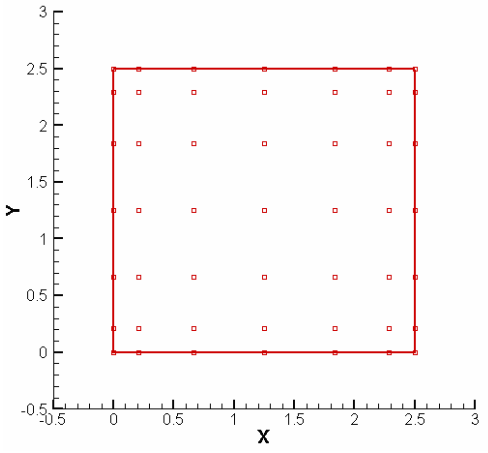

(a)

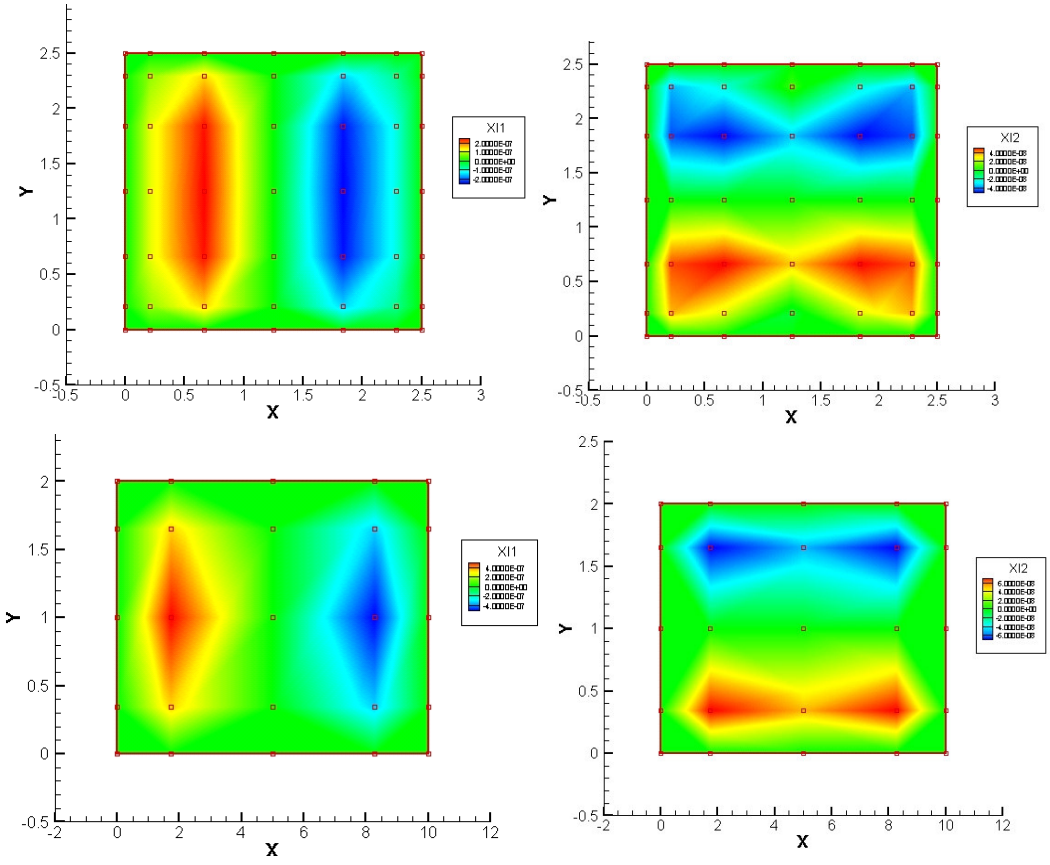

(b)

Figure 5.4 (a) Computational domain of the Y-periodic unit cell (b) contour plot of the elastic corrector function [χ_i^{kl}]

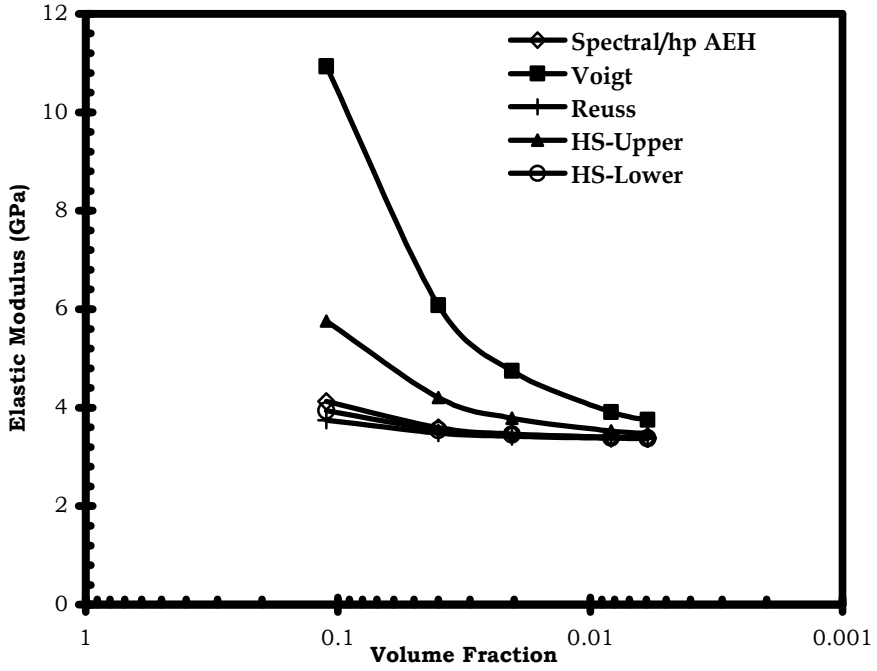

Figure 5.5 Variation of the AEH based homogenized elastic-material constants and comparison with the Voigt, Reuss, Hashin-Shtrikman (HS) upper, and lower bounds

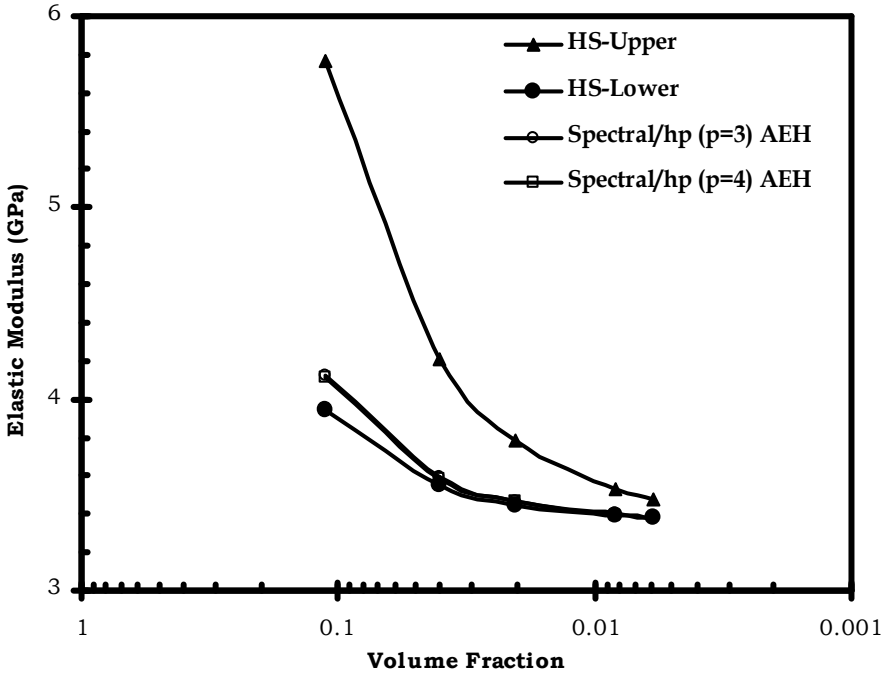

Figure 5.6 Variation of the AEH based homogenized elastic material constants and comparison with the Hashin-Shtrikman bounds for various spectral degrees

2. SPECTRAL/*hp* BASED AEH OF NANOCOMPOSITE STRUCTURES

Polymer-based composites reinforced with carbon fibers have been widely used in advanced structures. Use of CNT as potential composite reinforcements has many advantages over conventional fibers. The enhanced mechanical strength of CNT is one of the primary advantages. Few theoretical works have been undertaken to ascertain the effective properties of CNT-based polymers and experimental studies have found a 25% to 40% increase in strength [27]. CNT-based nanocomposites are analyzed by considering neat, functionalized and embedded CNTs as being dispersed in a matrix and the atomic interactions between the atoms of the CNT and matrix is studied by MD simulations [19, 20, 27, 30, 120]. The problem is different from a conventional fiber composite material as the fiber phase interacts with the matrix phase through molecular interactions. In a conventional composite material analysis, the material/mechanical properties of the participating phases are widely studied. This is however not the case with the nanometric sized fibers, as the material properties are still being debated and even weak molecular interactions are found to alter the overall properties drastically [2, 12]. Another multiscale method involves the use of micromechanical schemes to model the mesolevel and subsequently use the continuum formulation for scaling the domain of interest [52]. The obvious drawback of such an approach is that the local variations in morphology and structure are not considered or do not translate to the macroscopic scale.

a. NANO-MESOSCALE COUPLING

The elastic property calculated from the atomistic simulations helps in the multiscale formulations to estimate the macroscale properties of the CNT and CNT-reinforced composite structures. These simulations can be carried out by considering the volume averaging of the various measures in a mechanical straining process. For an elastic composite material, the effective constitutive relations are given by the volume average

of the stress (σ) and strain (ε) [22]. Similarly, for each phase k, on the micro/nano scale the constitutive relation can be given as

$$\left\langle \sigma \right\rangle_{tot}^{k} = C^{k} \left\langle \varepsilon \right\rangle_{tot}^{k} \tag{5.28}$$

In which $\left\langle . \right\rangle_{tot}^{k}$ is the volume-averaged state of phase k, including the matrix, fiber and any interphase layers [13], C represents the elastic moduli and α, β are the Cartesian co-ordinates. The volume averaging of the state variables are given in equation (5.29) and for an N particles ensemble is given in equation (5.30). The average stresses due to the atomic ensemble is equal to the average stress due to volume averaging in an EC thereby establishing the relationship between the material constants derived from molecular dynamic simulation and volume averaging for use in the micromechanical techniques from an earlier publication by the author [12].

$$\left\langle \overline{\sigma}_{\alpha\beta} \right\rangle_{EC} = \frac{1}{V} \int_{\Omega} \sigma_{\alpha\beta} dv \,; \qquad \left\langle \overline{\varepsilon}_{\alpha\beta} \right\rangle_{EC} = \frac{1}{V} \int_{\Omega} \varepsilon_{\alpha\beta} dv \,; \qquad \left\langle \overline{\sigma}_{\alpha\beta} \right\rangle_{EC} = C \left\langle \overline{\varepsilon}_{\alpha\beta} \right\rangle_{EC} \tag{5.29}$$

$$\left\langle \overline{\sigma}_{\alpha\beta} \right\rangle = \frac{1}{N} \sum_{i=1}^{N} \sigma_{\alpha\beta} \,; \qquad \left\langle \overline{\varepsilon}_{\alpha\beta} \right\rangle = \frac{1}{N} \sum_{i=1}^{N} \varepsilon_{\alpha\beta} \,; \qquad \left\langle \overline{\sigma}_{\alpha\beta} \right\rangle = C \left\langle \overline{\varepsilon}_{\alpha\beta} \right\rangle \tag{5.30}$$

Let us now consider a cylindrical RVE of a CNT-reinforced composite structure. Considering an axisymmetric model of the plane as shown in Figure 5.7a, a finite element mesh of the half plane can be constructed and AEH can be used to extract the homogenized mesoscale material property (see Figure 5.7b). A neat CNT and functionalized nanocomposite ensemble are studied in this chapter. Perfect load transfer is assumed in many of the works in CNT-composite models [2] and in cases where this perfect condition is not achieved, the effective load transfer is enhanced using functionalization of the CNTs.

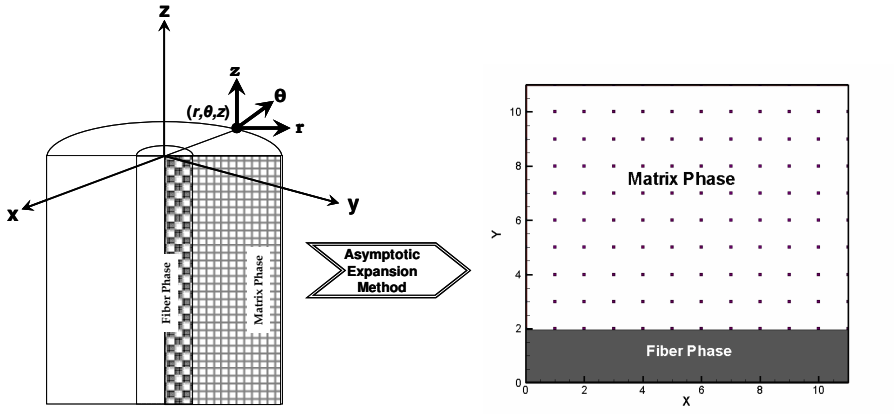

(a) (b)

Figure 5.7 (a) Homogenization of a nanocomposite RVE and (b) computational domain of the Y-periodic unit cell

b. NUMERICAL ANALYSIS

The following material properties are taken in the numerical simulation.

Matrix Phase: E = 610 MPa; ν = 0.3

Fiber Phase: Neat CNT, E = 922 GPa; ν = 0.3;

Functionalized CNT = 872 GPa; ν = 0.3.

Embedded CNT = 648.3 GPa; ν = 0.3.

The variation of the elastic corrector function, which is also dependant on the position of the fiber phase, is shown in Figure 5.8. The elastic corrector function which is dependant on the position of the fiber directly influences the homogenized material property. The effect of various volume fractions of the fiber phase is studied for a polynomial expansion degree 2 and it can be seen that the homogenized properties obtained by the method described in this chapter lies within the Voigt-Reuss bounds for neat, functionalized and CNT embedded in matrix respectively as shown in Figures 5.9 a, b and c respectively. The difference between the two methods is due the difference in the solution strategy in Song et al. [158] which is a three dimensional analysis while this chapter uses a two dimensional analysis. The effect of the aspect ratio on the effective

property is also carried out and it can be seen that there is negligible effect on the variation of the aspect ratio of the fiber on the overall effective property as shown in Figures 5.10. Thus it can be seen from the above analysis that use of higher order finite element is advantageous in the estimation of the effective proprieties of composite structures without resorting to intense computational resources, forming the major contribution of this work.

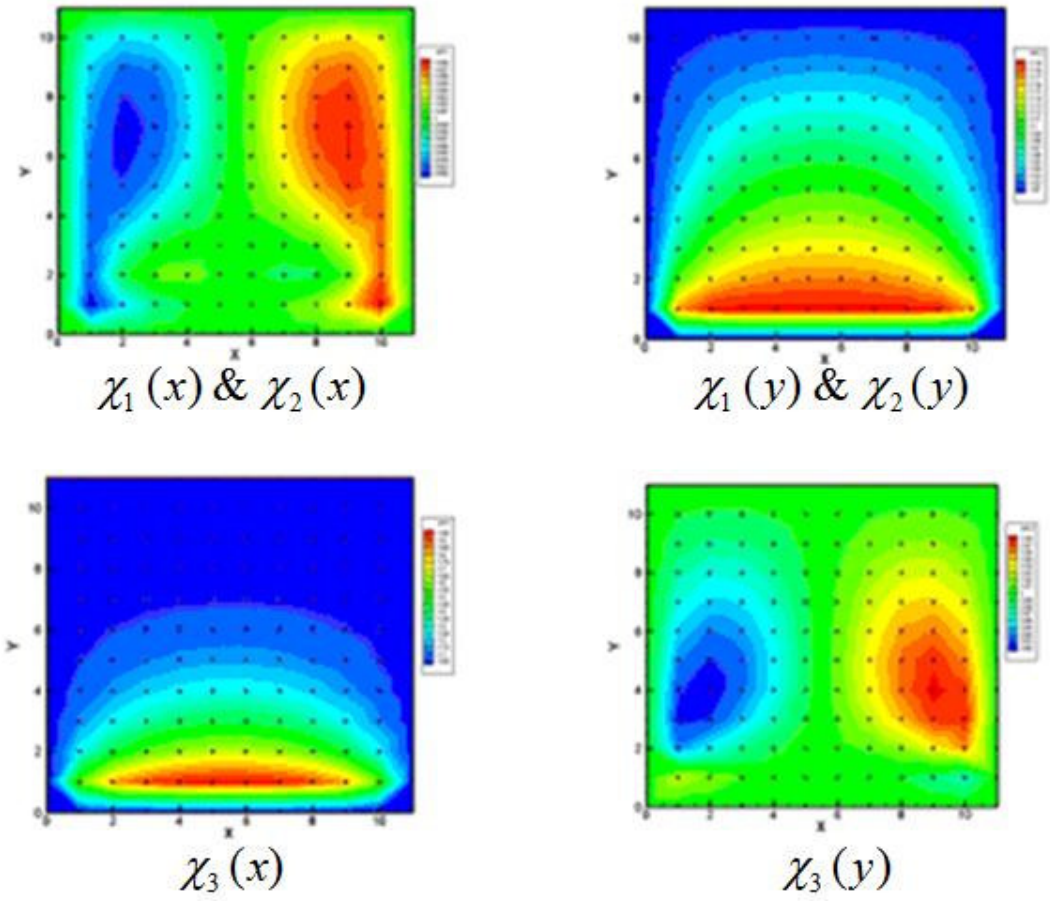

Figure 5.8 Contour plot of the elastic corrector functions [χ_i^{kl}]

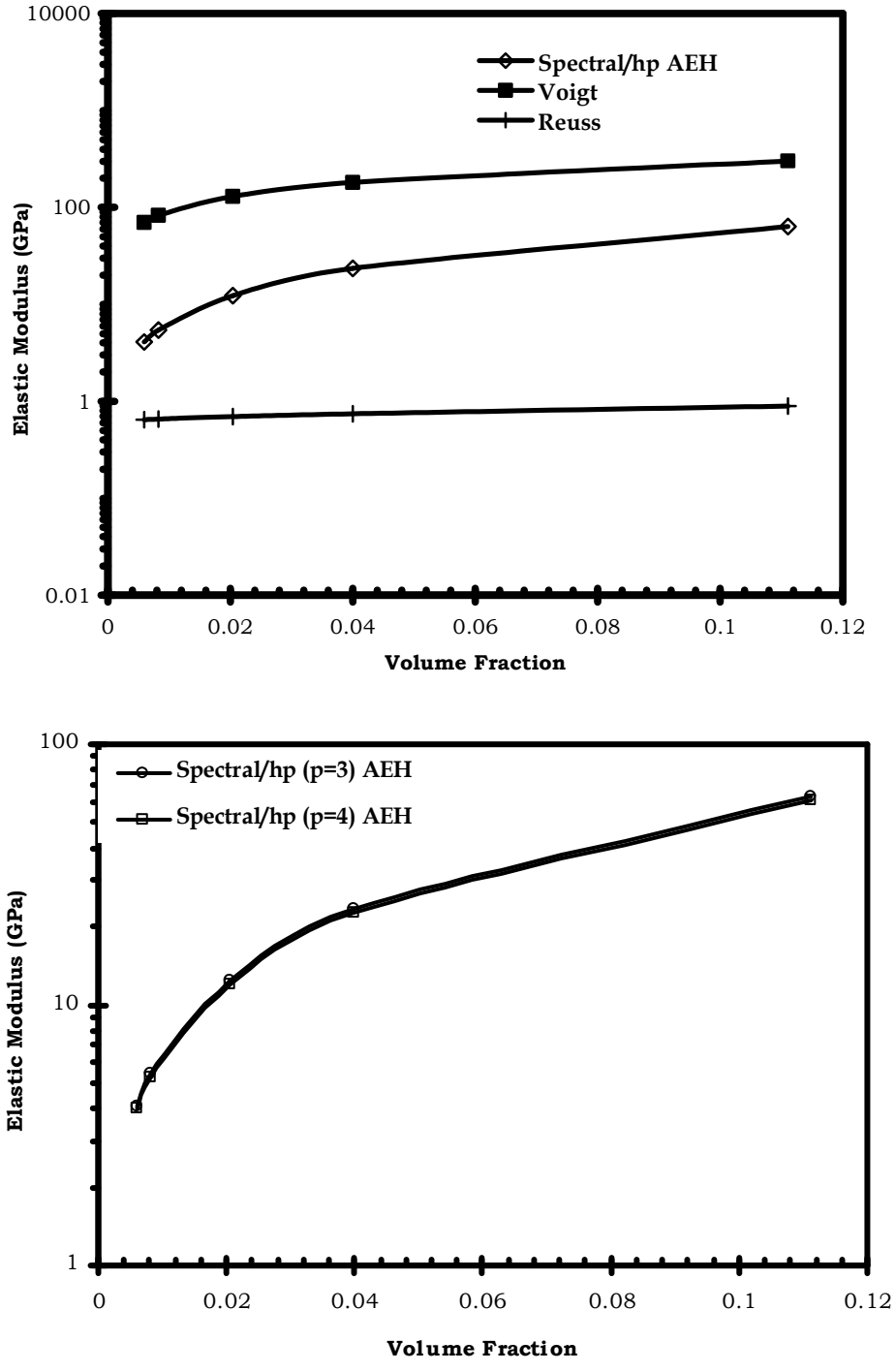

(a) Neat CNT

Figure 5.9 Variation of axial elastic modulus with spectral degrees for various CNT volume fractions

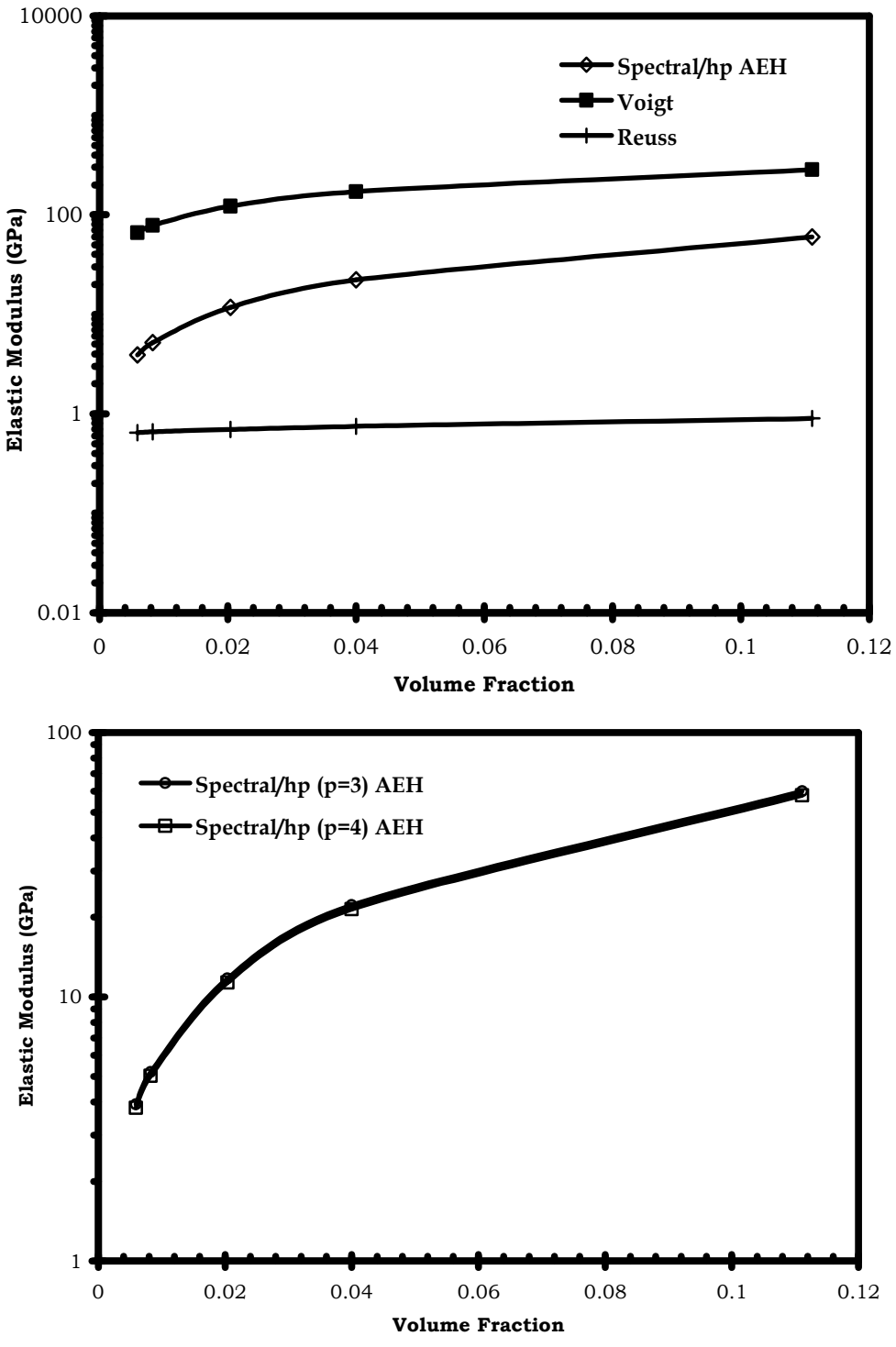

(b) Functionalized CNT

Figure 5.9 Continued

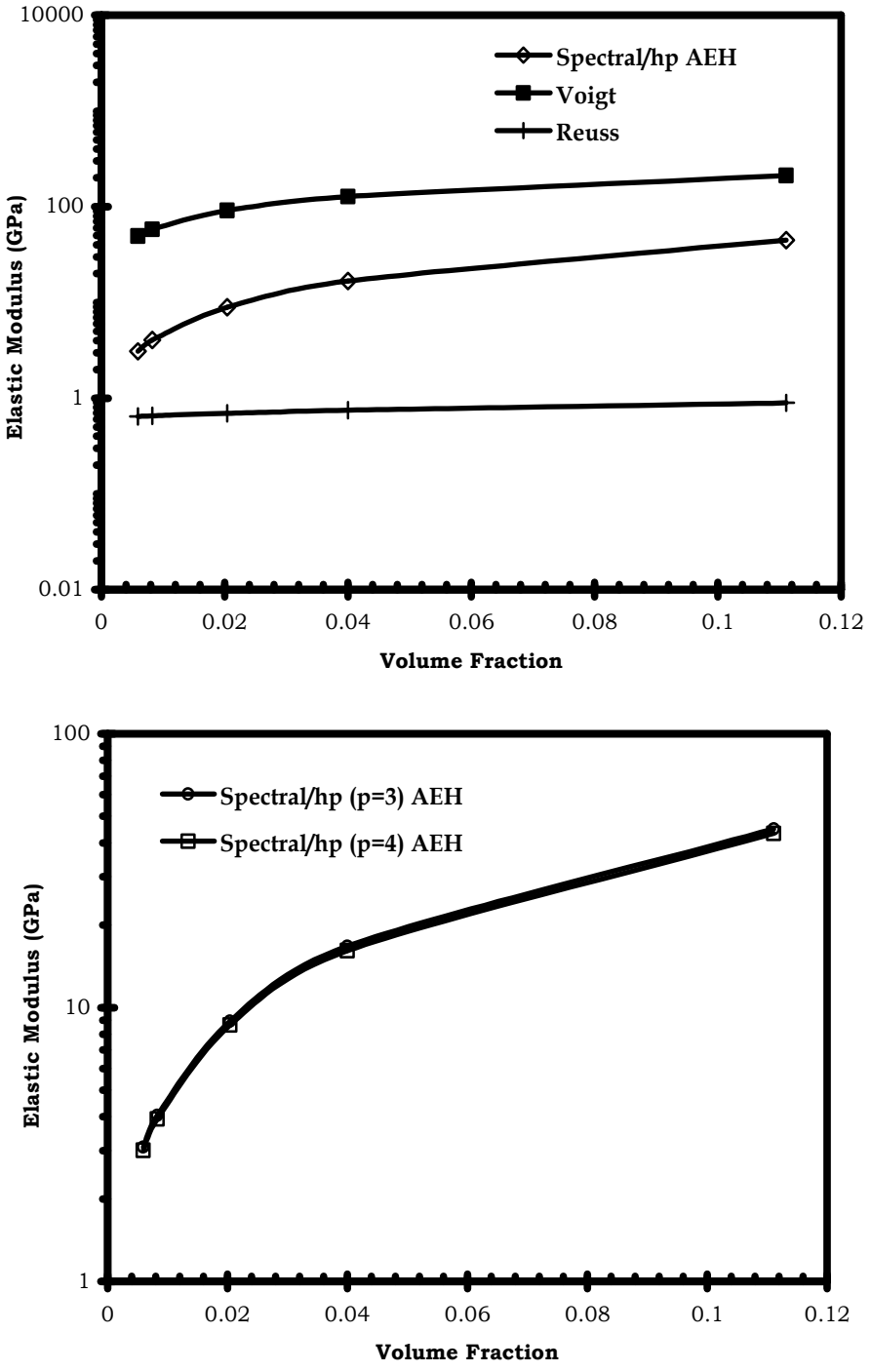

(c) CNT embedded in a Matrix

Figure 5.9 Continued

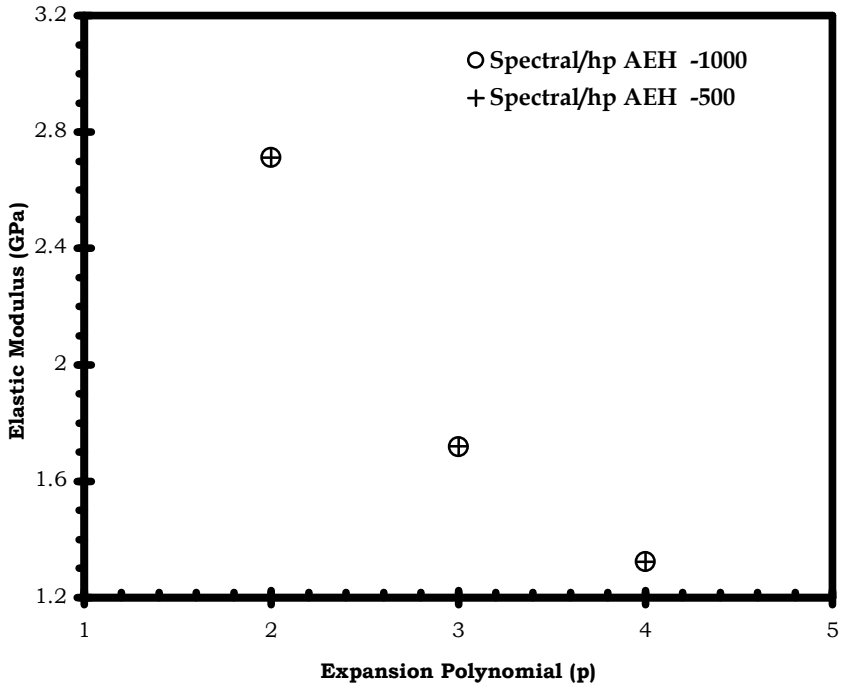

Figure 5.10 Variation of elastic stiffness with neat CNT volume fraction with spectral degree for fiber aspect ratio of 500 and 1000

3. ANALYSIS OF PLLA NANOFIBERS

Orientation and extension of molecules in a polymer melt affects the crystallization kinetics, structure and morphology. In an entangled polymer, one of the most common crystallization formations is the Shish-Kebab structure [100-102]. The innermost portion of a Shish-Kebab structure is a long and macroscopically smooth extended chain which is crystalline in nature, called a shish. The kebabs are folded chain crystalline structures entangling the shish. The direction of growth of the kebab is normal to the shish [88]. For polymeric nanofibers, AFM imaging also reveals a ''Shish-Kebab'' structure [87, 102]. In a previous work by the authors, the analysis of the elastic properties of the PLLA nanofibrous ensemble was estimated by homogenization of the Shish-Kebab model. It is assumed that the homogenized shish axial modulus is obtained from the crystalline modulus using molecular dynamics simulations and the kebabs modulus is

obtained form the average of the modulus of the RVE in all the directions (see Figure 5.11) [54].

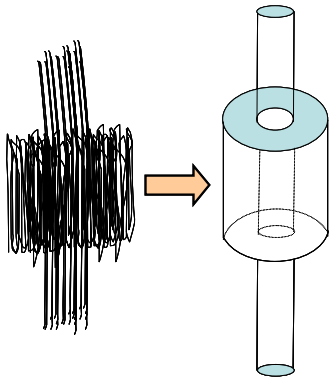

Figure 5.11 Shish-Kebab model and homogenized equivalent continuum Shish-Kebab model

Let us now consider a cylindrical RVE of an equivalent Shish-Kebab cylindrical model as shown in Figure 5.11. Considering an axisymmetric model of the plane as shown in Figure 4a, one can construct a finite element mesh of the half plane and, using the spectral/*hp* AEH finite element, the homogenized mesoscale material property can be obtained.

The following material properties are used in the numerical simulation.

Average Shish modulus of 5.14445 GPa

Crystalline modulus: 9.4425 GPa

Average Poisson's Ratio=0.4

The homogenized elastic constants in the mesoscale are shown in Figure 5.12 for varying fiber phase volume fractions. A good comparison of the elastic modulus with Unnikrishnan et al. [54] is observed, where the authors [54] presented homogenized values and compared it with experimental results. The variation of the elastic modulus was also plotted against varying fiber volume fraction for different expansion polynomial order as shown in Figure 5.13, and it can be see that greater convergence is obtained using higher order elements. It should also be noted that the values obtained using this method results in an effective modulus within the H-S bounds.

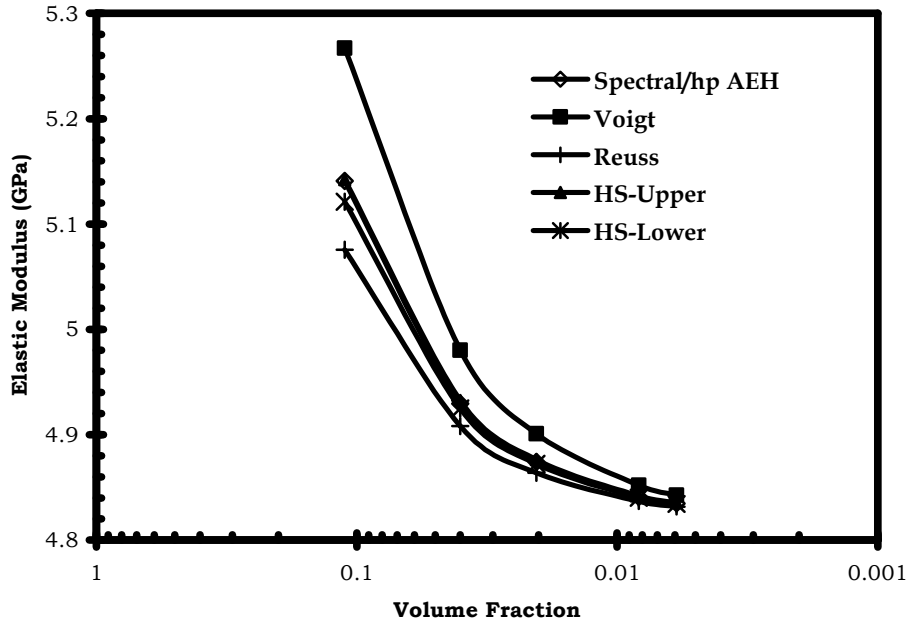

Figure 5.12 Variation of elastic constants for various volume fractions of shish phase

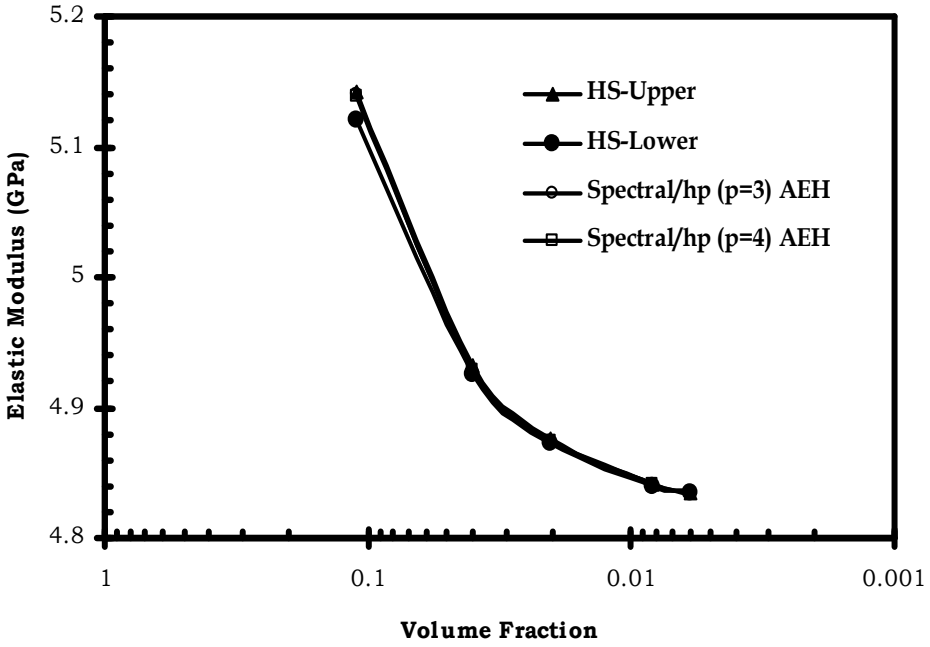

Figure 5.13 Variation of elastic constants for various volume fractions of shish phase for various spectral degrees

D. CONCLUSIONS

For the accurate and reliable estimation of the properties of nanocomposites, an efficient multiscale modeling strategy is imperative. In the case of problems in micro- or nanoscale systems and devices, the continuum theories cannot be applied naively. Fundamental molecular interactions need to be studied to scale up the properties to the continuum level by multiscale techniques. Such a framework should be able to unify and improve the existing methods of analysis and most importantly these methods should be able to provide adequate mathematical stability and accuracy. In this chapter, a multiscale computational strategy for the analysis of heterogeneous nanocomposites is presented. The chapter also deals with the effect of higher order finite element methods on the developed multiscale analysis strategy. The two-scale asymptotic expansion homogenization (AEH) method is used to estimate the mechanical properties of nanocomposites.

CHAPTER VI

CONCLUSIONS

A. SUMMARY AND CONCLUDING REMARKS

In this work, a novel multiscale modeling strategy is proposed for the analysis of Carbon Nanotube (CNT) fiber reinforced composite structures with CNTs of various morphologies and chiralities and polymeric nanofibers. This research provides a strong interlinking from the atomistic scale to the macroscale. With a full-scale mathematical basis, the proposed strategy is applied to the analysis of CNT reinforced nanocomposite structures and polymeric nanofibers. This research provides a sound theoretical and computational tool for the analysis and design of an enhanced strength nanocomposite using CNTs and nanofibers.

Analysis of Silicon doped CNT to estimate the elastic properties were presented in Chapter II and some of the significant conclusions were enumerated. The MD simulation was carried out using Tersoff-Brenner potential for isothermal strain conditions and the elastic modulus was obtained by the energy method. The doped CNT was found to be unstable at higher doping percentages the test temperature. Silicon atoms were found to attain an equilibrium position above the tubular structure of the CNT which had been verified earlier by ab-initio studies.

In Chapter III, the mechanical properties are determined for the central CNT when a functionalized CNT or other CNT structures was embedded in a matrix structure. The effect of chemical functionalization on the stiffness of CNTs along the tubule axis is estimated, and the functionalized CNT atomistic unit was found to be stable under various conditions. The stability of the CNT affected by the substitutional changes was studied by monitoring the structural change in the CNT profile under various loading conditions. These properties help in establishing the use of functionalized CNTs in composite structures.

Multiscale modeling to obtain the effective elastic modulus of the PLLA nanofiber having a Shish-Kebab model was shown in Chapter IV. The analysis was carried out at the atomistic level using MD simulation, to obtain the crystalline elastic modulus, and the homogenization of the Shish-Kebab model was carried out using micromechanical methods. The modified elastic constants were obtained and used in the proposed homogenized-continuum chain model to obtain the macroscale homogenized elastic modulus of the nanofiber. The simulations showed excellent correlation with that of experiments, without involving any experimental data in the analysis. In Chapter V, a multiscale computational strategy for the analysis of heterogeneous nanocomposites was presented. The two-scale asymptotic expansion homogenization (AEH) method was used to estimate the mechanical properties of nanocomposites and nanofibers. The effect of higher order of the polynomial expansion on the homogenized material property was also studied in this chapter.

B. TOPICS OF ONGOING AND FUTURE RESEARCH

In this dissertation work, only the mechanical characteristics of nanotube and nanocomposite systems were considered. However, for a truly multifunctional application, one needs to look into the thermal and electronic properties.

As an ongoing research it is only naturally for the estimation of the thermal properties of nanotube systems. It has therefore let to the study of thermal analysis of nanotube systems in the atomistic scale as well as in the mesoscale. The thermal conductivity analysis of a nanotube system having pure water and water with additives are currently under study. The aim of this study would be to quantify the effect of the admixture on the interfacial thermal resistance by molecular dynamic simulations. Here, some preliminary results on the estimation of the interfacial thermal resistance analysis are presented.

A (5,5) single-walled nanotubes with a diameter of 7Å immersed in water has been used in the analysis. The simulations are carried out on a CNT with 200 carbon atoms, corresponding to a nanotube length of~23.0 nm, and 435 water molecules and

the carbon and hydrogen atoms are modeled explicitly (see Figure 6.1). In the simulations the entire systems was minimized and later equilibrated for 1ps (1000steps). The temperature scaling was carried out in 10ps as an NVT ensemble (10,000 steps). During the minimization and NVT processes, the atoms in the periodic unit cell are allowed to equilibrate within the fixed MD cell. Periodic boundary conditions are applied in all directions.

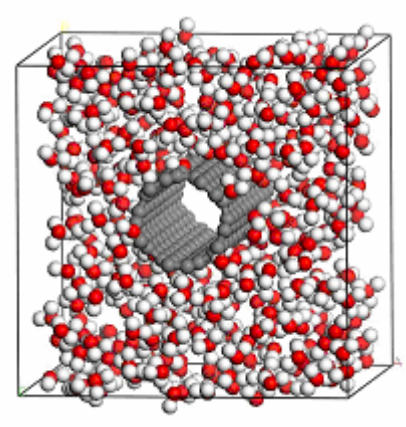

Figure 6.1 Initial state of unit cell with SWNT immersed in water

In the equilibration simulations, the atoms in the nanotube are heated instantaneously to 500K, 750 and 1000K by rescaling the velocities of carbon atoms in the nanotube. The system is allowed to relax without any thermostating effects. It is normally seen that the decay of the temperature is of an exponential order [159]. This decay of the temperature from the nanotube to the surrounding matrix molecules is limited by the interfacial thermal resistance. [160]. Under such conditions, the time constant, τ, of the decay depends on the nanotube heat capacity, C_T and the thermal resistance of the nanotube-matrix interface R_k

$$\tau = \frac{R_k \, C_T}{A_T} \tag{6.1}$$

where A_T is the area of the nanotube and C_T / A_T is the heat capacity per unit area of the SWNT and is usually taken as 5.6 x 10^{-4} J/m^{2}K [161-163]. The cooling profile of the two

ensembles against the MD time step is shown in Figures 6.2. Further details of the analysis will be presented in† [164].

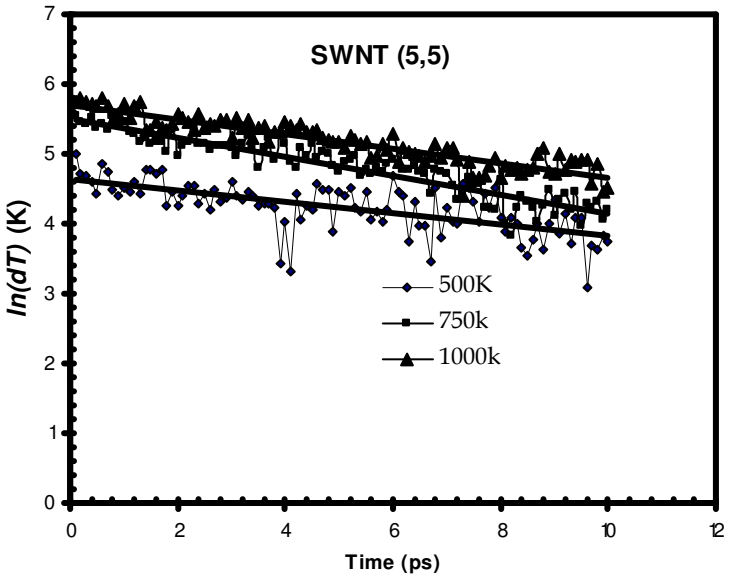

Figure 6.2 Cooling profile of SWNT in water

The obtained interfacial thermal resistance is now used in various effective medium theories to ascertain the effect on the overall thermal conductance of the composite system. The effective conductivities are found to be bounded by the Hashin-Shtrikman bounds which are established by micromechanical methods. The multiscale computational strategies developed in Chapter V can be used for the estimation of the macroscopic thermal conductivities.

REFERENCES

[1] Baughman, R. H., Zakhidov, A. A., and de Heer, W. A., 2002, "Carbon nanotubes--the route toward applications," Science, **297**, pp. 787-792.

[2] Chandra, N., Namilae, S., and Shet, C., 2004, "Local elastic properties of carbon nanotubes in the presence of stone-wales defects," Physical Review B (Condensed Matter and Materials Physics), **69**(9), pp. 094101-094112.

[3] Dresselhaus, M. S., Dresselhaus, G., and Eklund, P., 1996, *Science of fullerenes and carbon nanotubes: Their properties and applications*, Academic Press, New York.

[4] Jin, Y., and Yuan, F. G., 2003, "Simulation of elastic properties of single-walled carbon nanotubes," Composites Science and Technology, **63**, pp. 1507-1515.

[5] Lau, K. T., Chipara, M., Ling, H., and Hui, D., 2004, "On the elastic moduli of carbon nanotubes for nanocomposite structures," Composite Engineering, Pt. B, **35B**(2), pp. 95-101.

[6] Liao, L., and Li, S., 2001, "Interfacial characteristics of a carbon nanotube-polystyrene composite system," Applied Physics Letters, **79**(25), pp. 4225-4227.

[7] Mylvaganam, K., and Zhang, L., 2004, "Nanotube functionalization and polymer grafting: An ab-initio study," Journal of Physical Chemistry B, **108**, pp. 15009-15012.

[8] Mylvaganam, K., and Zhang, L. C., 2004, "Important issues in a molecular dynamics simulation for characterising the mechanical properties of carbon nanotubes," Carbon, **42**(10), pp. 2025-2032.

[9] Qian, D., Wagner, G. J., Liu, W. K., Yu, M.-F., and Ruoff, R. S., 2002, "Mechanics of carbon nanotubes," Applied Mechanics Reviews, **55**(6), pp. 495-533.

[10] Sears, A., and Batra, R. C., 2004, "Macroscopic properties of carbon nanotubes from molecular-mechanics simulations," Physical Review B (Condensed Matter and Materials Physics), **69**(23), pp. 235406-235410.

[11] Thostenson, E. T., and Chou, T. W., 2003, "On the elastic properties of carbon nanotube-based composites: Modeling and characterization," Journal of Physics D: Applied Physics, **36**(5), pp. 573-582.

[12] Unnikrishnan, V. U., and Reddy, J. N., 2005, "Characteristics of silicon doped carbon nanotube reinforced nanocomposites," International Journal for Multiscale Computational Engineering, **3**(4), pp. 437-450.

[13] Unnikrishnan, V. U., Reddy, J. N., and Rostam-Abadi, F., in review, "Mechanics of the core nanotube in nanocomposites, nanoropes, and functionalized nanotube systems."

[14] Yakobson, B. I., Brabec, C. J., and Bernholc, J., 1996, "Nanomechanics of carbon tubes: Instabilities beyond linear response," Physical Review Letters, **76**(14), pp. 2511-2514.

[15] Zhao, Q., Nardelli, M. B., and Bernholc, J., 2002, "Ultimate strength of carbon nanotubes: A theoretical study," Physical Review B, **65**(14), pp. 144105-144110.

[16] Blonski, S., Brostow, W., and Kuba´t, J., 1994, "Molecular-dynamics simulations of stress relaxation in metals and polymers," Physical Review B, **49**(10), pp. 6494 - 6500.

[17] Che, I., Cagın, T., and W. A. Goddard, I., 1999, "Studies of fullerenes and carbon nanotubes by an extended bond order potential," Nanotechnology, **10**, pp. 263-268.

[18] Srivastava, D., Wei, C., and Cho, K., 2003, "Nanomechanics of carbon nanotubes and composites," Applied Mechanics Reviews, **56**, pp. 215-230.

[19] Odegard, G. M., Harik, V. M., Wise, K. E., and Gates, T. S., 2003, "Constitutive modeling of nanotube-reinforced polymer composites," Composites, Science and Technology, **63**, pp. 1671-1687.

[20] Frankland, S. J. V., Harik, V. M., Odegard, G. M., Brenner, D. W., and Gates, T. S., 2003, "The stress-strain behavior of polymer-nanotube composites from molecular dynamics simulation," Composites Science and Technology, **63**, pp. 1655-1661.

[21] Reddy, J. N., 2004, *Mechanics of laminated composite plates and shells: Theory and analysis*, CRC Press Boca Raton, FL.

[22] Odegard, G. M., Gates, T. S., Nicholson, L. M., and Wise, K. E., 2002, "Equivalent-continuum modeling of nano-structured materials," Composites Science and Technology, **62**(14), pp. 1869-1880.

[23] Fisher, F. T., Bradshaw, R. D., and Brinson, L. C., 2003, "Fiber waviness in nanotube-reinforced polymer composites i: Modulus predictions using effective nanotube properties," Composites Science and Technology, **63**(11), pp. 1689-1703.

[24] Dereli, G., and Özdoğan, C., 2003, "Structural stability and energetics of single-walled carbon nanotubes under uniaxial strain," Physical Review B, **67**(3), pp. 035416-035421.

[25] Laborde-Lahoz, P., Maser, W., Martinez, T., Benito, A., Seeger, T., Cano, P., Villoria, R., and Miravete, A., 2005, "Mechanical characterization of carbon nanotube

composite materials," Mechanics of Advanced Materials and Structures, **12**(1), pp. 13-19.

[26] Iijima, S., 1991, "Helical microtubules of graphitic carbon," Nature, **354**(6348), pp. 56-58.

[27] Griebel, M., and Hamaekers, J., 2004, "Molecular dynamics simulations of the elastic moduli of polymer-carbon nanotube composites," Computer Methods in Applied Mechanics and Engineering, **193**(17-20), pp. 1773-1788.

[28] Dalgic, S., 2007, "The eam based effective pair potentials for the dynamic properties of liquid cu," Materials Chemistry and Physics, **103**(1), pp. 183-189.

[29] Reddy, J. N., 2002, *Energy principles and variational methods in applied mechanics*, John Wiley, New York.

[30] Frankland, S. J. V., Caglar, A., Brenner, D. W., and Griebel, M., 2002, "Molecular simulation of the influence of chemical cross-links on the shear strength of carbon nanotube-polymer interfaces," Journal of Physical Chemistry. B, **106**(12), pp. 3046 -3048.

[31] Namilae, S., Chandra, N., and Shet, C., 2004, "Mechanical behavior of functionalized nanotubes," Chemical Physics Letters, **387**(4-6), pp. 247-252.

[32] Brenner, D. W., 1990, "Emperical potential for hydrocarbons for use in simulating the chemical vapor deposition of diamond films," Physical Review B, **42**, pp. 9458-9471.

[33] Frankland, S. J. V., and Brenner, D. W., 1999, "*Materials applications of carbon nanotubes: Hydrogen storage and polymer-nanotube composites*," National Meeting of the American Chemical Society New Orleans, LA, p. 38953.

[34] Tersoff, J., 1989, "Modeling solid-state chemistry: Interatomic potentials for multicomponent systems," Physical Review B, **39**(8), pp. 5566-5568.

[35] Zhang, L., and Tanaka, H., 1997, "Towards a deeper understanding of wear and friction on the atomic scale - a molecular dynamics analysis," Wear, **211**, pp. 44-53.

[36] Chowdhury, S. C., and Okabe, T., 2007, "Computer simulation of carbon nanotube pull-out from polymer by the molecular dynamics method," Composites Part A: Applied Science and Manufacturing, **38**(3), pp. 747-754.

[37] Robertson, D. H., Brenner, D. W., and Mintmire, J. W., 1992, "Energetics of nanoscale graphitic tubules," Physical Review B, **45**(21), pp. 12592 - 12595.

[38] Salvetat, J. P., Briggs, G. A. D., Bonard, J. M., Bacsa, R. R., and Kulik, A. J., 1999, "Elastic and shear moduli of single-walled carbon nanotube ropes," Physical Review Letters, **82**, pp. 944-947.

[39] Baierle, R. J., Fagan, S. B., Mota, R., da Silva, A. J. R., and Fazzio, A., 2001, "Electronic and structural properties of silicon-doped carbon nanotubes," Physical Review B, **64**(8), pp. 085413-085416.

[40] Harik, V. M., 2002, "Mechanics of carbon nanotube: Applicability of the continuum beam models," Computational Materials Science, **24**, pp. 328-342.

[41] Vodenitcharova, T., and Zhang, L. C., 2003, "Effective wall thickness of a single-walled carbon nanotube," Physical Review B, **68**(16), pp. 165401-165404.

[42] Fagan, S. B., da Silva, A. J. R., Mota, R., Baierle, R. J., and Fazzio, A., 2003, "Functionalization of carbon nanotubes through the chemical binding of atoms and molecules," Physical Review B, **67**(3), pp. 033405-033408.

[43] Fagan, S. B., Mota, R., Baierle, R. J., da Silva, A. J. R., and Fazzio, A., 2003, "Ab initio study of an organic molecule interacting with a silicon-doped carbon nanotube," Diamond and Related Materials, **12**(3-7), pp. 861-863.

[44] Fagan, S. B., Mota, R., daSilva, A. J. R., and Fazzio, A., 2004, "Substitutional si doping in deformed carbon nanotubes," Nano Letters, **4**(5), pp. 975-977.

[45] Fazzio, A. R., J. Baierle, S. B. Fagan, R. Mota, and Silva, A. J. R. d., 2001, "*Ab initio study of si doped carbon nanotubes: Electronic and structural properties*," Proc. of Materials Research Society, p. 675.

[46] Petaccia, L., Goldoni, A., Lizzit, S., and Larciprete, R., 2005, "Electronic properties of clean and li-doped single-walled carbon nanotubes," Journal of Electron Spectroscopy and Related Phenomena, **144**, pp. 793-797.

[47] Srivastava, D., Menon, M., and Cho, K., 2001, "Anisotropic nanomechanics of boron nitride nanotubes: Nanostructured "Skin" Effect," Physical Review B, **63**(19), pp. 195413-195417.

[48] Khabashesku, V. N., Margrave, J. L., and Barrera, E. V., 2005, "Functionalized carbon nanotubes and nanodiamonds for engineering and biomedical applications," Diamond & Related Materials, **14**(3-7), pp. 859-866.

[49] Qian, D., Liu, W. K., and Ruo, R. S., 2003, "Load transfer mechanism in carbon nanotube ropes," Composites Science and Technology, **63**, pp. 1561-1569.

[50] Gou, J., Liang, Z., Zhang, C., and Wang, B., 2005, "Computational analysis of effect of single-walled carbon nanotube rope on molecular interaction and load transfer of nanocomposites," Composites: Part B, **36**, pp. 524-533.

[51] Wei, C., Srivastava, D., and Cho, K., 2002, "Thermal expansion and diffusion coefficients of carbon nanotube-polymer composites," Nano Letters, **2**(6), pp. 647-650.

[52] Reddy, J. N., 2006, *An introduction to the finite element method*, McGraw-Hill, New York.

[53] Calvert, P., 1999, "A recipe for strength," Nature, **399**, pp. 210-211.

[54] Unnikrishnan, V. U., Unnikrishnan, G. U., Reddy, J. N., and Lim, C. T., 2007, "Atomistic-mesoscale coupled mechanical analysis of polymeric nanofibers," Journal of Materials Science, **in press**.

[55] Unnikrishnan, G. U., Unnikrishnan, V. U., and Reddy, J. N., 2007, "Constitutive material modeling of cell: A micromechanics approach," Journal of Biomechanical Engineering, **129**, pp. 1-9.

[56] Bradshaw, R. D., Fisher, F. T., and Brinson, L. C., 2003, "Fiber waviness in nanotube-reinforced polymer composites: Ii. Modeling via numerical approximation of the dilute strain concentration tensor," Composites Science and Technology, **63**(11), pp. 1705-1722.

[57] Ding, W., Eitan, A., Chen, X., Dikin, D. A., Fisher, F. T., Andrews, R., Brinson, L. C., Schadler, L. S., and Ruoff, R. S., 2003, "Direct observation of polymer sheathing in carbon nanotube-polycarbonate composites," Nano Letters, **3**(11), pp. 1593-1597.

[58] Garg, A., and Sinnott, S. B., 1998, "Effect of chemical functionalization on the mechanical properties of carbon nanotubes," Chemical Physics Letters, **295**(4), pp. 273-278.

[59] Qin, L. C., and S., I., 2000, "*Twisting of single-walled carbon nanotube bundles*," Proc. of Materials Research Society Symposium, pp. 33-38.

[60] Fisher, F. T., and Brinson, L. C., 2003, "*Macroscale experimental evidence of a reduced-mobility non-bulk polymer phase in nanotube-reinforced polymers*," 44th AIAA/ASME/ASCE/AHS Structures, Structural Dynamics, and Materials Conference Norfolk, VA, pp. 1702-1706.

[61] Sandler, J., Broza, G., Nolte, M., Schulte, K., Lam, Y.-M., and Shaffer, M. S. P., 2003, "Crystallization of carbon nanotube and nanofiber polypropylene composites," Journal of Macromolecular Science: Part B - Physics, **B42**, pp. 479 - 488.

[62] Barber, A. H., Cohen, S. R., and Wagner, H. D., 2003, "Measurement of carbon nanotube--polymer interfacial strength," Applied Physics Letters, **82**(23), pp. 4140-4142.

[63] Wacker, G., Bledzki, A. K., and Chate, A., 1998, "Effect of interphase on the transverse young's modulus of glass/epoxy composites," Composites, **29A**, pp. 619-626.

[64] Al-Haik, M., Hussaini, M. Y., and Garmestani, H., 2005, "Adhesion energy in carbon nanotube-polyethylene composite: Effect of chirality," Journal of Applied Physics, **97**(7), pp. 074306-074305.

[65] Martel, R., Schmidt, T., Shea, H. R., Hertel, T., and Avouris, P., 1998, "Single- and multi-wall carbon nanotube field-effect transistors," Applied Physics Letters, **73**(17), pp. 2447-2449.

[66] Avouris, P., Hertel, T., Martel, R., Schmidt, T., Shea, H. R., and Walkup, R. E., 1999, "Carbon nanotubes: Nanomechanics, manipulation, and electronic devices," Applied Surface Science, **141**, pp. 201-209.

[67] Zhao, Y., Tong, T., Delzeit, L., Kashani, A., Meyyappan, M., and Majumdar, A., 2006, "Interfacial energy and strength of multiwalled-carbon-nanotube-based dry adhesive," Journal of Vacuum Science & Technology B: Microelectronics and Nanometer Structures, **24**(1), pp. 331-335.

[68] Hertel, T., Walkup, R. E., and Avouris, P., 1998, "Deformation of carbon nanotubes by surface van der waals forces," Physical Review B, **58**(20), pp. 13870 - 13873.

[69] Li, X., and Weinan, E., 2005, "Multiscale modeling of the dynamics of solids at finite temperature," Journal of the Mechanics and Physics of Solids, **53**(7), pp. 1650-1685.

[70] Benseddiq, N., Belayachi, N., and Nait Abdelaziz, M., 2006, "Multiscale approach to the behaviour and damage of the heterogeneous elastic-viscoplastic materials," Theoretical and Applied Fracture Mechanics, **46**(1), pp. 15-25.

[71] Li, S., Gupta, A., Liu, X., and Mahyari, M., 2004, "Variational eigenstrain multiscale finite element method," Computer Methods in Applied Mechanics and Engineering, **193**(17-20), pp. 1803-1824.

[72] Unnikrishnan, V. U., Reddy, J. N., and Rostam-Abadi, F., 2004, "Mechanics of carbon nanotube based composites with molecular dynamics and mori-tanaka methods," International Conference on Scientific and Engineering Computations Singapore.

[73] Mura, T., 1997, *Micromechanics of defects in solids*, Martinus Nijhoff, Hague, The Netherlands.

[74] Marzari, N., and Ferrari, M., 1992, "Textural and micromorphological effects on the overall elastic response of macroscopically anisotropic composites," Journal of Applied Mechanics-Transactions of the Asme, **59**(2), pp. 269-275.

[75] Schjodt-Thomsen, J., and Pyrz, R., 2001, "The influence of stochastic interfacial parameter distribution on the stiffness of composites with complex fibre orientation," Composites Science and Technology, **61**, pp. 697-704.

[76] Schjodt-Thomsen, J., and Pyrz, R., 2001, "The mori-tanaka stiffness tensor: Diagonal symmetry, complex fibre orientations and non-dilute volume fractions," Mechanics of Materials, **33**, pp. 531-544.

[77] Inai, R., Kotaki, M., and Ramakrishna, S., 2005, "Structure and properties of electrospun plla single nanofibres," Nanotechnology, **16**, pp. 208-213.

[78] Lim, T. C., M. Kotaki, Yong, T. K. J., Yang, F., Fujihara, K., and Ramakrishna, S., 2004, "Recent advances in tissue engineering applications of electrospun nanofibers," Materials Technology (Nano Bio-engineering Special), **19**(1), pp. 20-27.

[79] Lim, T. C., and Ramakrishna, S., 2005, "Next-generation applications for polymeric nanofibers," Nanotechnology global strategies, industry trends and applications, J. Schulte, ed., John Wiley & Sons, London, pp. 137-147.

[80] Ramakrishna, S., Fujihara, K., Ganesh, V. K., Teo, W. E., and Lim, T. C., 2005, "Science and engineering of polymer nanofibers," Functional nanomaterials, K. E. Geckeler, and E. Rosenberg, eds., American Scientific Publisher, Valencia.

[81] Ramakrishna, S., Fujihara, K., Teo, W. E., Lim, T. C., and Ma, Z. W., 2005, *An introduction to electrospinning and nanofibers*, World Scientific, Singapore.

[82] Zammaretti, P., and Jaconi, M., 2004, "Cardiac tissue engineering: Regeneration of the wounded heart," Current Opinion in Biotechnology, **15**, pp. 430-434.

[83] Tan, E. P. S., and Lim, C. T., 2006, "Characterization of bulk properties of polymer nanofibrous scaffolds from nanomechanical properties of single nanofibers," Journal of Biomedical Materials Research - Part A, **77A**(3), pp. 526-533.

[84] Freed, L. E., Vunjak-Novakovic, G., Biron, R. J., Eagles, D. B., Lesnoy, D. C., Barlow, S. K., and Langer, R., 1994, "Biodegradable polymer scaffolds for tissue engineering," Bio/Technology, **12**, pp. 689-693.

[85] Moran, J. M., Pazzano, D., and Bonassar, L. J., 2003, "Characterization of polylactic acid-polyglycolic acid composites for cartilage tissue engineering," Tissue Engineering, **9**(1), pp. 63-70.

[86] Lee, K. H., Kim, H. Y., Khil, M. S., Ra, Y. M., and Lee, D. R., 2003, "Characterization of nano-structured poly(1-caprolactone) nonwoven mats via electrospinning," Polymer, **44**, pp. 1287–1294.

[87] Tan, E. P. S., and Lim, C. T., 2005, "Nanoindentation study of nanofibers," Applied Physics Letters, **87**, pp. 123106-123109.

[88] Dukovski, I., and Muthukumar, M., 2003, "Langevin dynamics simulations of early stage shish-kebab crystallization of polymers in extensional flow," Journal of Chemical Physics, **118**, pp. 6648-6655.

[89] Northolt, M. G., and Hout, R. V. d., 1985, "Elastic extension of an oriented crystalline fiber," Polymer, **26**(2), pp. 310-316

[90] Tan, E. P. S., and Lim, C. T., 2006, "Nanomechanical characterization of nanofibers - a review," Composites Science & Technology, **66**(9), pp. 1099-1108.

[91] Richardson, I. D., and Ward, I. M., 1970, "Molecular reorientation and deformation in polymers i. Calculation of refractive indices for a general deformation," Journal of Physics D: Applied Physics, **3**(5), pp. 649-662.

[92] Northolt, M. G., 1980, "Tensile deformation of poly(p-phenylene terephthalamide) fibres, an experimental and theoretical analysis," Polymer, **21**(10), pp. 1199-1204.

[93] Northolt, M. G., and Baltussen, J. J. M., 2002, "The tensile and compressive deformation of polymer and carbon fibers," Journal of Applied Polymer Science, **83**(3), pp. 508-538.

[94] Northolt, M. G., Roos, A., and Kampschreur, J. H., 1989, "Birefringence, compliance, and viscoelasticity of poly(ethylene terephthalate) fibers," Journal of Polymer Science: Part B: Polymer Physics, **27**(5), pp. 1107-1120.

[95] Kalb, B., and Pennings, A. J., 1980, "General crystallization behaviour of poly(-lactic acid)," Polymer, **21**(6), pp. 607-612.

[96] Hoogsteen, W., Postema, A. R., Pennings, A. J., and ten Brinke, G., 1990, "Crystal structure, conformation, and morphology of solution-spun poly(l-lactide) fibers," Macromolecules, **23**, pp. 634-642.

[97] De-Santis, P., and Kovacs, A. J., 1968, "Molecular conformation of poly (s-lactic acid)," Biopolymers, **6**(3), pp. 299-306

[98] Yamane, H., Sasai, K., and Takano, M., 2004, "Poly(d-lactic acid) as a rheological modifier of poly(l-lactic acid): Shear and biaxial extensional flow behavior," Journal of Rheology, **48**(3), pp. 599-609.

[99] Fujita, M., and Doi, Y., 2003, "Annealing and melting behavior of poly(l-lactic acid) single crystals as revealed by in situ atomic force microscopy," Biomacromolecules, **4**(5), pp. 1301 -1307.

[100] Somania, R. H., Yanga, L., Zhub, L., and Hsiao, B. S., 2005, "Flow-induced shish-kebab precursor structures in entangled polymer melts," Polymer, **46**, pp. 8587-8623.

[101] Welch, P., and Muthukumar, M., 2001, "Molecular mechanisms of polymer crystallization from solution," Physical Review Letters, **87**(21), pp. 218302-218305.

[102] Zussman, E., Rittel, D., and Yarin, A. L., 2003, "Failure modes of electrospun nanofibers," Applied Physical Letters, **82**(22), pp. 3958-3960.

[103] Tan, E. P. S., and Lim, C. T., 2004, "Physical properties of a single polymeric nanofiber," Applied Physics Letters, **84**(9), pp. 1603-1605.

[104] Thelen, S., Barthelat, F., and Brinson, L. C., 2004, "Mechanics considerations for microporous titanium as an orthopaedic implant material," Journal of Biomedial Materials Research, **69A**, pp. 601-610.

[105] Leenslag, J. W., and Pennings, A. J., 1987, "High-strength fibers by hot drawing of as-polymerized poly(l)lactide," Polymer Communications, **28**(4), pp. 92–94.

[106] Leenslag, J. W., and Pennings, A. J., 1987, "High-strength poly(l-lactide) fibres by a dry-spinning/hot-drawing process " Polymer, **28**(10), pp. 1695-1702.

[107] Ward, I. M., 1967, "The influence of pre-orientation on the optical and mechanical anisotropy of drawn polymers," British Journal of Applied Physics, **18**, pp. 1165-1175.

[108] Baltussen, J. J. M., and Northolt, M. G., 2001, "The viscoelastic extension of polymer fibres: Creep behaviour," Polymer, **42**, pp. 3835–3846.

[109] Baltussen, J. J. M., Northolt, M. G., and van der Hout, R., 1997, "The continuous chain model for the elastic extension of polymer fibers in the glassy state," Journal of Rheology, **41**(3), pp. 549-573.

[110] Ruotsalainen, T., Turku, J., Heikkilä, P., Ruokolainen, J., Nykänen, A., Laitinen, T., Torkkeli, M., Serimaa, R., ten Brinke, G., Harlin, A., and Ikkala, O., 2005, "Towards internal structuring of electrospun fibers by hierarchical self-assembly of polymeric comb-shaped supramolecules," Advanced Materials, **17**(8), pp. 1048 - 1052.

[111] Demir, M. M., Yilgor, I., Yilgor, E., and Erman, B., 2002, "Electrospinning of polyurethane fibers," Polymer, **43**(11), pp. 3303-3309.

[112] Yuan, X. Y., Mak, A. F. T., and Yao, K. D., 2003, "Surface degradation of poly(l-lactic acid) fibres in a concentrated alkaline solution," Polymer Degradation and Stability **79**(1), pp. 45-52.

[113] Broz, M. E., Vander Hart, D. L., and Washburn, N. R., 2003, "Structure and mechanical properties of poly(d,l-lactic acid)/poly(e-caprolactone) blends," Biomaterials **24**, pp. 4181-4190.

[114] Cicero, J. A., and Dorgan, J. R., 2001, "Physical properties and fiber morphology of poly(lactic acid) obtained from continuous two-step melt spinning," Journal of Polymers and the Environment, **9**(1), pp. 1-10.

[115] Lim, J. Y., Kim, S. H., Lim, S., and Kim, Y. H., 2002, "Improvement of flexural strengths of poly(l-lactic acid) by solid-state extrusion," Macromolecular Chemistry and Physics, **202**(11), pp. 2447 - 2453.

[116] Fambri, L., Pergoretti, A., Fenner, R., Incardona, D., and Migliaresi, C., 1997, "Biodegradable fibres of poly(l-lactic acid) produced by melt spinning," Polymer, **38**(1), pp. 79-85.

[117] Balac, I., Milovancevic, M., Tang, C.-y., Uskokovic, P. S., and Uskokovic, D. P., 2004, "Estimation of elastic properties of a particulate polymer composite using a face-centered cubic fe model," Materials Letters, **58**(19), pp. 2437-2441.

[118] Mezghani, K., and Spruiell, J. E., 1998, "High speed melt spinning of poly(l-lactic acid) filaments," Journal of Polymer Science: Part B: Polymer Physics, **36**, pp. 1005–1012.

[119] Li, L. X., and Wang, T. J., 2005, "A unified approach to predict overall properties of composite materials," Materials Characterization, **54**(1), pp. 49-62.

[120] Bensoussan, A., Lions, J. L., and Papanicolaou, G., 1978, *Asymptotic analysis for periodic structures*, North-Holland., New York.

[121] Sanchez-Palencia, E., 1980, *Non-homogeneous media and vibration theory: Lecture notes in physics*, Springer-Verlag, Berlin ; New York.

[122] Wu, X., and Ohno, N., 1999, "A homogenization theory for time-dependent nonlinear composites with periodic internal structures," International Journal of Solids and Structures, **36**(33), pp. 4991-5012.

[123] Cao, L.-Q., 2005, "Iterated two-scale asymptotic method and numerical algorithm for the elastic structures of composite materials," Computer Methods in Applied Mechanics and Engineering, **194**(27-29), pp. 2899-2926.

[124] Chen, C.-M., Kikuchi, N., and Rostam-Abadi, F., 2004, "An enhanced asymptotic homogenization method of the static and dynamics of elastic composite laminates," Computers & Structures, **82**(4-5), pp. 373-382.

[125] Chung, P. W., and Namburu, R. R., 2003, "On a formulation for a multiscale atomistic-continuum homogenization method," International Journal of Solids and Structures, **40**, pp. 2563-2588.

[126] Chung, P. W., and Tamma, K. K., 1999, "Woven fabric composites: Developments in engineering bounds, homogenization and applications," International Journal of Numerical Methods in Engineering, **45**(12), pp. 1757-1790.

[127] Chung, P. W., Tamma, K. K., and Namburu, R. R., 2000, "A micro/macro homogenization approach for viscoelastic creep analysis with dissipative correctors for heterogeneous woven-fabric layered media," Composites Science and Technology, **60**(12-13), pp. 2233-2253.

[128] Chung, P. W., Tamma, K. K., and Namburu, R. R., 2001, "Asymptotic expansion homogenization for heterogeneous media: Computational issues and applications," Composites Part A: Applied Science and Manufacturing (Incorporating Composites and Composites Manufacturing),, **32**(9), pp. 1291-1301.

[129] Chung, P. W., Tamma, K. K., and Namburu, R. R., 2004, "A computational approach for multi-scale analysis of heterogeneous elasto-plastic media subjected to short duration loads," International Journal for Numerical Methods in Engineering, **59**, pp. 825-848.

[130] Marusic-Paloka, E., 1997, "Asymptotic expansion for a flow in a periodic porous medium," Comptes Rendus de l'Academie des Sciences - Series IIB - Mechanics-Physics-Chemistry-Astronomy, **325**(7), pp. 369-374.

[131] Meguid, S. A., and Kalamkarov, A. L., 1994, "Asymptotic homogenization of elastic composite materials with a regular structure," International Journal of Solids and Structures, **31**(3), pp. 303-316.

[132] Maday, Y., and Patera, A. T., 1989, *Spectral element methods for the incompresssible navier-stokes equations*, ASME, New York.

[133] Karniadakis, G. E., and Sherwin, S. J., 1999, *Spectral/hp element methods for cfd*, Oxford University Press, Oxford.

[134] Hill, A. A., and Straughan, B., 2006, "A legendre spectral element method for eigenvalues in hydrodynamic stability," Journal of Computational and Applied Mathematics, **193**(1), pp. 363-381.

[135] Hesthaven, J. S., 2000, "Spectral penalty methods," Applied Numerical Mathematics, **33**(1-4), pp. 23-41.

[136] Pontaza, J. P., and Reddy, J. N., 2003, "Spectral/hp least-squares finite element formulation for the navier-stokes equations," Journal of Computational Physics, **190**(2), pp. 523-549.

[137] Blackburn, H. M., and Sherwin, S. J., 2004, "Formulation of a galerkin spectral element–fourier method for three-dimensional incompressible flows in cylindrical geometries," Journal of Computational Physics, **197**, pp. 759–778.

[138] Clayton, J. D., and Chung, P. W., 2006, "An atomistic-to-continuum framework for nonlinear crystal mechanics based on asymptotic homogenization," Journal of the Mechanics and Physics of Solids, **54**, pp. 1604-1639.

[139] Takano, N., Ohnishi, Y., Zako, M., and Nishiyabu, K., 2000, "The formulation of homogenization method applied to large deformation problem for composite materials," International Journal of Solids and Structures, **37**, pp. 6517-6535.

[140] Hernandez, E., Goze, C., Brenier, P., and Rubio, A., 1998, "Elastic properties of c and bxcynz composite nanotubes," Physical Review Letters, **80**, pp. 4502-4505.

[141] Meunier, V., Nardelli, M. B., Roland, C., and Bernholc, J., 2001, "Structural and electronic properties of carbon nanotube tapers," Physical Review B, **64**(19), pp. 195419-195425.

[142] Pontaza, J. P., and Reddy, J. N., 2004, "Space–time coupled spectral/hp least-squares finite element formulation for the incompressible navier–stokes equations," Journal of Computational Physics, **197**, p. 418.

[143] Weinan, E., and Engquist, B., 2003, "Multiscale modeling and computation," Notices of the AMS, **50**(9), pp. 1062-1070.

[144] Song, Y. S., and Youn, J. R., 2006, "Asymptotic expansion homogenization of permeability tensor for plain woven fabrics," Composites Part A: Applied Science and Manufacturing, **37**(11), pp. 2080-2087.

[145] Takano, N., Zako, M., Okazaki, T., and Terada, K., 2002, "Microstructure-based evaluation of the influence of woven architecture on permeability by asymptotic homogenization theory," Composites Science and Technology, **62**(10-11), pp. 1347-1356.

[146] Petersen, S., Dreyer, D., and von Estorff, O., 2006, "Assessment of finite and spectral element shape functions for efficient iterative simulations of interior acoustics," Computer Methods in Applied Mechanics and Engineering, **195**(44-47), pp. 6463-6478.

[147] Nool, M., and Proot, M. M. J., 2005, "A parallel least-squares spectral element solver for incompressible flow problems on unstructured grids," Parallel Computing, **31** pp. 414-438.

[148] Melenk, J. M., 2002, "On condition numbers in hp-fem with gauss-lobatto-based shape functions," Journal of Computational and Applied Mathematics, **139**, pp. 21-48.

[149] Tufo, H. M., Fischer, P. F., Papka, M. E., and Blom, K., 1999, "*Numerical simulation and immersive visualization of hairpin vortices*," ACM/Institute of Electrical and Electronics Engineers, Inc., Supercomputing 1999 Conference Portland, Oregon, United States, pp. 62-77.

[150] Fischer, P., 1997, "An overlapping schwarz method for spectral element solution of the incompressible navier-stokes equations," Journal of Computational Physics, **133**, pp. 84-101.

[151] Zumbusch, G. W., 1996, "Symmetric hierarchical polynomials and the adaptive h-p-version," Houston Journal of Mathematics, **22**, pp. 529-540.

[152] Giraldo, F. X., 2003, "Strong and weak lagrange-galerkin spectral element methods for the shallow water equations," Computers and Mathematics with Applications, **45**, pp. 97-121.

[153] Giraldo, F. X., and Warburton, T., 2005, "A nodal triangle-based spectral element method for the shallow water equations on the sphere," Journal of Computational Physics **207**, pp. 129-150.

[154] Song, Y. S., and Youn, J. R., 2006, "Evaluation of effective thermal conductivity for carbon nanotube/polymer composites using control volume finite element method," Carbon, **44**(4), pp. 710-717.

[155] Lukkassen, D., Persson, L. E., and Wall, P., 1995, "Some engineering and mathematical aspects on the homogenization method," Composites Engineering, **5**(5), pp. 519-531.

[156] Abdelmoula, R., and Leger, A., 2005, "Local and global effects of small holes periodically distributed on a surface embedded in an axisymmetrical elastic medium," European Journal of Mechanics - A/Solids, **24**(1), pp. 89-109.

[157] Unnikrishnan, V. U., Unnikrishnan, G. U., and Reddy, J. N., in preparation, "Spectral/hp based asymptotic expansion homogenization of heterogeneous media: Analysis of nanostructures."

[158] Song, Y. S., and Youn, J. R., 2006, "Modeling of effective elastic properties for polymer based carbon nanotube composites," Polymer, **47**(5), pp. 1741-1748.

[159] Yao, N., and Lordi, V., 1998, "Young's modulus of single-walled carbon nanotubes," Journal of Applied Physics, **84**(4), pp. 1939-1943.

[160] Jiajun, W., and Xiao-Su, Y., 2004, "Effects of interfacial thermal barrier resistance and particle shape and size on the thermal conductivity of aln/pi composites," Composites Science and Technology, **64**(10-11), pp. 1623-1628.

[161] Clancy, T. C., and Gates, T. S., 2006, "Modeling of interfacial modification effects on thermal conductivity of carbon nanotube composites," Polymer, **47**(16), pp. 5990-5996.

[162] Huxtable, S. T., Cahill, D. G., Shenogin, S., Xue, L., Ozisik, R., Barone, P., Usrey, M., Strano, M. S., Siddons, G., Shim, M., and Keblinski, P., 2003, "Interfacial heat flow in carbon nanotube suspensions," Nature of Materials, **2**(11), pp. 731-734.

[163] Shenogin, S., Xue, L., Ozisik, R., Keblinski, P., and Cahill, D. G., 2004, "Role of thermal boundary resistance on the heat flow in carbon-nanotube composites," Journal of Applied Physics, **95**(12), pp. 8136-8144.

[164] Unnikrishnan, V. U., D. Banerjee, and J. N. Reddy, in review, "Atomistic-mesoscale thermal analysis of carbon nanotube systems."

VITA

Vinu Unnithan Unnikrishnan received his Bachelor of Technology degree in Civil Engineering from the University of Kerala in 1999. He completed his Master of Science degree in 2002, from the Indian Institute of Technology Madras in Civil Engineering with a specialization in Structural Engineering. He worked on the error estimation of nonlinear finite element methods in the distributed computing environment.

He joined the doctoral program at Texas A&M University in September 2002 and graduated in August 2007. His research interests include multiscale mechanical and thermal analysis of nanomechanical structures and computational analysis of heterogeneous structures and biomechanics.

Mr. Vinu Unnikrishnan may be reached through Professor J. N. Reddy (jnreddy@tamu.edu) in the Mechanical Engineering Department, Texas A&M University, College Station TX 77843-3123.